

The Norwegian University of Science and Technology

Department of Chemical Engineering

Kinetic and deactivation studies of hydrodesulfurization catalysts

by

Petr Steiner

A Dissertation Submitted in Partial Fulfillment of the Requirements for the Degree

Doctor Ingeniør

December 2002

ACKNOWLEDGEMENT

It is dark outside, norwegian winter with its long nights is almost in the highest peak and here I am, sitting behind the computer and finishing my thesis. It seems to be the best time to look back on the time I have spent here in Trondheim. When I started my Ph. D. study almost four and half years ago, I would never believe that the time will pass so quickly. Well, it seems to be true that when you have work to do, time is flying. During that time I have met a lot of nice and interesting people and I would like to mention especially prof. Edd A. Blekkan. Our long discussions, which were not necessarily just about the science, his skilled guidance throughout my Ph.D., and a lot of other small, but important things made him an unforgettable person in my life. I would like to thank to him for giving me the possibility to come to Trondheim to start a Ph.D. study and it is also mainly thanks to him that I am now sitting here with that good feeling about finishing the thesis. His corrections and comments were of great value and importance. Edd, thank you very much for all the help I have received.

I have also spent six wonderful months in the Technical University of Delft in The Netherlands in the group of prof. Jacob A. Moulijn. The topic of the work I did there was very closely related to the subject of my thesis and the time spent there was incredibly productive. I was lucky enough to be able to work on the functional experimental setup and for that I have to thank Bas M. Vogelaar, Dutch Ph.D. student. He made the setup almost ready before my arrival and after adjusting just the small details, I could measure without any delays. A perfect work, Bas! The cooperation with Bas and regular meetings every Friday during the lunch with Dr. A. D. van Langeveld made my stay very productive and meaningful. The interesting discussions with prof. Moulijn helped me very much to stay on the right track and use the designated time to the fullest. I would like to thank to all three for the great help during the finalizing of my thesis, when their corrections and suggestions were priceless. I am grateful to the whole catalysis group in Delft for being so friendly, helpful, and supportive during my short stay in their environment. Thank you all for the big help you were to me, especially after the incident I had in the laboratory.

I am grateful to the hydrotreating group in the Statoil research centre in Trondheim for letting me do some analytical work on their GC-AED. I especially thank to Bodil Thorvaldsen who

taught me how to use this delicate instrument. I have enjoyed very much my stay in the Statoil research centre and working in the team of dedicated people.

I would also like to thank to Dr. Håkon Bergem and Mr. Rune Myrstad for letting me perform the experiments on their apparatus and for teaching me how to use them. Without them the time I needed for the learning would be much longer. I have to thank to Håkon also for the continuous support and help during my experimental work.

I would also like to thank to the catalysis group on our department. Lisbeth was always a person on the right place and whenever I had any administrative problem, she was the one who solved it. I had nice colleagues in the lab and it would be a very long list to name them all. My special thanks belong to former diploma student Anastasia Virnovskaia, who had an active role in a part of my thesis and who made me realize that whatever your age is, you are as old as you feel inside. Nastya, you actually made me feel much younger and it was a pleasure to be your supervisor. Thank you.

I have met many Czechs here in Trondheim. Sometimes they made me feel like I have not left the Czech Republic at all. I am thankful for our regular meetings at Vækteren (and at Egon, after Vækteren burned down) and for the diverse parties and activities throughout the years. It was very nice to have someone with the same cultural background and the same language.

I would like to thank to all athletes from Trondheim Friidrett. You helped me to keep my sanity whenever I had some problems at work. Two hours a day I was out of this world, I was in a place where everything depends just on my skills and abilities and where your success depends only on the way you have trained. Thank you for accepting me into the group and for treating me like your own. You are the only real Norwegian friends I have made here.

I would also like to acknowledge the Foundation of Josefa, Marie and Zdenky Hlavkovich for the travel grant to cover some of my expenses connected with the move to Norway. Appreciation is extended to NTNU, The Norwegian Research Council, Statoil, and SINTEF for providing resources and funding for my research. I would also like to thank AKZO Nobel Chemicals, TU Delft, and The Dutch Organization for Scientific Research for funding my stay in The Netherlands.

Last but not least, I would like to thank to my parents for all the support they gave me throughout my life. I appreciate your full support for all my decisions even if the consequence was to move away to Norway, for you almost unreachable. Finally, a very special thanks go to my close friend Zdenka, who was able (in her special way) to make me feel that I am not alone and that I have someone to share with all my successes and problems. I know it was very difficult since Norway is quite far away for the possibility to be there where we need each other, but that period is soon over and I hope for the best in the future. I appreciate greatly your patience and I thank you for being here with me on the day of my final exam.

Trondheim, December 2002

“I find that a great part of the information I have was acquired by looking up something and finding something else on the way.”

Franklin P. Adams (1881 - 1960)

ABSTRACT

Hydrodesulfurization is an important part of the hydrotreating process. More stringent regulations on the quality of fuels bring new requirements to the catalytic processes. The removal of sulfur has become a key issue in the oil refining and this work aims to address several aspects of the process.

Kinetic studies of the hydrodesulfurization reaction over conventional (molybdenum-based) and new (Pt/Y-zeolite) catalysts are reported. The hydrodesulfurization of both the real oil (light gas oil from Statoil Mongstad refinery) and model compounds (thiophene and dibenzothiophene) over a NiMo/ γ -Al₂O₃ catalyst were studied. In a high-pressure study of the light gas oil, substituted alkyl-DBTs were found to be the most difficult to desulfurize and the order of reactivity was found to be DBT > 4-MDBT > 4,6-DMDBT. Steric hindrance together with electronic effects were identified as possible reasons for this behavior. The difference in reactivities of the individual compounds was found to decrease with the increasing reaction temperature. A gas chromatograph equipped with the atomic emission detector (GC-AED) was used for the analysis of the individual components of the oil.

The initial deactivation and the steady-state kinetics were studied during the HDS of thiophene at atmospheric pressure. Unpromoted Mo/ γ -Al₂O₃, CoMo/ γ -Al₂O₃, NiMo/ γ -Al₂O₃, and phosphorus modified NiMo/ γ -Al₂O₃ were used for the deactivation study, while NiMo/ γ -Al₂O₃, CoMo/ γ -Al₂O₃, and Pt/Y-zeolite (with three different pretreatments) were used for the steady-state study. Several experiments related to the deactivation of Mo/ γ -Al₂O₃ and NiMo/ γ -Al₂O₃ catalysts prepared with the chelating agent (NTA) were also performed and NTA was found to have no significant effect on the activity of the catalysts.

In the deactivation study, a fast initial decrease in the activity was observed on all the catalysts. However, nickel promoted catalysts were found to be more resistant to deactivation than unpromoted ones. The presence of phosphorus slightly increased the activity of the catalyst towards the thiophene HDS, but had no effect on the deactivation behavior. Several methods to regenerate the catalyst were investigated. During the resulfiding experiments, a difference between Mo/ γ -Al₂O₃ and NiMo/ γ -Al₂O₃ was observed. Deactivation of the Mo catalyst was more severe with increasing temperature, while for the NiMo catalyst the opposite behavior was observed. Carbon deposition on catalysts followed the similar trend: More carbon was observed on the Mo catalyst at higher temperatures, while the opposite is true for NiMo. The restoration of

the activity of NiMo was complete, while the reactivation of the Mo catalyst was only partial. The results from the reactivation experiments with pure H₂ and inert gas (helium) suggest that several mechanisms of the restoration of activity exist: Resulfiding of the desulfided active sites, hydrogenation and removal of the deposited carbonaceous species, and the desorption of the reactants and products from the active sites of the catalyst. Based on the observed results, the higher hydrogenation activity of nickel is assumed to be the reason for the behavior. Hydrogenation causes the faster removal of the deposited carbonaceous species and this leads to the conclusion that the desulfiding of the active sites and the adsorption of the reaction species is significantly less pronounced on the NiMo/ γ -Al₂O₃ catalyst.

Characterization studies show differences between standard and NTA-based catalysts. The higher amount of carbon on the NTA catalysts is attributed to the presence of the carbon-containing precursor - NTA. The changes in the surface area and the pore volume were observed only during the sulfiding process. In the case of standard catalysts the surface area and the pore volume decreased, while for the NTA-based catalysts the opposite is true. No change in the surface area and the pore volume with the increasing time on stream indicates that the deactivation is not due to structural changes of the catalyst. The amount of sulfur was found to be constant during the time on stream for all the catalysts.

In the steady-state study of the HDS of thiophene, CoMo and NiMo catalysts were found to be equally active. The activity of the Pt/Y-zeolite catalyst was found to be comparable to conventional catalysts when based on the amount of active material, but a fast deactivation was observed. The product selectivities during the HDS of thiophene were found to be the same for all standard catalysts, but slightly different for the Pt/Y-zeolite catalyst. This was attributed to a higher hydrogenation activity of the Pt/Y-zeolite catalyst.

The inhibition effect of other sulfur compounds and aromatics on the high-pressure hydrodesulfurization of dibenzothiophene (DBT), the so-called "matrix effect" was studied. Thiophene and DMDS have the same inhibiting effect on the total conversion of DBT, but differences exist in the effect on the selectivities of the products at low concentrations. The results indicate that the inhibiting effect of H₂S on the direct desulfurization route is stronger than the effect of thiophene on the hydrogenation pathway. In the study of aromatics, both toluene and naphthalene affect the total conversion of DBT. Naphthalene was found to be a much stronger inhibitor and inhibits mainly the direct desulfurization pathway, while the hydrogenation route is more affected by the presence of toluene.

LIST OF SYMBOLS AND ABBREVIATIONS

A	Chromatographic area
A (in Arrhenius equation)	Pre-exponential factor
AED	Atomic emission detector
ASA	Amorphous silica alumina
a.u.	Arbitrary unit
BET	Brunauer-Emmett-Teller
BP	Biphenyl
C	Concentration
cat	Catalyst
CHB	Cyclohexylbenzene
DBT	Dibenzothiophene
DDS	Direct desulfurization
DMDBT	Dimethyldibenzothiophene
DMDS	Dimethyldisulfide
E_A	Activation energy
EXAFS	Extended X-ray absorption fine structure
F	Molar flow rate
FID	Flame ionization detector
FTIR	Fourier Transformation Infrared Spectroscopy
GC	Gas chromatography
HDA	Hydrodearomatization
HDM	Hydrodemetalization
HDN	Hydrodenitrogenation
HDO	Hydrodeoxygenation
HDS	Hydrodesulfurization
HHDBT	Hexahydrodibenzothiophene
HMS	Hexagonal mesoporous silica
HYD	Hydrogenation
i.d.	Inner diameter
k	Reaction rate constant
LCO	Light cycle oil
LGO	Light gas oil
LHHW	Langmuir-Hinshelwood-Houden-Watson
LHSV	Liquid hourly space velocity
MDBT	Methyldibenzothiophene

MFC	Mass flow controller
N.A.	Not available
N.D.	Not determined
NTA	Nitilotriacetic acid
o.r.	Order of reactivity
QEXAFS	Quick-scanning Extended X-ray absorption fine structure
r	Reaction rate
R	Universal gas constant
r.a.	Relative activity
RF	Response factor
RT	Retention time
STM	Scanning tunneling microscopy
T	Temperature
THDBT	Tetrahydrodibenzothiophene
TOS	Time on stream
uid.	Unidentified
USY	Ultra stable Y-zeolite
W	Weight of the catalyst
wt%	Weight percent
wtpm	Weight parts-per-million
X	Conversion
XPS	X-ray photoelectron spectroscopy
γ (in equations)	Reaction order with respect to inhibitor
θ (Hg intrusion)	Contact angle of Hg on the surface of a solid sample

LIST OF PUBLICATIONS AND PRESENTATIONS**LIST OF PUBLICATIONS***Paper I*

T. Mejdell, R. Myrstad, J. Morud, J. S. Rosvoll, P. Steiner and E. A. Blekkan: "A new kinetic model for hydrodesulfurization of oil products", in "**Studies in Surface Science and Catalysis**" (G. F. Froment and K. C. Waugh, eds.), Vol. 133, Elsevier Science B. V., 2001.

Paper II

Petr Steiner and Edd A. Blekkan: "Catalytic hydrodesulfurization of a light gas oil over a NiMo catalyst: Kinetics of selected sulfur components", *Fuel Processing Technology* **79(1)** (2002) 1.

Paper III

P. Steiner, B. M. Vogelaar, A. D. van Langeveld, S. Eijsbouts, J. A. Moulijn and E. A. Blekkan: "Deactivation of hydrotreating catalysts: Thiophene HDS and characterization of spent catalysts", *manuscript in preparation*.

Paper IV

B. M. Vogelaar, P. Steiner, A. D. van Langeveld, S. Eijsbouts and J. A. Moulijn: "Deactivation of Mo/Al₂O₃ and NiMo/Al₂O₃ catalysts during hydrodesulfurization of thiophene", *manuscript in preparation*.

Paper V

P. Steiner, A. Virnovskaia, E. A. Blekkan: "Inhibiting effect of sulfur compounds and aromatics on the hydrodesulfurization of dibenzothiophene over NiMo catalyst", *manuscript in preparation*.

LIST OF PRESENTATIONS

1. P. Steiner and E. A. Blekkan: "Deep catalytic hydrodesulfurization of light gas oil studied by GC/AED", TMR Summer School on Surface Science: Understanding Catalysis, 28 August - 3 September 1999, Dronten, The Netherlands
2. P. Steiner, R. Myrstad, B. Thorvaldsen, E. A. Blekkan: "Hydrodesulfurization of light gas oil - detailed product analysis", 12th International Congress on Catalysis, 9-14 July 2000, Granada, Spain
3. P. Steiner, E. A. Blekkan: "Catalytic hydrodesulfurization of light gas oil: Detailed product analysis and kinetics", 14th International Congress of Chemical and Process Engineering (CHISA 2000), 27-31 August 2000, Prague, The Czech Republic
4. T. Mejdell, R. Myrstad, J. Morud, J. S. Rosvoll, P. Steiner and E. A. Blekkan: "A new kinetic model for hydrodesulfurization of oil products", Reaction Kinetics and the Development and Operation of Catalytic Processes, 22-25 April 2001, Oostende, Belgium
5. P. Steiner, B. M. Vogelaar, A. D. van Langeveld, S. Eijsbouts, J. A. Moulijn, E. A. Blekkan: "The deactivation of hydrotreating catalysts during thiophene HDS", Nordic Catalysis Symposium, 27-28 November 2001, Trondheim, Norway
6. P. Steiner, B. M. Vogelaar, A. D. van Langeveld, S. Eijsbouts, J. A. Moulijn: "Deactivation of hydrotreating catalysts: Thiophene HDS and a characterization of spent catalysts", 223rd American Chemical Society National Meeting, 7-11 April 2002, Orlando, FL, USA
7. B. M. Vogelaar, P. Steiner, A. D. van Langeveld, S. Eijsbouts, J. A. Moulijn: "Activity and deactivation of HDS catalysts: Studying the active phase using CO as a probe molecule", 223rd American Chemical Society National Meeting, 7-11 April 2002, Orlando, FL, USA

8. P. Steiner, R. Myrstad, B. Thorvaldsen, E. A. Blekkan: “Hydrodesulfurization of light gas oil - detailed product analysis”, Colloquium in Chemical Reaction Engineering (CCRE 17) and Chemical Engineering in the Applications of Catalysis (CEAC), 12-14 June 2002, Trondheim, Norway

9. B. M. Vogelaar, P. Steiner, A. D. van Langeveld, S. Eijsbouts, J. A. Moulijn: “Activity and deactivation of HDS catalysts: Studying the active phase using CO as a probe molecule”, 4th International Tokyo Conference on Advanced Catalytic Science and Technology, 14-19 July 2002, Tokyo, Japan

10. A. D. van Langeveld, B. M. Vogelaar, P. Steiner, S. Eijsbouts, J. A. Moulijn: “Activity and deactivation of HDS catalysts: Studying the active phase using CO as a probe molecule”, 17th International Symposium on Chemical Reaction Engineering, 25-28 August 2002, Hong Kong, China

11. P. Steiner, B. M. Vogelaar, A. D. van Langeveld, S. Eijsbouts, J. A. Moulijn, E. A. Blekkan: “Deactivation of hydrotreating catalysts: Thiophene HDS and characterization of spent catalysts”, 15th International Congress of Chemical and Process Engineering (CHISA 2002), 25-29 August 2002, Prague, The Czech Republic

AUTHOR'S CONTRIBUTION

The author had an active role in all stages of the work reported in this thesis. The author was involved in planning and performance of all the experimental work. However, ing. Bas M. Vogelaar performed Raman Spectroscopy analysis and a service organization did the analysis of carbon and sulfur and determined the surface area and pore volume in the part of the work dealing with the deactivation studies. The author wrote Paper II, III, and V and was involved in writing Paper I and IV.

TABLE OF CONTENTS

ACKNOWLEDGEMENT	i
ABSTRACT	iv
LIST OF SYMBOLS AND ABBREVIATIONS	vi
LIST OF PUBLICATIONS AND PRESENTATIONS	viii
LIST OF PUBLICATIONS	viii
LIST OF PRESENTATIONS	ix
AUTHOR'S CONTRIBUTION	xi
TABLE OF CONTENTS	xii
1. INTRODUCTION	1
1.1 Hydrotreating processes	2
1.2 Hydrodesulfurization	4
1.3 Hydrodesulfurization catalysts - conventional and new types	5
<i>1.3.1 Conventional molybdenum-based catalysts</i>	<i>6</i>
<i>1.3.1.1 Unsupported and unpromoted molybdenum sulfide</i>	<i>6</i>
<i>1.3.1.2 Effect of support and promoters</i>	<i>7</i>
<i>1.3.1.3 Effect of preparation and pretreatment</i>	<i>13</i>
<i>1.3.1.4 Current hydrodesulfurization catalysts - properties and activity ..</i>	<i>16</i>
<i>1.3.2 New types of catalysts for hydrodesulfurization</i>	<i>18</i>
1.4 Reaction mechanism and kinetics	24
1.5 The inhibiting effect of other components of the oil ("matrix effect")	29
1.6 Deactivation of hydrotreating catalysts	32
1.7 Scope of the work	34
2. THEORY	36
2.1 Kinetic calculations for HDS of thiophene and DBT	36
2.2 Kinetic calculations for the inhibiting effect	38
2.3 Response factors during GC analyses	39
3. EXPERIMENTAL METHODS	40
3.1 High-pressure HDS of light gas oil	40
<i>3.1.1 Materials</i>	<i>40</i>
<i>3.1.2 Apparatus</i>	<i>40</i>
<i>3.1.3 Procedures</i>	<i>40</i>
<i>3.1.4 Analysis</i>	<i>41</i>
<i>3.1.4.1 Principle of GC-AED</i>	<i>42</i>
3.2 Deactivation studies during thiophene HDS at atmospheric pressure	44
<i>3.2.1 Materials</i>	<i>44</i>
<i>3.2.2 Apparatus</i>	<i>44</i>

3.2.3	<i>Procedures</i>	46
3.2.4	<i>Analysis and characterization</i>	47
3.3	Kinetics of thiophene hydrodesulfurization at atmospheric pressure	48
3.3.1	<i>Materials</i>	48
3.3.2	<i>Apparatus</i>	48
3.3.3	<i>Procedures</i>	50
3.3.4	<i>Analysis</i>	51
3.4	High-pressure studies of dibenzothiophene HDS and the “matrix effect”	52
3.4.1	<i>Materials</i>	52
3.4.2	<i>Apparatus</i>	52
3.4.3	<i>Procedures</i>	54
3.4.4	<i>Analysis</i>	56
4.	RESULTS	57
4.1	High-pressure HDS of light gas oil	57
4.1.1	<i>Use of GC-AED for analysis of light gas oil</i>	57
4.1.2	<i>Hydrodesulfurization activity of NiMo/γ-Al₂O₃</i>	59
4.1.3	<i>Kinetic studies</i>	61
4.2	Deactivation studies during thiophene HDS at atmospheric pressure	66
4.2.1	<i>Initial deactivation behavior</i>	66
4.2.2	<i>Reactivation experiments</i>	69
4.2.3	<i>Diluted flow of H₂ with inert (He)</i>	71
4.2.4	<i>Hydrodesulfurization of thiophene: Reaction products selectivity</i>	73
4.2.5	<i>Characterization of spent catalysts</i>	75
4.2.5.1	<i>Carbon and sulfur analysis</i>	75
4.2.5.2	<i>BET and Hg intrusion results</i>	80
4.2.5.3	<i>IR and Raman spectroscopy analysis</i>	82
4.3	Steady state kinetics of thiophene HDS at atmospheric pressure	84
4.3.1	<i>Kinetic behavior</i>	84
4.3.2	<i>Selectivity of reaction products of thiophene hydrodesulfurization</i>	87
4.4	High-pressure steady-state kinetics of DBT HDS and study of “matrix effect”	88
4.4.1	<i>DBT in n-heptane</i>	88
4.4.2	<i>Inhibition effect of sulfur compounds on the hydrodesulfurization of DBT</i>	90
4.4.3	<i>Inhibition effect of aromatics on the hydrodesulfurization of DBT</i>	91
4.4.4	<i>Selectivity of reaction products of hydrodesulfurization of DBT</i>	92
5.	DISCUSSION	95
5.1	High-pressure HDS of light gas oil from the Statoil Mongstad refinery	95
5.2	Hydrodesulfurization of thiophene at atmospheric pressure	99
5.2.1	<i>Catalyst deactivation during thiophene HDS</i>	99
5.2.1.1	<i>Initial deactivation behavior</i>	99
5.2.1.2	<i>Reactivation experiments</i>	103
5.2.1.3	<i>Diluted flow of H₂ with inert (He)</i>	105

5.2.1.4	<i>Surface area and porosity of studied catalysts</i>	106
5.2.2	<i>Steady state kinetics of thiophene HDS at atmospheric pressure</i>	106
5.2.2.1	<i>Commercial molybdenum based catalysts</i>	107
5.2.2.2	<i>Non-conventional catalyst - Pt/Y-zeolite</i>	107
5.2.2.3	<i>Selectivity of reaction products of thiophene HDS</i>	110
5.3	High-pressure steady-state kinetics of DBT HDS and study of “matrix effect”	114
5.3.1	<i>DBT in n-heptane</i>	114
5.3.2	<i>Effect of sulfur compounds on hydrodesulfurization of DBT</i>	116
5.3.3	<i>Effect of aromatics on hydrodesulfurization of DBT</i>	117
6.	CONCLUSIONS	119
7.	REFERENCES	123
	LIST OF APPENDICES	A0

1. INTRODUCTION

Oil refining as an industry developed during the 20th century to become an important part of modern life. One of the main objectives of processing is to reduce the very high carbon/hydrogen ratio of heavy oil. Nowadays, there is a lot of oil fields in the world and each of them produces crude oil of different quality based on many different characteristics and presence of impurities. The crude oils from different fields are often mixed together during the processing to obtain the final refined product of desired quality. In general, the products obtained from the crude oil can be divided into 7 groups:

- 1) Volatile products (propane and butane LPG, light naphtha)
- 2) Light distillates (gasolines, heavy naphtha, kerosene and jet fuels)
- 3) Middle distillates (automotive diesel, heating oils, gas oils)
- 4) Fuels oils (marine diesel, bunker fuels)
- 5) Lubricating oils (motor, spindle, machine oils)
- 6) Waxes (food and paper coating grade, pharmaceutical grade)
- 7) Bitumen (asphalt, coke)

Products in these groups are produced from distillation processes and treated to meet certain specifications. These specifications are the result of a compromise between desired performance characteristics in the product and the ability to make such product from the available crude oil and the processing facilities at hand. Wide variations in these specifications exist between different continents and even between countries.

Crude oil is a mixture of literally hundreds of hydrocarbon compounds ranging in size from the smallest, methane, with only one carbon atom, to large compounds containing 200 or more. Because of the large quantity of these compounds which exist in crude oil, only the simplest can be isolated to some degree of purity on a commercial scale. Generally, in refining projects, isolation of comparatively pure products are restricted to those compounds lighter than C₇s.

Not all compounds contained in the crude oil are pure hydrocarbons. The crude oil also contains certain inorganic impurities such as sulfur, nitrogen, oxygen, and metals. By far the most common of these impurities are the organic sulfur compounds called mercaptanes. The sulfur compounds with more complicated structure also exist such as disulfides, thiophenes,

benzothiophenes, and their substituted analogues. The sulfur compounds are very similar in their characteristics (e.g. vapor pressures) to hydrocarbons and this is why they cannot be isolated by distillation process on a commercial scale. The metals contained in the crude oil are mainly nickel, sodium, iron, and vanadium. Because of their low volatility they are found in the heavier products of crude oil. They only become a concern in certain cases when they can affect further processing of the oil. Also organic chloride compounds are not usually removed from crude oil as a product, but the corrosive effect of these compounds on parts of refinery plants is always a source of concern.

The last troublesome group of organic compounds are unsaturated hydrocarbons. Unsaturated aliphatic compounds, which are usually not present in the original crude oil, but are often formed during the refining processes, are unstable and readily combine with themselves or other similar compounds to form polymers. The polymers then can become a precursor to a coke formation and cause the catalyst deactivation. Another group of unsaturated hydrocarbons, aromatics, are usually very stable and they are a source of concern mainly because of their environmental and health effects.

1.1 Hydrotreating processes

Oil refining is a very complex procedure and there are many individual processes for the obtaining of desired products, which are mentioned earlier. Catalytic reforming, hydrotreating, fluid catalytic cracking, hydrocracking, and thermal cracking are the most important chemical processes.

Hydrotreating is a group of very important processes and it has been studied extensively for many decades. The hydrotreating process saturates unsaturated hydrocarbons and removes a significant amount of the impurities present in the raw distillate streams by reaction with H_2 . Hydrotreating is today used extensively for improving the quality of final products and the related hydrocracking process is used for conversion of heavy feedstocks. The former process usually implies only small changes in overall molecular structure, while a significant change in a molecular weight occurs during the latter one. Hydrotreating also plays an essential role in pretreating streams for other refinery processes. More severe environmental legislation with respect to harmful emissions [1] has triggered an increased interest in both basic and applied research within hydrotreating catalysis. Although there are significant variations from region to

region, it is clear that the environmental regulations will pose a major driving force for introducing more hydrotreating capacity in refineries. Deep desulfurization and aromatics reduction become increasingly important in order to provide environmentally more acceptable reformulated fuels. As a result of this increased role of hydrotreating, a majority of all refinery streams undergo hydrotreating today. These new challenges have a very strong impact on the current refining facilities and will continue to have the effect in the near future, e.g. as shown in an article dealing with the influence of sulfur limitations by Swaty *et al.* [2].

As was mentioned earlier, the impurities removed during hydroprocessing are mainly metals and compounds containing sulfur, nitrogen, and oxygen. The sulfur is the most common, but at the same time the least tolerable of these impurities. However, because of the steep increase in the consumption of the refined products from crude oil, crude oils of lower quality have to be processed and that requires, in addition to hydrodesulfurization (HDS), conversion of large molecules to smaller ones, the removal of metals (hydrodemetalization, HDM), nitrogen (hydrodenitrogenation, HDN), and in some cases also oxygen (hydrodeoxygenation, HDO). Another possible way to obtain hydrotreated products of desired quality could be a hydrotreating of blends of several distillate fractions. A study of the effects of catalytic hydrotreating on diesel quality by using feedstocks prepared with different oil blends was done by Ancheyta-Juárez and coworkers [3, 4]. Their results show that diesel specifications in sulfur content and cetane number could be reached through single stage hydrotreating of these blends at moderate hydrotreating operating conditions. The deeper understanding of the hydrotreating and need for products of better quality also led to the development of the processing of crude oils using two reaction stages, as is presented by Ancheyta *et al.* [5] or Reinhoudt *et al.* [6]. Ancheyta [5] shows that crude oil quality can be substantially improved by hydroprocessing in two stages with different catalyst in each: The result of the first stage reaction was removal of metals, while hydrodesulfurization was a main reaction in the second stage. Different behavior in heteroatoms removals, hydrocracking, and pore size distribution of catalysts after reaction were thus observed in each reaction stage. The similar idea, but only for hydrodesulfurization, was presented in [6], where the application of a separate deep HDS reactor following the conventional HDS process, in which a tailor-made catalyst for the effective removal of the remaining (refractory) sulfur compounds could be applied, is suggested. Sie [7] suggests the same division to two stages based on his kinetic studies.

The term “hydrotreating” is very often used as a synonym for hydrodesulfurization, because the removal of sulfur remains to be the main goal of the hydrotreating process. An example could

be the hydrotreating (desulfurization) of naphtha and diesel. There is a small difference in the flow of H₂ between these two processes, because naphtha hydrotreating uses once-through H₂ and diesel hydrotreating uses recycle of H₂, but both processes are aimed mainly at converting organic sulfur compounds to H₂S, which is then removed as a gas. From all the information given above one can see that hydrodesulfurization has been the most important part of the hydrotreating process during its history and will be thus introduced individually in the following chapters.

1.2 Hydrodesulfurization

In the refinery, sulfur in the form of organic compounds is removed from the distillate streams by a process called hydrodesulfurization (HDS), where compounds containing sulfur undergo reaction with hydrogen and form the corresponding hydrocarbon and hydrogen sulfide. H₂S is then removed as a gas. The reaction of aliphatic compounds is schematically shown in Equation (1-1), where *R* stands for alkyl.



A similar reaction applies to aromatic and polyaromatic sulfur compounds, where a desulfurized hydrocarbon and H₂S again are the final products. However, the mechanism of the reaction of sulfur compounds containing aromatic ring(s) is not as simple as presented in Equation (1-1), but can proceed through several reaction pathways, as is schematically shown for thiophene in Figure 1-1.

More details will be presented in chapter 1.4 about the mechanism and kinetics of individual compounds. There it will be shown that a similar reaction network exists for all polyaromatic sulfur compounds.

Hydrodesulfurization is a heterogeneously catalyzed reaction. Supported metal sulfides have been found to be the best catalysts for the HDS reaction. Both molybdenum and tungsten sulfides are active catalysts in the hydrodesulfurization reaction. Nowadays however, mainly molybdenum based catalysts are used worldwide in the processes connected with sulfur removal. Different promoters have been tested and nickel and cobalt were found to give the highest enhancement of the activity towards desired products. Alumina support has a very important role in the activity and stability of the hydrodesulfurization catalyst as well and the γ -phase is the most suitable for the operation.

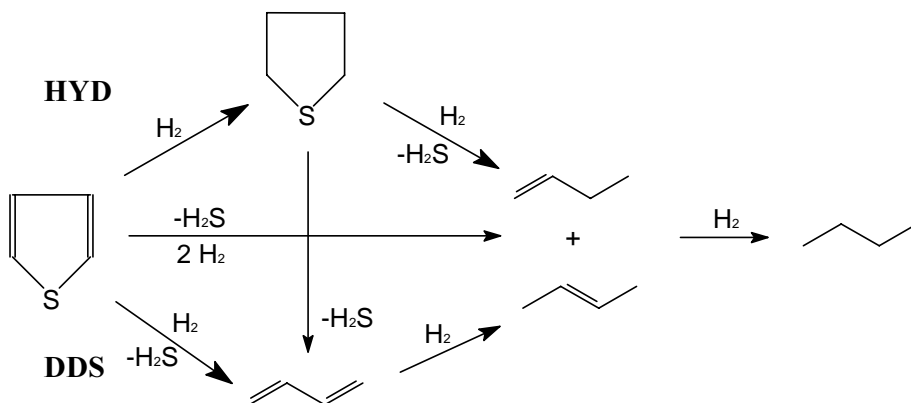


Figure 1-1 Reaction scheme for thiophene hydrodesulfurization (adapted from [8]).

1.3 Hydrodesulfurization catalysts - conventional and new types

The catalyst selection for certain process is based on studies of activity, selectivity and lifetime. This is usually a very long and difficult task. And then, once the suitable catalyst giving the desired product quality at a reasonable costs is found, the search for a better catalyst starts immediately. In hydroprocessing, the selection of a catalyst depends mainly on the required conversion and characteristics of the processed feedstock. As was mentioned before, the characteristics of feed vary quite a lot and the amount of impurities and the physical properties thus determine the choice of the catalyst. This suggests that a universal catalyst or a catalytic system suitable for hydroprocessing of the feeds from different crudes does not exist. With respect to the chemical and physical properties, a wide range of hydroprocessing catalysts have been developed for commercial applications. The focus in the following chapters will be given to hydrodesulfurization catalysts. In chapter 1.3.1 the conventional molybdenum based catalysts will be reviewed, namely cobalt-molybdenum (CoMo) and nickel-molybdenum (NiMo) supported on $\gamma\text{-Al}_2\text{O}_3$. The results of the search for new and more active catalysts will then be summarized in chapter 1.3.2.

1.3.1 Conventional molybdenum-based catalysts

There is a very few processes working with virtually the same catalyst for many decades and hydrodesulfurization belongs to them. The conventional sulfidic form of molybdenum-based catalysts supported on $\gamma\text{-Al}_2\text{O}_3$ have been used for a quite long time now (see e.g. [9], [10] and references therein). These typical hydrodesulfurization catalysts and the effects of support and promoters as well as preparation methods will be reviewed in this chapter.

As was mentioned before, the typical hydrodesulfurization catalysts contain nickel or cobalt as a promoter and are $\gamma\text{-Al}_2\text{O}_3$ supported. However, unsupported catalysts were found to be active in HDS as well and that is why the next chapter will be dedicated to MoS_2 .

1.3.1.1 Unsupported and unpromoted molybdenum sulfide

Unsupported molybdenum sulfide catalysts have often been used as model catalysts for hydrotreating reactions. Based on their nature, these catalysts are used in slurry processes which can accommodate heavy feedstocks with residual matters. However, the primary function required for the catalysts in slurry processes is not hydrodesulfurization but hydrogenation (HYD), because the major role of the catalyst is to quench thermally produced radicals by supplying active hydrogen species. So the catalyst's HDS activity was not studied very thoroughly. Nevertheless, several studies have been done on the effect of preparation of these catalysts on their catalytic activity. Daage and Chianelli [11] present the "rim-edge" model for the $\text{Mo}/\text{Al}_2\text{O}_3$ catalyst and report that a difference exists between the rim and edge active sites during the HDS of dibenzothiophene (DBT). Sulfur hydrogenolysis was obtained on both rim and edge sites, while the hydrogenation of DBT occurred exclusively on the rim sites. Alonso *et al.* [12] and Busetto *et al.* [13] investigated the effect of preparation on the catalyst activity towards HDS of DBT and thiophene, respectively. Alonso found that higher surface area and improved catalytic performance can be achieved when the right preparation method is used. A similar result was found by Del Valle *et al.* [14]. However, their preparation method increased the surface area, but decreased the activity of the catalyst towards DBT HDS. They mention that the high catalytic activity of the edge and rim sites in the hydrodesulfurization reaction is probably not the only factor affecting the activity towards HDS reaction. The same result with regard to the activity of rim and edge sites was reported by Iwata *et al.* [15], who studied the effect of preparation of

unsupported molybdenum sulfide on the activity towards the model test reactions, namely HYD of 1-methylnaphthalene and HDS of DBT. They found a strong effect of the crystal structure on the activity of the catalyst. The poorly crystallized structure provided a larger number of catalytically active sites than the well-crystallized structure. The presence of more edges and bent basal planes was identified as the reason for observed behavior. A similar effect of the catalyst structure was found also in [16], again by Iwata *et al.*, where a study of the catalytic activity of unsupported MoS₂ shows that the catalyst is actually active in the primary upgrading of heavy oils. Its activity towards hydrogenation of aromatic rings was associated with the inflection on the basal plane that correspond to the rim sites of crystalline MoS₂ microdomains.

This chapter shows that an unpromoted MoS₂ catalyst is active in HDS as well, but at much lower degree when compared to supported and promoted catalysts. The effects of support and promoters on the activity of HDS catalysts will be presented next.

1.3.1.2 Effect of support and promoters

Many different supports have been tested and many combinations are presently being investigated (see chapter 1.3.2), but the typical support for commercial hydrotreating catalysts continues to be γ -Al₂O₃.

Alumina was found to be effective as a support for hydrotreating catalyst already in the beginning of the industrial application of the process. Alumina as a good choice with respect to the activity enhancement is mentioned in several reviews (e.g. Schuit and Gates [17], Ratnasamy and Sivasanker [18], Grange [19], and references therein). Among the many Al₂O₃ phases, the γ -phase was found to be the most active one, as was reported by Ledoux *et al.* [20]. Ledoux studied the role of the crystallinity of the alumina support on the HDS activity of CoMo catalysts. The effect of support is clearly not only to anchor active metals of the catalyst, but also enhance its catalytical properties. The very important role of the support in modification of acid properties of the sulfide phase of the catalyst was recently reported by Maugé *et al.* [21], who used FTIR to study the surface properties. They show that the unsupported molybdenum sulfide catalyst has weaker acidic properties as well as a higher metallic character of the Mo sites as compared with those of MoS₂ supported on alumina. Again, not only the presence of support, but also its properties have a strong influence on the catalytic activity. Similar results to those of Ledoux *et al.* [20] were reported by Sakashita *et al.* [22], who also claims that the surface orientation of

alumina supports affects the catalytic functionality, such as activity towards HYD and HDS. This was evaluated by using a model compound reaction and showed quite a large dependence of the catalytic activity and selectivity on the microstructures of MoS₂ clusters. These were affected by the surface orientation of γ -Al₂O₃. It is clearly visible that the catalysts activity towards hydrodesulfurization is significantly improved by supporting the active metals on γ -Al₂O₃.

The effect of promoters on catalytic activity of alumina-supported molybdenum sulfide has been studied thoroughly for many decades. In the hydrotreating reactions, the function of the promoter is to enhance the catalyst activity in the sense of increasing the conversion and improving reactivities of the components which are difficult to remove. The best promoters for hydrotreating reactions, especially for hydrodesulfurization, were found to be nickel and cobalt (Topsøe *et al.* [8]). Tungsten instead of molybdenum supported on alumina was also found to be active in hydrotreating (Topsøe *et al.* [8], Voorhoeve and Stuiver [23]), but the properties of molybdenum based catalysts were found to be more suitable for hydrodesulfurization reactions. In the literature, the majority of studies is dedicated to the CoMo system and the mechanism of promoting effects of other metals is always described on the basis of information obtained from the CoMo system.

During the years of development of better and better characterization techniques, the idea behind the promoting mechanism of cobalt has undergone a certain development. In the 70's, Schuit and coworkers [17, 24-27] presented the first detailed model of the structure of CoMo/Al₂O₃ catalysts, the so-called monolayer model. In this model, the outer alumina layer was called "surface layer", the adjacent Mo layer was termed the "monolayer", and the top layer consisting of only anions was the "capping layer". In the calcined state, the molybdenum species were assumed to be bonded to the surface of the alumina forming mentioned monolayer. Interaction of the molybdenum with the alumina was believed to occur via oxygen bridges resulting from reaction with surface OH groups. Cobalt (present as Co²⁺) was assumed to be in tetrahedral positions in the surface of the alumina, replacing Al³⁺ ions. The promotional effect of cobalt was suggested to result from an increase in the stability of the Mo monolayer caused by the presence of replaced aluminium cations in the surface layer adjacent to the monolayer. Mo³⁺ ions, produced in the presence of hydrogen from Mo⁶⁺ ions by removal of some of the S²⁻ ions from the capping layer, were believed to be the catalytically active sites.

At approximately the same time, another model was presented by Voorhoeve and Stuver [23, 28]. In the intercalation model they assumed that the sulfided catalyst contains MoS_2 (WS_2) slabs on the surface of the alumina. Each slab consists of Mo atoms sandwiched between two hexagonal, close-packed planes of sulfur atoms. The Co(Ni) atoms are then believed to occupy octahedral intercalation positions in the van der Waal's gap between the slabs. Active sites were assumed to be sulfur-deficient metal sites, or anion vacancies, the activity of which does not depend on the coverage of the surface with sulfur. The promotion effect was related to an increase in the concentration of Mo^{3+} (or W^{3+}) ions caused by the presence of the promoter atoms ($\text{Co}^0 + 2\text{Mo}^{4+} = 2\text{Mo}^{3+} + \text{Co}^{2+}$). Later on, based on calculations, the "pseudo-intercalation" model was presented, which restricted intercalation of Co(Ni) atoms to the edge surfaces of the lattice of MoS_2 (Topsøe *et al.* [8] and references therein, Huisman *et al.* [29]). Both monolayer and intercalation system seem to be present on the catalyst simultaneously and operate in combination, each of them facilitating different reaction pathways of the hydrodesulfurization reaction (Schuit and Gates [17]).

Another model based on Mo being present as MoS_2 is the contact synergy model of Delmon and coworkers ([30, 31], Grange [19]; also Topsøe *et al.* [8] and references therein). The promoting effect of Co is here attributed to a contact between the Co_9S_8 and MoS_2 phases, which results in spill-over of hydrogen from Co_9S_8 to MoS_2 , thereby enhancing the intrinsic activity of MoS_2 .

The development of new characterization methods, like *in situ* Mössbauer spectroscopy, extended X-ray absorption fine structure (EXAFS) spectroscopy, and infrared spectroscopy, enabled Topsøe and coworkers [32-40] to provide the most detailed structural description of CoMo catalysts and a new explanation of the promoting effect, widely accepted today. The Co-Mo-S phase was shown to be MoS_2 -like structures with the promoter atoms located at the edges in five-fold coordinated sites (tetragonal pyramidal-like geometry). The Co-Mo-S structure was studied mainly on supported catalysts, but the work of Candia *et al.* [41] shows that it is possible to find the same structure on unpromoted catalysts as well.

The early investigations on Co-Mo-S showed that the Co promoter atoms are accessible at the surface of the molybdenum phase, which is present as two-dimensional MoS_2 structures on the alumina surface (Topsøe *et al.* [8] and references therein). Based on these results, Ratnasamy and Sivasanker [18] proposed that Co may be located at the edges of the MoS_2 crystallites (Co is not

intercalated between the MoS₂ slabs). They also claimed that a maximum of one Co ion can be incorporated per two Mo ions in this manner. By this process, cobalt lends structural stability to the MoS₂ crystallites and suppresses the excessive formation of anion vacancies (usually present in the unpromoted Mo/Al₂O₃ catalysts) at crystallite edges. In the case of unpromoted catalysts, highly acidic anion vacancies on the edges lower the structural stability of MoS₂ crystallites and are also much faster deactivated in the presence of unsaturated molecules. This is the reason why the promoted catalysts perform much better in a steady-state operation, when compared to unpromoted ones [42]. While this seems to be a widely accepted mechanism of the promoting effect of cobalt, it is possible to find conflicting ideas, as is the case of work done by Chiplunker *et al.* [43], who claims that the promoting effect of cobalt can be attributed to the creation of anion vacancies through substitution of Mo⁴⁺ by Co²⁺ ions. While the fact that the active sites are located on the edges and/or rims of the catalyst surface is generally believed to be true, the pinning up of anion vacancies as the active sites is a controversial issue. Not only Chiplunker [43], but also review by Startsev [44] points out that the anion vacancies are considered to play a role of catalytically active centers. Grimblot [45] in his review on Co(Ni)-MoS₂ supported catalysts asked: “Does the promoter enhance the catalytic activity, probably by electron transfer, of the Mo edge site or does it provide new sites?”. The EXAFS study done by Leliveld *et al.* [46] actually shows that both concepts might be true and the structural model presented by Topsøe might have to be extended. Leliveld proposes a structural model that involves two types of active sites for HDS on the sulfided Co-promoted molybdenum catalyst. The first type consists of a sulfur vacancy that is only associated with the promoter atoms, which is created at low temperatures. At higher temperatures, the second type of site is produced by removal of sulfur atoms that are bonded to both Co and Mo atoms.

The Co-Mo-S structure is not a single, bulk phase with a fixed overall Co:Mo:S stoichiometry. Rather, it should be seen as a family of structures with a wide range of Co concentrations, ranging from pure MoS₂ up to essentially full coverage of the MoS₂ edges by Co. STM images presented by Lauritsen *et al.* [47] clearly show changes to the MoS₂ structure when promoted by cobalt (Figure 1-2). The Co atoms in Co-Mo-S structure may not all have identical properties due to different edge-site geometries [48], Co-Co interactions [33, 34], and changes in sulfur coordination (Topsøe *et al.* [49]). It was also observed by means of Mössbauer emission spectroscopy that an interaction between Co and neighboring Mo atoms exists in the Co-Mo-S structure (Topsøe *et al.* [50]). Both single and multiple slab Co-Mo-S structures (Type-I [33] and

Type-II [38] Co-Mo-S) have been observed depending on preparation and activation parameters, presence of additives, type of support, metal loading, etc. For alumina-supported catalysts, the single slab structures interact strongly with the support, probably via Mo-O-Al linkages located at the edges. For the multiple slab form, these interactions are small [51].

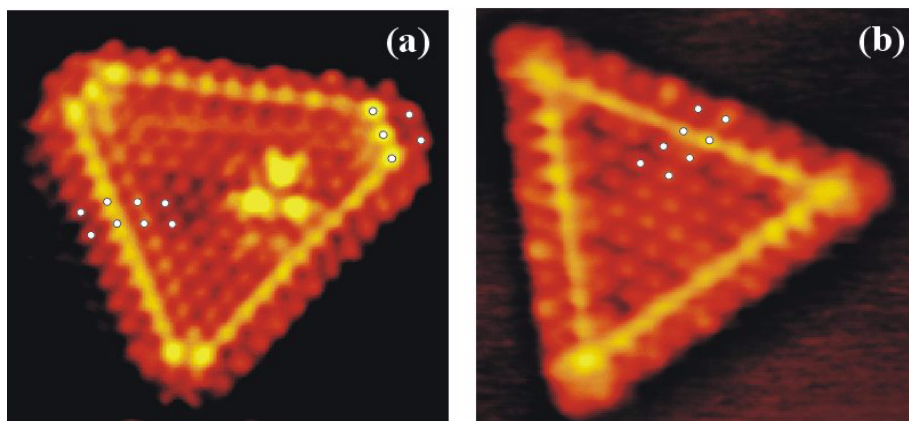


Figure 1-2 (a) STM image of a single-layer Co-Mo-S nanocluster. (b) Triangular single-layer MoS₂ nanocluster (adapted from Lauritsen *et al.* [47]).

The combined results from activity, Mössbauer, and IR spectroscopy studies have shown that most of the catalytic activity is linked to the presence of the promoter atoms in Co-Mo-S. The *in situ* studies showed that phases other than Co-Mo-S may be present in typical alumina-supported CoMo catalysts (Figure 1-3). Thus the presence of promoter atoms in such phases has to be taken into account for the explanation of the activity behavior of Co-Mo-S model.

The mechanism of HDS and promoting effect of cobalt was also investigated using ³⁵S radioisotope pulse tracer method (Gachet *et al.* [52], Kabe and coworkers [53, 54], Kogan *et al.* [55]). Gachet observed three types of sulfur and reports that only one type, so-called labile sulfur, participates in the reaction [52]. Kabe observed an increase in the amount of labile sulfur with the addition of cobalt, suggesting that Co makes sulfur more mobile and thus creating more active sites. The promotion effect of Co was also attributed to the decrease in the strength of sulfur-molybdenum bond in its presence and thus facilitating the subsequent desorption of H₂S from active sites [53, 54]. The labile sulfur was found to be involved mainly in direct desulfurization route of DBT [56]. The similar study with ³⁵S-labeled DBT on the Ni promoted catalyst was done

by Qian *et al.* [57] and conclusions about the promotion effect were the same as in the case of cobalt.

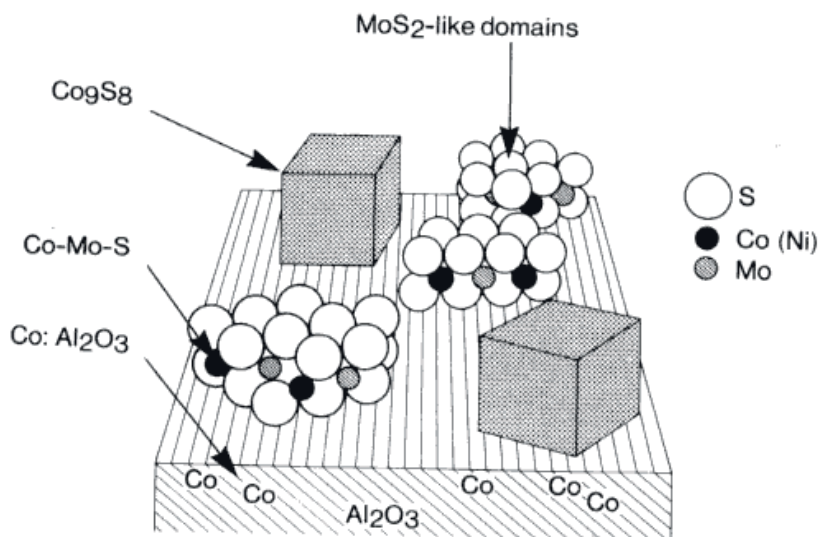


Figure 1-3 Schematic representation of the different phases present in typical alumina-supported catalyst (adapted from [38]).

Several other models emerged in the last years (Topsøe *et al.* [8] and references therein). These models are results of the studies on the electronic effects, hydrogen spill-over, conductivity measurements, and other methods. The models are usually just a modification of the widely accepted mechanisms and since it is not essential to know the details for the purpose of this work, these models will not be reviewed here.

Since the CoMo catalyst was the one used in the majority of hydrodesulfurization processes, a large amount of data was obtained on the Co-Mo-S structure. However, nickel promoted catalysts have been recently rediscovered as an interesting choice with regard to deep hydrodesulfurization. Already after a few basic studies, the similarity between NiMo and CoMo catalysts was observed. Thanks to a large amount of data on the Co-Mo-S structure, not so thorough studies from scratch were necessary on the NiMo catalyst and an analogous promoting effect of Ni atoms and the Ni-Mo-S structure closely similar to Co-Mo-S was reported by Topsøe and coworkers [37, 49, 50]. However, small differences in the structure still exist, as is presented by Canosa Rodrigo *et al.*

[58]. They report the results of the characterization of NiMo/ γ -Al₂O₃ by the means of Raman spectroscopy, XPS, and other methods. In their model, Ni²⁺ ions are present mainly in the topmost atomic layer, but their concentration can be reduced with increasing calcination temperature by the diffusion into the support matrix. In contrast to CoMo/ γ -Al₂O₃, Ni²⁺ is not specifically concentrated between the molybdate layer and the support surface. There is evidence in the literature suggesting that a difference between the promoting effects of Co and Ni exist, but the structural models are believed to be very similar. The similarity between the structure of cobalt and nickel promoted catalysts was also found in the work of Crajé *et al.* [59]. Their work raises some questions about the Co-Mo-S model and they notice that the results from characterization studies are of limited value if the exact experimental details are not provided to allow repetition of the work. The study by Nielsen *et al.* [60] on the nature of the active phase on NiMo catalyst shows a high activity of Ni edge sites. Thus the general concept of the active sites located on the edges and/or rims is the same for Co and Ni promoted catalysts. A study done by Kushmerick and Weiss [61] on Ni/unsupported-MoS₂ by the means of STM suggests another two additional effects of the metal promoters on MoS₂: They bind reactants to unreactive portions of the catalytic surface and transport reactants to active sites on the anisotropic catalytic surface. However, differences were also observed, as can be demonstrated by the work of Breysse *et al.* [62], who report a strong promoting effect of Co on the direct desulfurization route, while Ni promoted hydrogenation properties of the catalyst. Nevertheless, the structural models of active sites do not seem to differ between Ni and Co promoted catalysts. There are obviously some differences between the promotion effects of different metals and these will be reviewed both in chapter 1.3.1.4 on the currently used hydrodesulfurization catalysts and in 1.4, which focuses on the kinetics of HDS.

1.3.1.3 Effect of preparation and pretreatment

Catalysts used in this work were mainly commercial ones prepared by the companies specialized in the making of hydrotreating catalysts. The preparation and activation methods were not studied in detail and will only be briefly reviewed here.

The difference between the catalysts prepared by the standard impregnation method and with complexing agent was the only effect of preparation studied here. Nitrilotriacetic acid (NTA) was

used during the preparation as a complexing agent. Again, the catalyst was not prepared during this work, but was supplied by the cooperating company.

According to Cattaneo *et al.* [63], the role of the chelating ligand (NTA) is believed to be a change in the sulfiding mechanism of Ni, which subsequently leads to a higher dispersion of the promoter. The positive or negative effect of NTA on the hydrodesulfurization reaction depends on the ratio between Ni and NTA. The presence of the chelating ligand also affects the sulfiding of Mo. The effect is explained by changing the temperature of sulfiding. When Ni is complexed by ligands, as well as in the absence of nickel, Mo will interact with the support and form compounds with a larger interval of sulfidation temperature. NTA thus aids the formation of more regular MoS₂ slabs by decreasing the temperature of sulfiding. In QEXAFS, regular MoS₂ slabs show the highest Mo-S coordination number, which indicates a complete saturation of the MoS₂ edges and thus more active catalyst. In agreement with this idea, a significant increase in the activity of catalysts prepared with the chelating ligand, both promoted and unpromoted, was reported by Vissenberg [64], Hensen [65], Reinhoudt *et al.* [66], and Robinson *et al.* [67]. The same enhancement of activity was observed for CoMo catalyst in the work of Coulier *et al.* [68]. The positive effect of NTA and other complexing ligands on the hydrodesulfurization of benzothiophene and DBT over the CoMo catalyst was also reported by Shimizu *et al.* [69]. However, in the same article they show no enhancement effect on the NiMo catalyst. A missing enhancement is explained by the already high activity of the NiMo catalyst towards the reaction and thus leaving very little space for the promotion effect of complexing agents. To make the picture more complex, Venezia *et al.* [70] studied CoMo/SiO₂ catalyst prepared by addition of NTA to the impregnation solution and they also found an improvement in the catalyst activity. The enhancement effect of NTA was attributed to the presence of small pores in the SiO₂ support, which can optimize the NTA procedure.

The effects of conditions during the activation of the catalysts on their activity were not studied and only a few basic facts about the activation step, which is a sulfiding of the catalyst, will be reviewed in this section. The catalyst is usually delivered in the oxidic state and has to be sulfided *in situ* before the reaction. The sulfiding procedure is usually specific to each catalyst. In general, the oxidic precursor is transformed to the sulfidic state by reaction with the sulfiding agent during this step. The nature of the activation molecules is various and thiophene, H₂S, dimethyldisulfide, CS₂ or a spiked feed can be employed. The sulfiding process is combined with the reduction by

H₂. The whole process is usually done in the excess of both sulfiding and reducing agent and the effect of the different approaches is not very significant.

However, several studies on the effect of the sulfiding procedure has been done. Janssens *et al.* [71] reports that an active and selective hydrotreating catalyst can be obtained by (partially) sulfiding of nickel. Grimblot *et al.* [72] studied the changes in the structure of catalysts during the sulfidation process. Glasson *et al.* [73] also suggested that the sulfidation state plays an important role in the catalytic activity. Geantet *et al.* [74] showed different sulfidation mechanism of catalysts with different metals. It was reported that there exists a difference in the sulfidation process between Co alone and Co+Mo on alumina. Nielsen *et al.* [75] showed the effect of sulfiding on the dispersion of the MoS₂ phase in Mo/Al₂O₃ catalyst. The study done by Qian *et al.* [76] shows that there is not a significant difference in the sulfidation between the nickel and cobalt promoted catalysts. The amount of sulfur accumulated on the catalysts increased with increasing sulfiding temperature for both catalysts. However, they report a difference in the result of sulfiding between promoted and unpromoted catalysts. Below 300 °C, there is no difference and it is assumed that only Mo is sulfided. To sulfide promoter atoms, the sulfiding temperature has to be between 300 and 400 °C. At 400 °C, the sulfidation states of catalysts were close to the stoichiometric states.

The increasing demand for progressively lower sulfur contents in fuels has resulted in motivation for the improvement of hydrotreating catalysts currently in use. Standard Co(Ni)-Mo/ γ -Al₂O₃ catalysts are being modified with additives and impregnation stabilizers. These additives may either change the chemistry of the HDS process or improve the promoter atoms distribution. During the last decade, phosphorus addition has become a popular choice as a stabilizer during the preparation of highly active hydrotreating catalysts. The effect of phosphorus addition on conventional NiMo/ γ -Al₂O₃ and CoMo/ γ -Al₂O₃ catalysts was studied by Mertens *et al.* [77] and a more pronounced effect on NiMo was found. Kwak *et al.* [78] studied the effect of phosphorus addition on the CoMo/Al₂O₃ catalyst in HDS of DBT and 4,6-DMDBT and identified two ways of the catalyst modification by P. They attributed the increased activity to enhanced metal distribution and increased Brønsted acidity. The effect of P was found to be dependent on the reactant. In DBT HDS, phosphorus promoted HYD more than direct desulfurization (DDS), while for 4,6-DMDBT the opposite trend was found. It is clear that the Brønsted acidity plays a more significant role in the case of 4,6-DMDBT, because the enhanced acidity allows isomerization of the sterically hindered molecules and increases their reactivity. The enhancing effect of

phosphorus was found to be dependent on the way of preparation, as reported by de Back *et al.* [79]. For a CoMo/Al₂O₃ catalyst, increased stability and activity was found when P, Mo, and Co were impregnated in one step. In contrast, when P was impregnated first, dispersion of the active metals was very low, because P occupied a part of the anchoring sites of the molybdate anions on the support.

The effect of phosphorus addition on the HDS of thiophene over the NiMo/Al₂O₃ catalyst was studied by Atanasova *et al.* [80] and Spojakina *et al.* [81]. The presence of phosphorus was found to increase the dispersion of the active component (promoter) and to decrease the coke formation, hence increasing the hydrodesulfurization activity. The optimum composition of the polymolybdate surface structures was found at 1 wt% phosphorus present. Hydrotreating catalysts with phosphorus addition were also studied by Chadwick and coworkers [82-84]. The addition of phosphorus to the conventional NiMo/ γ -Al₂O₃ catalyst increased the HDS activity and the maximum in enhancement was found to be again at about 1 wt% of P added to the catalyst [82]. They suggested that the effect of P could be to promote the formation of an oxide precursor for a Ni-Mo-S phase and thus the promotional effect to be secondary and not direct as is the case of metals (Ni, Co). Phosphorus promoted NiMo/ γ -Al₂O₃ catalyst was studied also in [83], but only in hydrogenation reaction. In a later paper the same group reported on Fe/alumina HDS catalyst [84]. The addition of phosphorus during the preparation was again found to increase the HDS activity of the catalyst. The effect of phosphorus on W/Al₂O₃ catalyst was studied by Cruz *et al.* [85] and also in their work the increase in activity was found. Moreover, they report that the conditions during the preparation with P, namely pH, have no significant effect on the promotional effect. They also found a stronger effect on the HDS reaction compared to HDN, suggesting that the phosphorus affects the distribution of active sites in favor of HDS reaction. Addition of phosphoric acid to Mn₂O₃-NiO catalyst, thus creating a phosphate-promoted catalyst, was also found to increase HDS activity, as Yamamoto *et al.* [86] reports.

1.3.1.4 Current hydrodesulfurization catalysts - properties and activity

In general, CoMo/ γ -Al₂O₃ is noted for its HDS activity whereas NiMo/ γ -Al₂O₃ is known for its HDN and HYD activity. However, this does not mean that CoMo is always preferred for HDS. The reason is that NiMo catalyst is very flexible in a performance towards both HDN and HDS of different feedstocks, while CoMo catalysts only exhibit reasonable HDN activity on lighter

feedstock (Galiasso *et al.* [87]). Thus the choice of catalyst also depends on the type and amount of impurities in the processed feedstock. In Figure 1-4, a decision tree for matching catalysts with the feeds proposed by Kellett *et al.* [88] is shown. From this decision tree, it is apparent that once the process conditions are known, the main consideration is whether the feed is straight run or a secondary feed stream from cracking processes. The boiling range of the feedstock is usually not

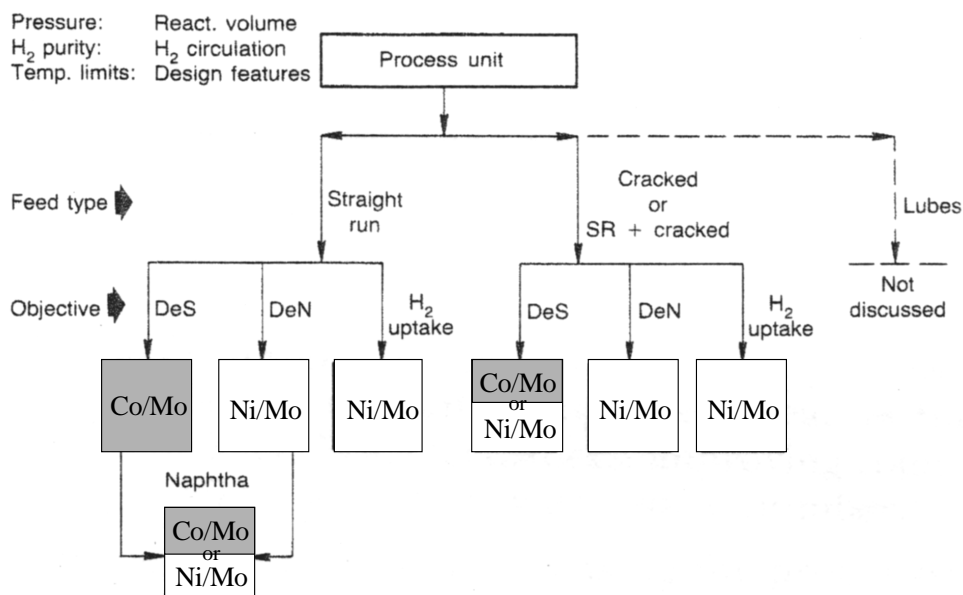


Figure 1-4 The decision tree for a catalyst selection (adapted from Kellett *et al.* [88]).

a major consideration. Thus the choice between CoMo and NiMo catalyst is based on the feedstock and desired properties of the final product. A new hydrotreating “toolkit” [89] consisting of several catalysts with different properties could be an example of the versatility of hydrotreating catalysts.

In this work, light gas oil (LGO) was used as a feedstock. LGO contains a wide range of organic sulfur compounds, which are distributed nonuniformly in their boiling range and this nonuniformity depends on the origin of the crude oil. Such a high number of individual components is very difficult to identify. However, with the help of new analytical methods, e.g. GC-AED, which will be presented in detail in chapter 3.1.4.1, it was possible to identify most of them, as is reported in [90] and also by Kabe and coworkers [91, 92]. Regarding the catalyst, the

work by Kabe together with the decision tree in Figure 1-4 show that CoMo would be the most suitable catalyst for hydrodesulfurization of LGO. This agrees with the literature, where CoMo was found to show slightly higher activity towards the HDS reaction and to have lower hydrogen consumption than NiMo. In the literature, the use of CoMo catalyst supported on γ -Al₂O₃ is reported for many years (see e.g. Topsøe *et al.* [8], review by Landau [93], and references therein). The CoMo catalyst was also used in several other works and the methyl-substituted dibenzothiophenes were found to be the most difficult to desulfurize over CoMo, as is reported by Kabe *et al.* [91], Ishihara *et al.* [94], and Zhang *et al.* [95]. It seems that CoMo catalyst dominates the hydrodesulfurization chemistry of LGO and that NiMo/ γ -Al₂O₃ was neglected in the studies of the hydrodesulfurization reactions because of its lower activity. However, several studies on NiMo have been done, where the catalyst was tested as a possible HDS catalyst for the gas oil. A nice comparison of both catalysts were done by Ma *et al.* [96, 97] and they confirmed the dependency of the catalyst activity on the processed feed. CoMo was found to be a better catalyst for lighter fractions, while NiMo was more active towards the heavier fractions. Zhang *et al.* [95] studied both the NiMo and the CoMo catalyst as well and they report a better activity of the NiMo catalyst towards the substituted DBTs present in the LGO. This higher activity when compared to CoMo was attributed to the difference in the activity of both catalysts for the hydrogenation of aromatic rings of DBTs.

Previous paragraphs were dealing mainly with the studies of real oil fractions. As for model compounds and model studies, a lot of different types of catalysts have been studied during many decades. NiMo/ γ -Al₂O₃ and CoMo/ γ -Al₂O₃ will be reviewed in detail in chapter 1.4, since they were used in this work. For the general view on the diversity of the studied catalysts, new types of hydrotreating catalysts will be reviewed in the following chapter.

1.3.2 New types of catalysts for hydrodesulfurization

A strong demand for cleaner fuels asks more from the old processes and it seems that the activity of the catalysts used successfully for a long time might be insufficient. During the last decade a search for a new process, including a new catalyst, has been going on. As is pointed out in the review by Furimsky [10], the effort of finding new catalysts has two main approaches. One approach is based on the modification of the support by various additives (e.g. phosphorus, boron, or other elements) or replacing conventional γ -Al₂O₃, while still using the same active metals.

Another approach includes development of novel active phases to replace traditional Mo and W sulfides. It is also possible to use totally new types of catalysts in the sense of changing both support and active metals.

In this work, conventional molybdenum based catalysts supported on alumina were used. Thus the topic of new catalysts obtained by the change of active metals or support will be reviewed only briefly, since it is beyond the scope of the current work. However, Pt catalyst supported on Y-zeolite, originally a hydrocracking catalyst, was tested during a few experiments. Hence the new catalysts based on noble metals and zeolites will be reviewed in more detail later on.

As was mentioned already in chapter 1.3.1.3, there is a lot of options for the modification of the catalyst support (Mertens *et al.* [77]). Phosphorus was found to be one of the best additives for the preparation of highly active hydrotreating catalysts. The main conclusions were that an addition of phosphorus increased the HDS activity in all presented works and the effect was attributed to the improvement of dispersion of the active metal and increase of the acidity of the catalyst. In the same way, other elements were also studied as an additive. Ocelli and Debies [98] studied the effect of boron on a NiMo catalyst that also contained HY zeolite in an alumina matrix. They report that the macroporosity and a greater metal availability (caused by the presence of boron during the preparation) is responsible for the enhanced HDN activity observed during the upgrading of a vacuum gas oil. The effect of boron addition on HDS activity of NiMo/ γ -Al₂O₃ catalyst was studied by Lewandowski and Sarbak [99] and Li *et al.* [100]. As in the case of phosphorus, the addition of boron led to an increase in the acidity of the catalyst and an improvement in the hydrocracking ability. The maximum of the enhancement was found at about 1 mol% of B₂O₃ which was in a good agreement with the dispersion of active metal phases and the hydrogenation ability of the catalyst [100]. Similar results were obtained for the study of aluminium borate supported catalysts in the HDS of real oil fractions. Chen and Tsai [101, 102] observed an optimum amount of B₂O₃ to be about 4 wt%. The explanation of the effect is again an increase in the acidity of the catalyst and the reason is suggested to be the increased amount of the Co-Mo-O precursors for the active Co-Mo-S phase. A very similar effect of the fluorine addition was found in the works of Kwak and coworkers [103, 104]. However, there seems to be a difference in the effect of fluorine on different catalysts. For CoMoS/Al₂O₃ catalyst, fluorine increases the catalyst acidity and the metal dispersion and both these effects lead to an increase in the activity. On the other hand, fluorine at NiWS/Al₂O₃ causes decrease in the dispersion of active species, which causes decrease in the activity, and in the same time fluorine enhances the

sulfidation of the catalyst, which increases the activity. Consequently, the overall activity of fluorinated NiWS/Al₂O₃ catalyst is determined by two opposite trends, whose contributions to catalytic activity vary with the preparation conditions. In summary, addition of phosphorus and boron has been found to have only positive effect on the activity of hydrotreating catalysts, while the effect of fluorine depends on the catalyst used.

Another way to modify the support is to use different oxides or create binary oxides with alumina. TiO₂, ZrO₂, and SiO₂ are usually used for this purpose, as is shown in the study by Okamoto *et al.* [105], who studied the effect of support on activity of the CoMo sulfide model catalysts. Segawa and coworkers [106-108] studied binary mixtures of TiO₂ and Al₂O₃ and observed increased activity in the HDS of dibenzothiophenes. They report the promotion in favor of the hydrogenation route and also observed a higher reducibility of oxidic precursors to sulfides on the binary oxide, thus increasing the number of active sites for HDS reaction. They also report that the binary oxide with alumina is more active than just pure TiO₂ as a support. A similar study on pure TiO₂ support was done by Coulier *et al.* [109]. An unpromoted Mo catalyst with TiO₂ as a support was found to be more active than an Al₂O₃-supported counterpart, while a Ni promoted catalyst was not affected. The suggested reason is the promotion behavior of Ti on an unpromoted catalyst in the same way as Ni and Co do in promoted catalysts. In promoted catalysts Ni and Co have a higher affinity to the edge sites of MoS₂ and any effect of Ti is absent. In agreement with previous studies, Coulier also observed an increase in the hydrogenation activity of the catalyst. Other authors found an enhancing effect of TiO₂ addition on the HDS reaction too [110-114]. However, in several papers it is noticed that the degree of increase of the activity is strongly dependent on the feed to desulfurize [112, 113]. A TiO₂-ZrO₂ support was also studied [115, 116] and the initial catalyst activity was found to be higher compared to Al₂O₃-supported catalysts, but fast deactivation was observed [116]. ZrO₂ was studied as a pure support [117, 118], but also in mixtures with Al₂O₃ and SiO₂. Catalysts supported on Al₂O₃-ZrO₂ were found to be more active than pure alumina supported ones in HDS reaction, although the improvement was somewhat limited with the real feedstock [119]. ZrO₂-Al₂O₃ and ZrO₂-SiO₂ supports were studied by Damyanova *et al.* [120]. They report a significant increase in the molybdenum dispersion with a small amount of Zr added, especially on silica. ZrO₂-Al₂O₃ supported Mo catalysts showed higher Lewis acidity than ZrO₂-SiO₂ supported ones. The HDS activity has a maximum at low Zr content, which was related to higher Mo dispersion. Kostova *et al.* [121] studied the effect of Zr

addition on SiO₂ support and report a decrease in the total acidity of the catalyst when Zr is added. Zr was also found to increase the hydrogenation activity of catalysts. They also studied different types of silicas and found catalysts supported on hexagonal mesoporous silica (HMS) more active in HDS than the ones supported on normal silica, mainly because of higher surface area and porosity of HMS. Different forms of SiO₂ as a support were also studied by many others [68, 70, 122-125]. MgO has been tested as a support as well, but the results are not fully clear and controversial views on the effect on HDS activity can be found [126-128]. Carbon as the support was also a subject of many studies with enhancement in activity observed in many cases [129-137]. Supports based on mesoporous materials like MCM-41 also show promising activity for deep desulfurization [138-141].

Another example of possible supports are zeolitic materials. The zeolite most used is that of type Y, but also X-zeolite has been studied. Co, Ni, and Mo supported on zeolites are known to be more active in hydrocracking catalysis than in HDS [142, 143]. However, some studies have been done on the activity in hydrodesulfurization reactions. The preparation method of zeolite supported molybdenum and CoMo catalysts was found to have a significant effect on the HDS activity [143-145]. Bataille *et al.* [146] and Isoda *et al.* [147] report that the acidity of zeolites can strongly influence the reactivities of the sterically hindered molecules like 4,6-DMDBT, because the acidic function promotes skeletal isomerization to more reactive isomers. Welters *et al.* [148] also observed an increase in the HDS of thiophene with increasing acidity of the zeolitic structure and they attributed this to a synergy between the small metal sulfide particles located inside the zeolite pores and the acidic support. Sarbak studied NiMo catalysts supported on X- and Y-zeolites modified with anions [149] and cations [150, 151]. Anions (like fluoride) introduced to the zeolitic structure lead to increased HDS activity [149]. This is explained by the increase of the strength of the Lewis acid sites, which make hydrogenolysis of the C-S bond easier. But a fast deactivation of the studied zeolite catalysts was observed as well. Also catalysts with the addition of cations into the zeolitic structure were found to be active in the HDS reaction [150, 151]. In general, zeolites characterized by a higher SiO₂/Al₂O₃ ratio are more active [151].

In summary, many different combinations and types of supports were tested for HDS reactions with different results. The most promising seems to be combination TiO₂-Al₂O₃, which is more acidic and allows better desulfurization of the refractory compounds, and also the newly emerged HMS support, because of its unique properties (a high surface area and porosity). Zeolites can also be used as an active support for new hydrodesulfurization catalysts, but as yet the high

deactivation rate makes them less interesting. It seems that in industrial operations the conventional catalysts will still prevail for quite some time.

There is a lot of work done on the changes of the active and promoting metals. The largest group tested in hydrodesulfurization reactions is the noble metal group. The activity of a series of transition metals was studied in the HDS reaction and a typical volcano plot (Figure 1-5) was found with the maximum for Ru and Os [152, 153]. Some studies on unsupported noble metals have been done [152, 154], but a majority of work has been done on supported Ir [155], Re [156, 157], Ru [158-161], Pd, and Pt. Platinum and palladium were supported on conventional γ - Al_2O_3 [162-164], new amorphous silica alumina (ASA) support [6, 155, 165, 166], or mesoporous silicate FSM-16 [167].

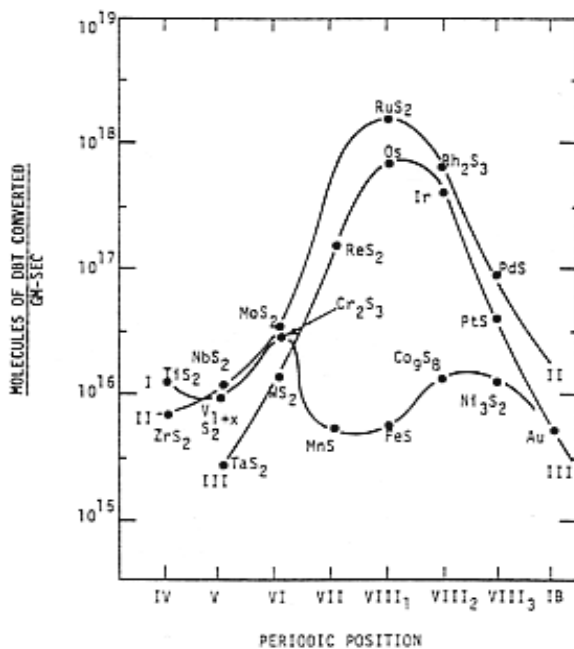


Figure 1-5 Periodic trends for HDS of DBT at 400 °C (adapted from [153]).

To summarize the main conclusions from the works presented in the previous paragraph, noble metal catalysts are active in HDS reactions, but their activity depends on the preparation method. They also deactivate relatively fast [162], are sensitive to inhibition by H_2S [6, 165], and their

sensitivity towards nitrogen containing inhibitors depends on the support [155]. That also means that the suitability of the catalyst for a real feedstock cannot be evaluated by a single-component study alone [6]. Data from the ^{35}S radioisotope tracer method indicates that the mechanism of HDS on the noble metal catalyst is different from that on the conventional Mo-based catalyst [163]. The higher hydrogenation activity of noble metals and the stronger acidity of the ASA support improve reactivities of sterically hindered molecules, where the hydrogenated intermediate facilitates the desulfurization reaction [6, 165, 166]. In the case of bimetallic catalysts, a synergetic effect between metals was found [6, 163, 164].

Navarro *et al.* [168] studied the HDS activity of noble and semi-noble metals on a HY zeolite support. Under steady-state conditions, noble metals were more active than Ni in hydrodesulfurization of DBT. Surprisingly, their relative activities did not follow the volcano plot shown in Figure 1-5. The role of the support was found to be quite important in the HDS activity of the catalyst and even a pure HY zeolite without any metal performed well in the HDS of DBT. In all cases, the direct desulfurization route was found to be more important than the hydrogenation reaction. They also observed fast deactivation of Ni and Ru catalysts, while on Ir, Pt, and Pd catalyst the deactivation rate was very low. The resistance of Pt and Pd catalysts to poisoning was thus confirmed. The initial decrease in conversion was usually caused by the deactivation of the zeolitic support, whereas the gradual loss of activity with longer time on stream was attributed to the deactivation of the active metal. Pt supported on HZSM-5 zeolite was studied by Sugioka *et al.* [169]. A high and stable catalytic activity for the hydrodesulfurization of thiophene was observed and this activity was higher than that of a commercial $\text{CoMo}/\text{Al}_2\text{O}_3$ catalyst. They proposed a new mechanism of thiophene HDS involving hydrogen spill-over (Figure 5-3), which will be discussed in the appropriate discussion section. A similar system was also studied by Song [170]. His results seem to show promising direction in the design of sulfur tolerant catalysts. Sulfur resistance was divided into two types (type I is resistance to organic sulfur compounds, type II resistance to inorganic H_2S [171]) and each of the types could be enhanced by certain modifications. Type I by a structural design that uses shape-selective exclusion, and type II by modifying the electronic properties of metal species to weaken the sulfur-metal interaction or bond. Thiophene HDS on Pt supported zeolites was also studied by Simon *et al.* [172]. They observed that the thiophene decomposition occurred mainly on the Brönsted acid sites and Pt facilitates the hydrogen spill-over to metal surface. However, the spill-over was only observed if the Brönsted acid site and metal surface site were in close proximity.

Thus the mechanism of the reaction can be described with the same model as was proposed by Sugioka [169]. Also bimetallic catalysts, mainly combinations of Pt-Pd, were studied. Sugioka *et al.* [173] proposed the same mechanism for both Pt and Pt-Pd mixture in the HDS reaction and found the Pt-Pd supported on zeolite as a promising catalyst for further studies. Rades *et al.* [174] studied Pt-Pd catalyst supported on NaY zeolite by diffuse reflectance IR and report the formation of a highly dispersed Pt-Pd alloy. Le Bihan and Yoshimura [175] report a strong effect of the calcination temperature on the catalytic properties of Pd-Pt/USY catalyst modified by ytterbium. A very strong effect was found on the HDA behavior, while HDS was slightly affected by increasing temperature of calcination. These results indicate that the selectivity of HDS or HDA can be controlled by changing the calcination temperature of Pd-Pt/Yb/USY zeolite catalysts.

1.4 Reaction mechanism and kinetics

The hydrodesulfurization reactions are virtually irreversible at temperatures and pressures usually applied, roughly 300 to 450 °C and up to 10 MPa. The reactions are exothermic with heats of reaction of the order of 40 to 80 kJ/mol of hydrogen consumed [176].

The mechanism of the HDS reaction is fairly similar for all sulfur components. Sulfur compound reacts with hydrogen and a saturated hydrocarbon and H₂S are the final products. The mechanism for aliphatic compounds was already shown in chapter 1.2 (Equation (1-1)) together with the mechanism for thiophenic compounds, which follow the one presented in Figure 1-1. A slightly more complex mechanism is proposed for dibenzothiophenes (Figure 1-6). This mechanism was proposed in the late 70's by Houalla *et al.* [177] and is still widely accepted. As one can see, the C-S bond cleavage is not the only reaction, hydrogenation plays a significant role as well as isomerization steps. It is generally believed that the HDS¹ mechanism involves two reaction pathways - direct desulfurization route (DDS, sometimes called hydrogenolysis) and hydrogenation (HYD, by some authors referred to as hydrodesulfurization - HDS). However, the ratio between the HYD and DDS strongly depends on the catalyst and reaction conditions. Especially for thiophene, there are papers in the literature supporting all possible combinations of the suggested pathways.

1. For a better distinction between the names and to avoid confusion in this work, the abbreviation HDS will be used for the overall reaction and notations DDS and HYD will be used for individual pathways.

Houalla based the presented mechanism on the reaction behavior of DBT over a commercial CoMo/ γ -Al₂O₃ catalyst under conditions of practical interest. There is some controversy in the literature about the active sites for the reaction. Some authors suggest one site reaction (O'Brien *et al.* [178]), but most prefer a two site mechanism, where the hydrogenation reaction occurs on one type of sites and desulfurization on the other type [179, 180].

Since the cobalt promoted catalyst is the one mainly used in a commercial HDS process, most studies focus on this system. There are slight differences in activities of Co and Ni promoted catalysts and these are visible mainly in the different ratio between HYD and DDS routes. This issue was addressed previously (chapter 1.3).

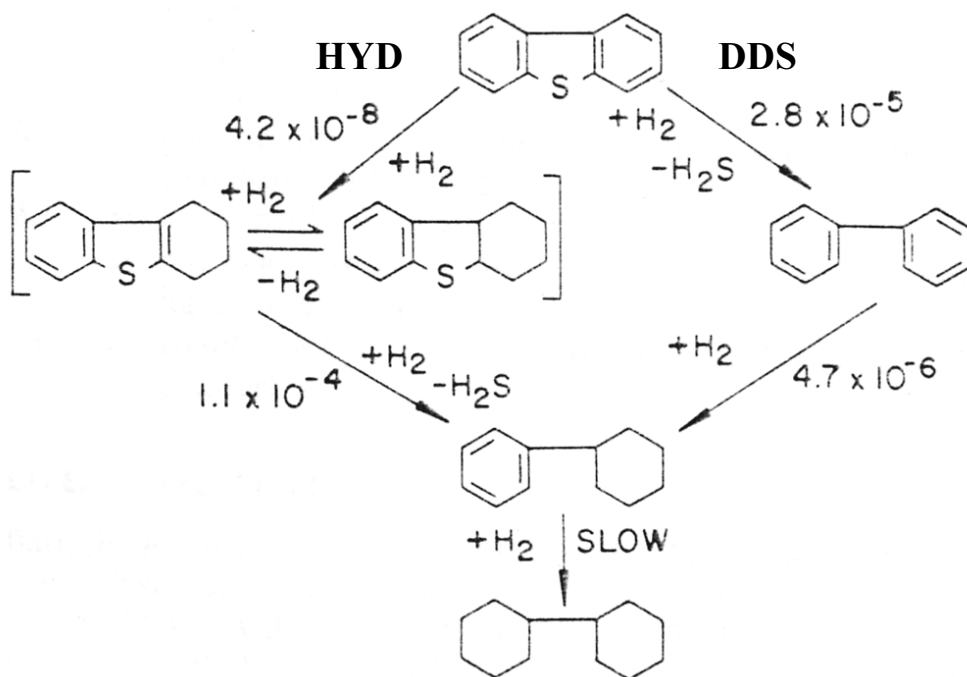


Figure 1-6 Mechanism of HDS of DBT (adapted from Houalla *et al.* [177]). Numbers indicate the relative rates of the individual reaction steps.

To successfully perform deep hydrodesulfurization, understanding the kinetics is of a great importance (Cooper and Knudsen [181]). Hence the kinetics of HDS of both real feedstock and model compounds has been studied very thoroughly by many groups.

There is a large amount of work on model compounds and catalysts, where inhibition can be controlled and detailed kinetics of individual compounds can be investigated. Both Ni and Co promoted catalysts have been studied and major interest was given to the refractory compounds, namely DBT, 4-MDBT, and 4,6-DMDBT. The work of Lamure-Meille *et al.* [182] and an overview by Shafi and Hutchings [183] point out several main conclusions: The order of reactivity is generally acknowledged to be 2,8-DMDBT > DBT > 4-MDBT > 4,6-DMDBT [67, 184] and the reason is considered to be steric hindrance (see Figure 1-7 and ref. [96]) and the electronic effects of the substituents in certain positions (the behavior and properties of 2,8-DMDBT will be discussed later). Hydrogenation of the aromatic ring prior to sulfur removal is generally thought to decrease this steric hindrance and, therefore, facilitate the HDS reaction [185]. The hydrogenation pathway was found to be preferred in the case of hindered DBTs and this preference increases with the size of substituent in the 4-, or 4,6-positions [186]. NiMo has evidently a higher hydrogenation activity and is thus more suitable for the HDS of hindered DBTs [187]. H₂S was found to be an inhibitor of HDS reactions [188].

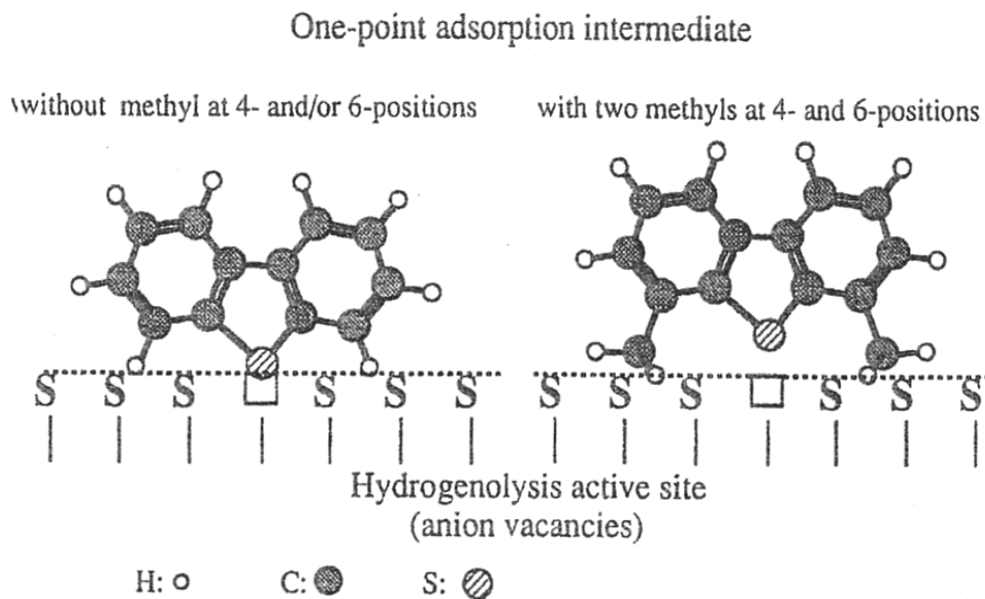


Figure 1-7 Schematic representation of steric hindrance (adapted from Ma *et al.* [96]).

Gates and coworkers [177, 184, 189, 190] were among the first to establish the mechanism of HDS of DBT on CoMo catalysts. They also studied other thiophenic compounds and observed the order of reactivity of substituted DBTs shown above. For benzothiophenes and dibenzothiophenes, no aromatic ring saturation was observed at the studied conditions, suggesting that hydrogenation is not a prerequisite step to C-S bond scission [189]. This observation was behind the mechanism presented in Figure 1-6 [177], showing two reaction pathways of HDS of DBT. It was also shown that electronic effects play a significant role in the reactivities of individual substituted alkyl-DBTs [190]. Singhal *et al.* [191] also present the idea that the hydrogenation of a C-C bond is the first step if the electron density of the sulfur atom is delocalized over an extensive π -system. Ma [96] concluded that the decrease of conjugation of π -electrons of the benzene ring with lone-pair electrons of sulfur increases the HDS reactivity of the substituted DBTs.

The rigorous kinetic study of the HDS of aromatic sulfur compounds over a CoMo/ γ -Al₂O₃ catalyst done by Froment and coworkers [192-196] confirmed the existence of two types of active sites, one for the hydrogenation (HYD) reaction and one for the hydrogenolysis (DDS) reaction. On both types of active sites the surface reactions between the reactants and competitively adsorbed hydrogen seem to be rate-determining. Sulfur components can undergo desulfurization with or without prior hydrogenation. Again, the observed order of reactivities was thiophene > DBT > 4-MDBT > 4,6-DMDBT.

Significantly less attention has been given to the study of HDS kinetics of model compounds over NiMo/ γ -Al₂O₃. HDS of polycyclic aromatic sulfur compounds was studied by Levaché *et al.* [197], who reports that the competition between the hydrogenation and the direct desulfurization is dependent on the electronic structure of the compound studied. Meille *et al.* [198, 199] studied HDS of alkyldibenzothiophenes over nickel promoted catalyst and found similar results as for CoMo catalysts. The order of reactivity was 2,8-DMDBT = DBT > 4-MDBT > 4,6-DMDBT, but they observed that the compounds have similar adsorption equilibrium constants. The difference in reactivity must then be due to different reaction rates of the adsorbed molecules. Steric hindrance and partial hydrogenation of the aromatic ring prior to C-S cleavage, as was explained in the case of CoMo catalyst, is the likely explanation. Even if the NiMo catalyst has not been studied as extensively as CoMo, the results from these studies show that there is virtually no difference between these two catalysts in their basic catalytic properties. There is, of course, a significantly higher hydrogenation activity over the nickel promoted catalysts (see e.g. Ledoux *et*

al. [200]), but the difference is really visible only in the case of the sterically hindered molecules and the processing of real feedstocks, as will be presented next.

The studies of different oil fractions have been given a significant attention recently. For example, the review by Landau [93] presents suggestions for technical solutions for the transfer from HDS to deep HDS of middle distillates, required nowadays by legislation in most countries. The main points would be to find more active catalyst, increase the severity of the process, and divide the process into two stages. On a slightly more detailed level, single fractions attract the major interest. HDS of heavy distillates over a NiMo/ γ -Al₂O₃ catalyst was studied by Katti *et al.* [201]. Several individual sulfur compounds were detected and pseudo-first-order kinetics was applied to their conversions. Substituted DBTs were found to be the most refractory components. They also tested a CoMo catalyst and found it to be more active per unit mass, but less active per unit surface area than NiMo. Diesel fuel was studied by van Looij *et al.* [202] and Vradman *et al.* [203]. An inhibition effect of aromatic and nitrogen containing compounds present in the oil was observed. Similarly, a sensitivity of the HDS activity of the catalysts to inhibiting components in oils under the industrial conditions was reported by Lecrenay *et al.* [204]. Hydrodesulfurization of light gas oil over a commercial CoMo/ γ -Al₂O₃ catalyst was studied by Kabe and coworkers [91, 205]. Alkyldibenzothiophenes, especially 4,6-DMDBT, were found to remain unreacted until very high HDS conversion level. Ma and coworkers [96, 97, 206, 207] studied the kinetics of hydrodesulfurization of gas oils over both NiMo and CoMo catalysts as well. Pseudo-first-order kinetics was applied to the data obtained with the help of detailed analysis of sulfur components in gas oils. Sulfur compounds were divided into several groups based on their reactivities, and substituted alkyldibenzothiophenes, in particular 4,6-DMDBT, were found to be the most difficult to desulfurize. The steric hindrance was identified as a reason (Figure 1-7). For the heavier fractions, hydrodesulfurization of alkyl-DBTs was strongly inhibited by the polyaromatics and nitrogen compounds present in the oil. Deep HDS of gas oils was studied in detail by Sie [7]. He did not divide the complex component mixture into groups, but described the kinetics of total sulfur removal as an approximately second-order reaction with sulfur as a pseudo-single component. Very similar reaction orders, between 1.7 and 2.0, were reported by Ancheyta *et al.* [208]. The second-order kinetics implies that with increasing depth of desulfurization the amount of catalyst needed increases steeply. Another consequence is the generation of large quantities of H₂S already in early stages of the reaction, which can cause serious problems since H₂S is known to be a strong inhibitor of HDS reaction. The solution for this problem can be a two-stage process,

as already mentioned. The easily desulfurized compounds are removed in the first stage and in the second one a different catalyst is used for removal of refractory components.

1.5 The inhibiting effect of other components of the oil (“matrix effect”)

The industrial feedstock is a complex mixture of different molecules, some of which can act as inhibitors. Depending on the quality, the crude oil contains varying amounts of aromatics and components containing nitrogen and oxygen. Sulfur compounds, which can be divided into several groups based on their reactivity, can act as inhibitors as well. And, of course, H_2S (as well as NH_3 and H_2O) as a product of hydrotreating reactions, also act as inhibitors. All these components of the oil somehow influence the reactivity of individual sulfur compounds and thus the HDS effectivity.

Schulz *et al.* [209, 210] studied the reactivity of the sulfur components in the real oil fractions and named this inhibiting behavior the “matrix effect”. They claim that this effect is predominantly due to other sulfur compounds in the oil and that the nitrogen containing components and aromatics do not have such a strong effect. Among the sulfur compounds, the heavier analogues of polyaromatic sulfur compounds have the strongest inhibiting effect. Their study shows that the effect is not caused only by the competitive adsorption. The addition of one H atom to the sulfur compounds causes the formation of very strongly chemisorbed stable intermediates, which are believed to be the inhibiting species. This is closely related to the change of electronic structure of the molecule, which affects the strength of adsorption and reactivity of the component. Ancheyta-Juárez *et al.* [211] studied also this inhibition effect and reported that the inhibiting effect of the components in oil decreases with increasing temperature. The complexity of this problem can be demonstrated by the work of Nagai and Kabe [212], who report a study on the simultaneous HDS, HDN, and HDO reactions. Nitrogen compounds were found to inhibit hydrogenation pathway (HYD) of DBT by a stronger adsorption on active sites at lower temperatures, while at higher temperatures they affected both reaction pathways. Sulfur and oxygen compounds retarded all reactions of desulfurization of DBT at all temperatures. Their study also supported the idea of two different sites for DDS and HYD reactions.

There has been a lot of studies done on the effect of sulfur compounds, mainly H_2S , on the hydrodesulfurization reaction. Lamure-Meille *et al.* [182] report that on both NiMo and CoMo catalysts H_2S strongly decreases the initial reaction rate of the HDS reaction of DBT and 4-

MDBT, and modifies the relative importance between hydrogenation and direct desulfurization routes in favor of HYD. But Lecrenay *et al.* [204] studied the effect of H₂S on HDS of 4,6-DMDBT and the product distribution showed that on a NiMo catalyst, the HYD route was more affected than DDS. On the other hand, the DDS route was more affected on a CoMo catalyst. They also observed a low promoting efficiency of Ni in the presence of H₂S. The inhibition effect was explained by the strong adsorption of H₂S on the catalytically active sites. Moreover, a similar inhibiting effect of aromatics in the feed on the HDS reaction of 4,6-DMDBT was found. Kasahara *et al.* [213] observed a strong inhibiting effect of H₂S on HDS of both benzothiophene and DBT over NiMo, CoMo, and Mo catalysts. This effect was more significant for DBT. In the case of benzothiophene the DDS was more inhibited than the HYD route and the opposite trend was found in the case of DBT. The ratio of rate constants between inhibited and non-inhibited reaction was approximately 0.03 over the NiMo catalyst and 0.11 over the CoMo catalyst. They also found that H₂S decreased the promotion effect of Ni added to the Mo-based catalyst. In a direct contrast to the study of Lecrenay [204], Shin *et al.* [214] report that on the NiMo/Al₂O₃ catalyst, H₂S prohibits the step of S elimination from substituted DBTs and thus retards DDS more than HYD. However, for 4,6-DMDBT both reaction pathways are affected in the same degree. A similar result was published by Kabe *et al.* [215], who studied the effect of H₂S on HDS of DBT and 4,6-DMDBT. Both the HYD and DDS routes were affected, but the inhibition was stronger for the DDS path. The inhibition was explained by the stronger adsorption of H₂S on the hydrogenolysis sites when compared to hydrogenation sites. Furthermore, the effect of Ni on NiMo catalysts is to weaken the inhibiting effect of H₂S. Kabe *et al.* [205] also report that in the oil, the retarding effect of H₂S is much stronger on HDS of DBT and 4-MDBT than on HDS of 4,6-DMDBT, which was hardly influenced on the CoMo catalyst. This was explained by assuming competitive adsorption between DBTs and H₂S. Detailed kinetic studies of the retarding effect of H₂S were also done by Leglise *et al.* [216] and Hiroshi *et al.* [217] with the use of LHHW kinetics. Singhal *et al.* [180] reported that on CoMo catalyst H₂S has no effect on the product selectivity, just on the total DBT conversion. However, with increasing temperature the selectivity to the DDS route increases, but CHB is mainly produced via the HYD route.

Regarding the effect of aromatics, some studies have been done in connection with studies of the effect of other components in oil. Kabe *et al.* [92] studied the effect of both H₂S and aromatics on desulfurization of LGO and found the aromatics to be much stronger inhibitors than H₂S. They

also observed a strong dependency of the effect of inhibition by H_2S on the sulfur compound desulfurized, while the same dependency was much lower in the case of inhibition by aromatics. Multiring aromatics were found to be much stronger inhibitors when compared to 1-methylnaphthalene. The majority of studies with the model compounds is aimed towards the effect of aromatics on the HDS of 4,6-DMDBT and very little work has been done in studying the effects on the HDS of DBT. Lecrenay *et al.* [204] describe the inhibiting effect of naphthalene on HDS of 4,6-DMDBT and the product distribution showed that the HYD route was more affected than the DDS route. Whitehurst *et al.* [188] observed as well that naphthalene inhibits all hydrogenation reactions but has only a small effect on direct desulfurization. Isoda *et al.* [218] studied the effect of naphthalene on the hydrodesulfurization of 4,6-DMDBT and they report that 10 wt% of naphthalene severely retarded the HDS reaction and that the NiMo catalyst preferred the hydrogenation of naphthalene to HDS of 4,6-DMDBT. Farag and coworkers [132, 219] report that 10 wt% of naphthalene inhibited both DDS and HYD pathways and the most affected was the desulfurization of hydrogenated intermediates. Moreover, 4,6-DMDBT was found to inhibit hydrogenation of naphthalene (so-called self-inhibition). Koltai *et al.* [220] report a strong inhibiting effect of polycondensed aromatics on the HDS of 4,6-DMDBT, while Katti *et al.* [201] report naphthalene to be only a weak inhibitor of dibenzothiophene hydrodesulfurization. The mixed results and conclusions from the literature indicate that the picture of the inhibiting effect of aromatic compounds is not clear.

As was mentioned earlier, nitrogen containing components of the oil also influence the hydrodesulfurization reaction. This effect was not studied in the present work, but for completing the picture of this complex problem, the effect of nitrogen compounds will be briefly reviewed. The poisoning effect of nitrogen compounds on the HDS of DBTs over $CoMo/Al_2O_3$ is the topic of several papers [221-224]. The most commonly studied nitrogen compounds are non-basic carbazole and basic quinoline. For the HDS reaction of DBT there was virtually no difference in the effect of basic and non-basic compounds [222]. However, the inhibiting effect was dependent on the properties of nitrogen compound in the case of HDS of 4,6-DMDBT [224]. In the experiments with a pulse feeding of nitrogen compounds, the observed effect of non-basic and basic compounds on the catalyst was different. When the feeding of nitrogen compounds was stopped, the catalyst activity was restored in a short time in the case of the non-basic nitrogen compound, which was found to easily desorb from the active sites. On the other hand, the basic compound was adsorbed very strongly and the catalyst was deactivated irreversibly. The same

result was reported by Nagai *et al.* [225] for a NiMo/Al₂O₃ catalyst. The inhibition by nitrogen compounds in the gas oil blends on the HDS reaction over a commercial CoMo catalyst was studied by Zeuthen *et al.* [226] and the conclusions were identical to the ones presented above. Most authors agree in the conclusion that basic nitrogen compounds are stronger poisons because of their affinity to acidic active sites of the catalyst [221, 223, 224]. The stronger acidic active sites are usually associated with the direct desulfurization pathway and this route is thus more affected by the basic nitrogen compounds than HYD. However, as in the case of H₂S and aromatics, this applies mainly to substituted DBTs, because their reactivities depend much more on the acidity of the catalyst when compared to unsubstituted DBT.

1.6 Deactivation of hydrotreating catalysts

Initial catalyst deactivation is a major issue in the refining industry and the replacement of the deactivated catalyst is an economically demanding and time-consuming procedure. However, the hydrotreating processes usually have a very long catalyst lifetime. Nevertheless, in the case of the heavy feed, the amount of impurities in crude oil, as well as the propensity of the oil to form coke, increases as the average molecular weight of the oil increases, and catalyst deactivation can become a significant problem. Coke formation is also an issue in catalytic hydroprocessing, since the feedstock contains many species which readily form coke. The questionnaire by Bos *et al.* [227] shows the problems of deactivation during the catalyzed processes. Many companies participating in the questionnaire complain about the complications resulting from the catalyst deactivation and to solve this problem is very difficult, because the relation between the deactivation and its cause cannot be determined *in situ*. That is why model studies with model compounds and real catalysts are done. The deactivation of commercial hydrotreating catalysts during thiophene HDS is studied in this work.

The deactivation of the catalysts in any process involves the loss of active sites. The basic causes are active site poisoning by strongly adsorbed species, active site coverage by deposits (coke, metals), pore mouth blockage/restriction, and sintering of active phase. This is also the case for hydroprocessing catalyst. The irreversible adsorption on the active site decreases the total number of sites available for reaction and this process may be more severe on the promoter sites. Sintering of the active slabs would reduce the total amount of sulfur vacancies. Pore mouth blocking makes the still working active sites unavailable for reaction, while pore mouth

restriction can accentuate diffusional limitations on reaction rates. And finally, rearrangement of the structure may disproportionately reduce certain site center configurations more than others, affecting catalyst selectivity as well as activity.

In hydroprocessing, the deactivation of catalyst also depends on the characteristics of the processed feed. For light feeds, deactivation of the catalyst is minimal and the process can operate for long periods of time before replacement of the catalyst. However, in hydroprocessing of heavy residues the catalyst deactivation can be severe. During commercial operation, the hydroprocessing catalysts invariably experience some degree of deactivation, depending on the feed. Review by Absi-Halabi *et al.* [228] shows that an initial deactivation is usually caused by coke, which appears to reach a pseudo steady-state (in terms of residual activity) rather rapidly. Continued deactivation over a longer period of time is then caused by metal deposits. And the final, total loss in activity is attributed to pore constriction and ultimate pore blocking. At this stage, the run has to be terminated and the catalyst batch replaced by a fresh one.

The catalyst deactivation (or inhibition) due to the competitive adsorption on the active sites, which can occur in the presence of the strongly adsorbing components in the feed, was already reviewed in chapter 1.5 dedicated to the so-called “matrix effect”. The deactivation caused by the other mechanisms will be presented next.

There has been a lot of work done on the deactivation of hydrotreating catalysts during the hydrotreating of the real oil. These studies are usually done through a longer period of time to simulate the conditions in the real process. A quite rapid coke deposition was identified as the main reason for deactivation during the studies of real oils [228-232]. Depending on the feed, about 15-25 wt% of coke was deposited during the first hours of the experiment and this was followed by a much slower increase with time on stream. In a longer time period, metal deposition becomes an important factor of the deactivation process.

Model compounds and model catalysts were used as well, but the results were not always transferable to the real process. Still the results can give a strong hint on the catalyst deactivation behavior during the industrial process. A paper by da Silva *et al.* [233] presents the study of activation and regeneration of the spent NiMo/Al₂O₃ catalyst after the hydrotreatment of the shale oil. Regarding the deactivation, they have observed a partial regeneration of the catalyst activity and attributed the non-regenerated part to the structural changes of the catalyst in the sulfided form. However, the conditions used for the hydrotreating of the shale oil are very different from the model studies.

Among the model compounds, thiophene is widely used for the detailed studies of different aspects of the HDS, because of the relatively simple reaction network and easy product identification. However, not many papers in the literature deal with the deactivation behavior of the hydrodesulfurization catalysts during the thiophene HDS. The most closely related paper to the work presented here report studies of the thiophene HDS over unpromoted MoS₂ catalyst. An infrared spectroscopic analysis by adsorbed CO was used for the study of the deactivation by Elst *et al.* [234]. They report a preferential coke deposition on the active sites of the catalyst to be the main reason for the catalyst deactivation. The amount and the chemical nature of the deposited coke was found to change during the time on stream and the possibility of rejuvenation by the H₂S/H₂ stream was reported. A study done by Pedraza *et al.* [235] introduces some interesting results on the unsupported and unpromoted MoS₂ catalyst, but this system is too distant from the work done here to use it as a reliable reference.

1.7 Scope of the work

The overall aim of this work was to study the kinetics of the hydrodesulfurization reaction over conventional catalysts (molybdenum-based) and test new catalysts for HDS (Pt/Y-zeolite). Kinetics of the individual components of the light gas oil were studied as well as the kinetics of model compounds (thiophene and dibenzothiophene). The NiMo/ γ -Al₂O₃ catalyst was chosen for the hydrodesulfurization of the light gas oil since this catalyst system is increasingly used and less studied than the CoMo system. For thiophene HDS, also unpromoted Mo, CoMo, phosphorus promoted NiMo catalyst, and Pt/Y-zeolite were used. Several experiments on the NiMo and Mo catalysts prepared with the chelating agent (NTA) were also performed.

The inhibiting effect of other components present in the oil on hydrodesulfurization is a very important issue. The kinetic behavior of the complex oil mixture was emulated by the study of the “matrix effect” on the HDS of DBT with added inhibiting compound. In this work, the inhibiting effect of sulfur compounds (DMDS and thiophene) and aromatics (toluene and naphthalene) was addressed and the results were comparable with the data in literature.

The fast initial deactivation of the hydrotreating catalysts was studied during the thiophene HDS and a characterization of the spent catalysts was done. Very little information was found in the literature and that is why a wide range of the hydrotreating catalysts was used. Reactivation experiments and the experiments with the different partial pressure of H₂ were also done. The

deactivated catalysts after different times on stream and different reaction procedures were then analyzed for the total amounts of carbon and sulfur in the sample. The surface area and pore volume were determined as well to see effect of deactivation on the structure of the catalyst.

2. THEORY

2.1 Kinetic calculations for HDS of thiophene and DBT

The kinetic expression can be based either on the Langmuir-Hinshelwood-Hougen-Watson (LHHW) theory or on a simple power law equation. In this work, power law expressions were used for the description of the kinetic behavior of the compounds studied. As was already mentioned, pseudo-first-order kinetics can be successfully applied for the description of the reaction of sulfur compounds during the HDS process. The design equation for a tubular reactor is given in Equation (2-1), where F_A is the molar flow rate of the component, W is the mass of the catalyst in grams and r'_A is the reaction rate.

$$-\frac{dF_A}{dW} = -r'_A \quad (2-1)$$

At any position in a flow system, F_A is defined according to Equation (2-2), where F_{A0} is a molar flow of the component into the system, X is the conversion of that component.

$$F_A = F_{A0} - F_{A0} \cdot X \quad (2-2)$$

Substituting Equation (2-2) into Equation (2-1) gives the differential form of the design equation for a plug-flow reactor:

$$F_{A0} \cdot dX = r'_A \cdot dW \quad (2-3)$$

Based on the similar studies in the literature, the reactions were assumed to be of the first order with respect to the sulfur compound. The reaction rate for the first order reaction can be calculated according to Equation (2-4), where k is the rate constant and C_{A0} is an inlet concentration of the reactant. Combining Equation (2-4) and Equation (2-3) we get Equation (2-5).

$$r'_A = -k \cdot C_{A0} \cdot (1 - X) \quad (2-4)$$

$$F_{A0} \cdot dX = -k \cdot C_{A0} \cdot (1 - X) \cdot dW \quad (2-5)$$

Integration of Equation (2-5) over the whole reactor leads to Equation (2-6) for the calculation of rate constant, where X represents the conversion of the studied sulfur compound calculated from the chromatograms according to Equation (2-7).

$$k = -\ln(1 - X) \cdot \frac{F_{A0}}{W \cdot C_{A0}} \quad (2-6)$$

$$X = 100 \% - \text{area \% of reactant peak from the total area} \quad (2-7)$$

The inlet concentration of thiophene was calculated assuming ideal gas, but the partial pressure of thiophene was calculated from the Antoine equation (Equation (2-8)).

$$\ln p_A [Pa] = -\frac{4400.8}{T[K]} + 23.929 \quad (2-8)$$

For DBT, the inlet concentration was given by the prepared solutions of 0.1 wt% of DBT in n-heptane. From the calculated rate constants, Arrhenius plots based on Equation (2-9) were drawn and the apparent activation energy was determined from the slope of the regression line.

$$\ln k = \ln A - \left(\frac{E}{R} \cdot \frac{1}{T} \right) \quad (2-9)$$

2.2 Kinetic calculations for the inhibiting effect

Basic assumptions for the reactor design equations are the same as in the case of model compounds and follow Equation (2-2) to Equation (2-3). However, in the equations for the reaction rate, the inhibiting effect of the added component was included. The reaction rate is then calculated according to Equation (2-10),

$$r'_A = -k \cdot C_{A0} \cdot (1 - X) \cdot C_P^\gamma \quad (2-10)$$

where C_P stands for the concentration of inhibitor and γ is the order with respect to the inhibiting compound. To estimate the reaction order with respect to the inhibitor, the reaction rate is calculated from the mole balance throughout the reactor according to:

$$-r'_A = \frac{F_{A0}}{W} \cdot X \quad (2-11)$$

Since the conversion of DBT in experiments with inhibiting compounds is much lower than 1 and does not significantly vary with the concentration of the inhibitor in the feed, the first part of the Equation (2-10) can be replaced by new rate constant k' and Equation (2-10) transfers to Equation (2-12).

$$r'_A = -k' \cdot C_P^\gamma \quad (2-12)$$

After the transformation to the logarithmic equation, Equation (2-13) is plotted and the reaction order γ with respect to inhibitor is determined from the slope of the line.

$$\ln r'_A = \gamma \cdot \ln C_P - \ln k' \quad (2-13)$$

The reaction order is then used back in Equation (2-10) and the reaction constant is calculated according to Equation (2-14):

$$k = \frac{r'_A}{(1-X) \cdot C_{A0} \cdot C_P^\gamma} \quad (2-14)$$

2.3 Response factors during GC analyses

The use of the flame ionization detector (FID) in the gas chromatographic analysis brings a small complication to the data evaluation. The response factor (RF) of the FID is generally different for every chemical compound. While for the non-branched aliphatic hydrocarbons the response factor is approximately 1, for more complicated structures and heteroatom-containing compounds it can vary from 0.2 to 1.2. The response factors for sulfur compounds were determined according to papers of Dietz [237] and Katritzky *et al.* [238]. A relative response factor equal to 1 was used for C₄ compounds produced by thiophene HDS. For thiophene, the RF is 0.67 and for tetrahydrothiophene it was estimated to be 0.70. The estimate was based on a structural similarity to compounds with known RF. For HDS of dibenzothiophene, relative response factors for DBT, cyclohexylbenzene, and biphenyl were 0.71, 0.96, and 0.90, respectively. A response factor of 0.75 for tetrahydro-/hexahydrodibenzothiophene was again estimated with the same assumptions as presented above.

3. EXPERIMENTAL METHODS

3.1 High-pressure HDS of light gas oil

3.1.1 Materials

The catalyst was a commercial NiMo/ γ -Al₂O₃, used as received from the suppliers. The feed used in laboratory experiments was a blended light gas oil (LGO) drawn from a commercial unit. The feed contained 1318 wtppm S determined by GC-AED. The bulk density was 853 kg/m³.

3.1.2 Apparatus

The apparatus used in this part of work is presented in Figure 3-1. It consists of an upflow fixed-bed reactor with off-line sample collection and analysis, and has been shown to represent the behavior of an industrial trickle-bed unit well [239]. The reactor is a stainless steel tube (1 m x 19.3 mm i.d.) with a total volume of 290 cm³. The length of the catalyst bed is adjusted by diluting with SiC particles (500-710 μ m) in a volume ratio 1:1. In the present experiments a catalyst volume of 50 cm³ was used, which gives a catalyst weight of about 42 g. The reactor is placed vertically in a heating block made of bronze and heated in an electric furnace with two separate heating zones. The reactor is equipped with an axial thermowell containing four thermocouples, three of which are in the catalyst bed.

3.1.3 Procedures

After closing the reactor and pressure-testing the unit, the system was flushed with N₂, the catalyst was dried overnight and traces of N₂ were removed by the H₂ flow. The catalyst was then pretreated (sulfided) according to instructions from the suppliers using a spiked feedstock (P = 3 MPa, LHSV = 1 h⁻¹, H₂/oil ratio = 200 Nm³/Nm³, final temperature 350 °C held for 4 hours). After the presulfiding step the temperature was adjusted to 250 °C, the feed was changed to the LGO used in the study, and the pressure was increased to that of the first planned experimental point. The conditions were adjusted and the system was left to stabilize for 48 hours before collecting the products for the analysis of the first experimental point. The conditions were then

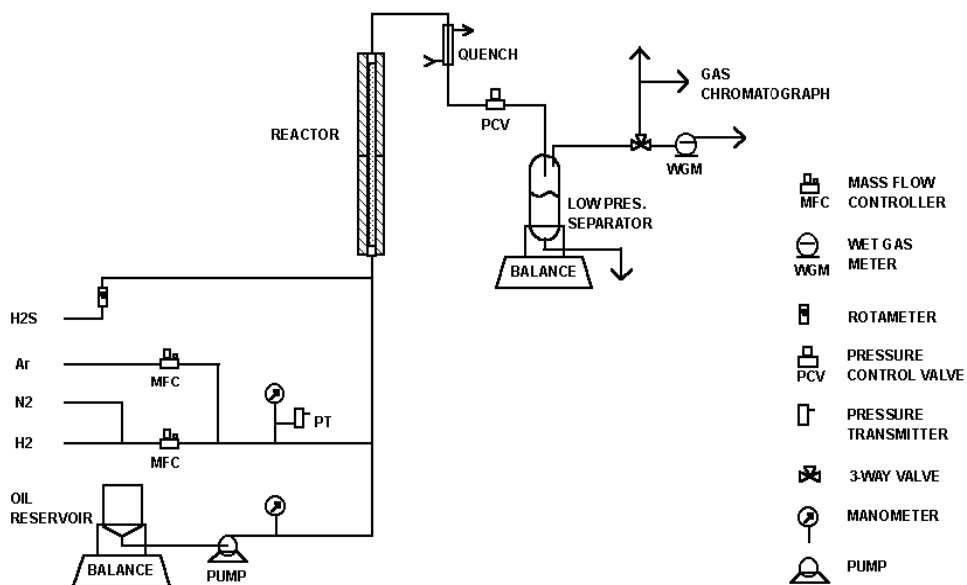


Figure 3-1 High pressure setup for hydrotreating of light gas oil.

adjusted to the next set-point and the procedure was repeated with a shorter time for stabilization. The same procedure was followed for all set-points. The samples were subsequently collected once in approximately every 24 hours. No deactivation of the catalyst was observed over the experimental period (5 weeks).

3.1.4 Analysis

The gas oil composition before and after the hydroconversion was analyzed by the sulfur sensitive GC-AED. In the GC (HP 6890) the non-polar capillary column Chrompac WCOT CP-Sil 5 CB (30 m x 32 μm x 5 μm) was used. In AED (HP G2350) the sulfur (181 nm) and carbon (179 nm) emission lines were used for detection. He was used as the carrier gas.

The samples were also analyzed for total sulfur using an ANTEK 7000NS conventional combustion analyzer.

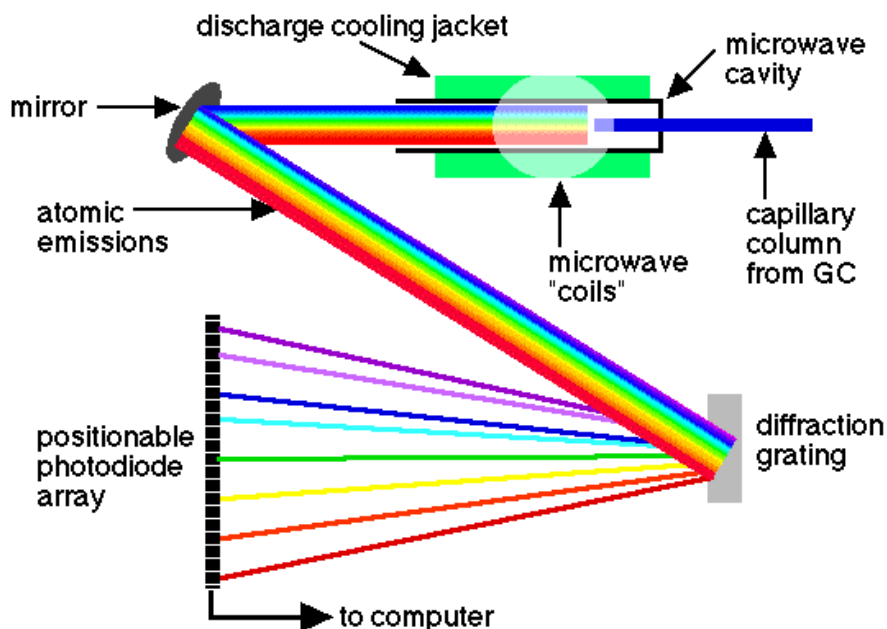


Figure 3-2 Principle of the atomic emission detector [240].

3.1.4.1 Principle of GC-AED

A gas chromatograph equipped with an atomic emission detector (GC-AED) was used for the off-line analysis of the collected samples. This detector is a useful alternative to the conventional ones. For instance, instead of measuring simple gas phase (carbon containing) ions created in a flame as with the flame ionization detector, or the change in background current because of electronegative element capture of thermal electrons as with the electron capture detector, the AED has a much wider applicability because it is based on the detection of atomic emissions¹.

The strength of the AED lies in the detector's ability to simultaneously determine the atomic emissions of many of the elements in analytes that elute from a GC capillary column. As eluants come off the capillary column they are fed into a microwave powered plasma (or discharge)

1. Atoms or molecules that are excited to high energy levels can decay to lower levels by emitting radiation (emission or luminescence). For atoms excited by a high-temperature energy source this light emission is commonly called atomic or optical emission.

cavity where the compounds are destroyed and their atoms are excited by the energy of the plasma. The light that is emitted by the excited particles is separated into individual lines via a photodiode array. The associated computer then sorts out the individual emission lines and can produce chromatograms made up of peaks from eluants that contain only a specific element. Schematic representation of the AED instrumentation is presented in Figure 3-2. The carrier gas is He, which is among the few elements not detected by the AED.

The combination of GC with AED can have advantageous applications in many fields of environmental chemistry. Applications include establishing the distribution of sulfur and metal compounds in petroleum feedstocks, screening for elements to quickly locate target or unknown peaks of interest in complex environmental matrices and easy quantification using virtually constant response factors (Agilent Technologies, Inc. [241]). Several groups have been studying and improving the properties and possible use of the GC-AED system. As an example, the retention-detection response relationships in the GC-AED were studied by Augusto and Valente [242], while Becker and Colmsjö [243] used GC-AED for quantification of polycyclic aromatic sulfur heterocycles.

In this work, the GC-AED method was used as a tool for a detailed analysis of LGO, to establish the distribution of sulfur compounds in petroleum feedstocks and products. Related to our work, the detection of sulfur and nitrogen compounds in refinery liquids by means of GC-AED was already done by Quimby *et al.* [244] and they optimized the method for the analysis of S and N compounds in gasoline through diesel-range materials. Kabe *et al.* [91] and Zhang *et al.* [95] used GC-AED to detect polyaromatic sulfur-containing compounds in the LGO with very good results. Stumpf *et al.* [245] also used GC-AED for an analysis of sulfur compounds in the gasoline range petroleum liquids. The sulfur sensitive GC-AED technique has already been found to be very useful in the molecular analysis of the sulfur components in LCO (Depauw and Froment [246]), medium cycle oil (Shin *et al.* [214]), and also in other applications [247-249].

It is clear that GC-AED is a powerful tool for sulfur analysis in the refining industry. It is a very sensitive (part-per-million levels) method and shows that the spectrum of sulfur compounds in the refinery liquids is very broad. However, the exact identification of all individual components is out of reach and only a few selected and well known compounds can be determined unequivocally.

3.2 Deactivation studies during thiophene HDS at atmospheric pressure

3.2.1 Materials

In this part of work the following catalysts were used: Mo/ γ -Al₂O₃, Mo(NTA)/ γ -Al₂O₃, NiMo/ γ -Al₂O₃, NiMo(NTA)/ γ -Al₂O₃, and two NiMoP/ γ -Al₂O₃ catalysts with different properties. NTA is an abbreviation for nitrilo-triacetic acid used as a chelating agent during the preparation. The fresh catalysts were supplied by AKZO Nobel Chemicals in extrudate form with the properties presented in Table 3-I. Prior to use, the extrudates were crushed and sieved to obtain a catalyst particle size in the range of 75-125 μ m. Thiophene (99+% without benzene, Acros Organics) was used as a model compound for this study.

Table 3-I: Composition and properties of catalysts used for the study of deactivation during thiophene HDS

	MoO ₃ (wt%) ^a	NiO (wt%) ^a	P ₂ O ₅ (wt%) ^a	Surface Area (m ² /g)	V _{pore} (cm ³ /g)
Mo	10.3	0	0	257	0.57
Mo (NTA)	10.1	0	0	150	0.40
NiMo	10.0	2.5	0	242	0.55
NiMo (NTA)	9.9	2.4	0	120	0.30
NiMoP (A)	20.0	4.8	5	195	0.48
NiMoP (B)	24.0	4.0	8	170 ^a	0.34 ^a

^a Analyses performed by AKZO Nobel (Amsterdam).

3.2.2 Apparatus

A schematic representation of the thiophene HDS setup used for the deactivation studies is shown in Figure 3-3. The reactions were carried out in a glass tube microreactor with a frit for holding the catalyst. To avoid hot spots in the catalyst bed, 0.5 g of the catalyst diluted with SiC (particle size \sim 400 μ m) in the 1:1 volume ratio was used. A piece of glass wool was placed above the catalyst bed to keep the catalyst bed in place. The reactor was heated using a programmable temperature controller and the temperature was monitored by a thermocouple positioned in the reactor directly on top of the catalyst bed. The parallel reactors enabled sulfiding of a catalyst for

the next experiment during the reaction in the first one. The off-gas stream passed through a bubble tank containing a NaOH solution, where H₂S was captured by forming Na₂S. NaOH pellets (Lamers&Pleuger, 95%) and indicator Indigo Carmine (Aldrich, dye content 85%) were used in the bubble tank for capturing the offgas. In the basic environment, Indigo Carmine has a yellow color which changes to blue in an acidic solution.

3.2.3 Procedures

The activation of the catalysts was done by transforming the metallic oxides to their corresponding sulfided phases. The sulfiding of catalysts was carried out by passing H₂ (30 ml/min) together with 10% H₂S/Ar (30 ml/min) mixture (H₂:H₂S ratio 10:1) through the reactor. The temperature was kept for 30 min at room temperature (usually between 28-30 °C) and then the reactor was heated up to the sulfiding temperature 405 °C at a heating rate of 10 °C/min (for the NTA catalysts the heating rate was 2 °C/min). After one hour at the constant sulfiding temperature the gas was switched from the sulfiding mixture to pure He flow (60 ml/min) and the temperature was decreased to the desired reaction temperature. The cooling under the He flow usually lasted for 20 min.

Immediately after the sulfiding step, the reaction was started by passing the H₂/thiophene mixture (in the majority of experiments, molar ratio = 22) or H₂/He/thiophene mixture (molar ratio of H₂/thiophene = 11) through the reactor. Gaseous thiophene was added to the H₂ or H₂/He gas stream by bubbling through liquid thiophene in a glass saturator kept at a constant temperature of 10 °C. The reaction temperature was between 250 and 400 °C (usually 400 °C for Mo catalysts and 300 °C for NiMo and NiMoP catalysts) and the pressure was 0.1 MPa. The reaction mixture flow was 110 ml/min. Immediately after the reaction, the gas was switched from H₂/thiophene or H₂/He/thiophene mixture to pure He and the reactor was cooled down. After 30 min, the He flow was switched off and the reactor was cooled down further without any gas flow. After cooling down to room temperature, the reactor was opened, the spent catalyst was then separated from the SiC by sieving and stored for characterization.

The restoration of the activity of the deactivated catalyst by resulfiding in H₂S/H₂ was studied as a helpful tool for getting insight into the mechanisms of the catalyst deactivation.

To check the effect of the H₂ partial pressure on the activity and coke deposition, experiments were carried out using a H₂ stream diluted 1:1 with He.

3.2.4 Analysis and characterization

Products were analyzed on-line by gas chromatograph equipped with a CHROMPAC column (50 m x 0.25 mm x 0.25 μm) with a CP-Sil 5 CB coating. Helium was used as a carrier gas. The temperature program used for the analysis was the following: initial temperature 30 °C was kept for 6 minutes, then increased at a heating rate of 15 °C/min to 175 °C and was kept there for 1 minute. The total time of the analysis was 18.5 minutes. An automatic sampler was used, the temperature of injector and detector (FID) was 250 °C. The main products were identified according to the Chrompack reference book [250], the relevant page from which is in Appendix A1.

The carbon and the sulfur content of the spent catalysts were measured using a "Leco CS 225" induction oven. An exactly determined amount of sample was combusted in a continuous O₂ gas flow. The C and S present in the sample were converted to CO₂ and SO₂, respectively, and the gas mixture was led through an infrared detector, which successively measured the CO₂ and SO₂ signals. Calibration of the analysis was done by use of a well-defined standard material. Each sample was measured twice as an independent duplicate to get information about the reproducibility.

BET surface areas were measured by means of a "Quantachrome Autosorb 6B" unit using N₂ physisorption at 77 K. Prior to the analyses, the samples were heated at 200 °C in vacuum for 16 hours. The pore size distribution was calculated by the Barrett-Joyner-Halenda (BJH) method applied to the desorption-branch of the isotherm.

Pore volume determinations were done using a "CE Instruments Pascal 140-440". Mercury intrusion curves were measured and the pore size distributions were calculated by the Washburn equation (assuming $\theta=140^\circ$).

Infrared (IR) spectra were acquired using a "Nicolet Magna-IR 550" FTIR spectrometer and a spectrum with a resolution of 4 cm⁻¹ was obtained by accumulating 256 scans. Pressed disks of the powdered catalyst were used for the analysis.

In situ Laser Raman spectroscopy experiments were performed with a "Renishaw Ramascope System 2000" coupled with a Leica microscope. The excitation source is a 514 nm, 20 mW Ar+

laser. Scattered Raman light is collected using a Leica 50x objective, filtered for Rayleigh scattering by a holographic filter, and directed to the spectrograph. The spectrograph is equipped with a moving grating and a Peltier-cooled CCD detector, which is read via a PC to obtain the Raman spectrum with a resolution of 2 cm^{-1} . Samples were prepared by cutting the catalyst particles (cylindrical extrudates) using a scalpel. Cross-section analysis was performed using a Prior automated XYZ stage coupled to the Raman software.

3.3 Kinetics of thiophene hydrodesulfurization at atmospheric pressure

3.3.1 Materials

In this part of work the following catalysts were used: commercial NiMo/ γ -Al₂O₃, commercial CoMo/ γ -Al₂O₃, and Pt/Y-zeolite (3Pt-C712-m1). The preparation of the Pt/Y-zeolite catalyst is described elsewhere [251]. The amount of Pt loaded on the zeolite was 0.3 wt%. Chemisorption measurements showed the metal dispersion of the catalyst (H:Pt) to be 0.03 and the Pt particle size 21.6 nm. The fresh commercial catalysts were supplied in extrudate form. Prior to use, the extrudates were crushed and sieved to obtain a catalyst particle size in the range of 75-125 μm . The Pt/Y-zeolite catalyst was in a powder form. The powder was tableted and tablets then crushed and sieved to obtain a catalyst particle size in the range of 75-125 μm . Thiophene (99+% without benzene, Acros Organics) was used as a model compound for this study.

3.3.2 Apparatus

The apparatus used in this part of work is shown in Figure 3-4. The reactions were carried out in a stainless steel tube microreactor with an inserted metal tube with a steel mesh supporting the catalyst, as presented in Figure 3-5. To avoid hot spots in the catalyst bed, 0.5 g of the catalyst diluted with SiC (88 μm) in a weight ratio 1:10 was used. An empty run without a catalyst was performed as well. The glass wool was placed below the catalyst bed to prevent the loss of fine particles of the catalyst by the flow of the reaction mixture. Above the catalyst bed, coarse SiC particles (1250 μm , ~20 g) were placed to obtain an evenly distributed temperature profile in the reaction mixture flow before the catalyst bed was reached. The reactor was heated using a programmable temperature controller and the temperature was monitored by a thermocouple

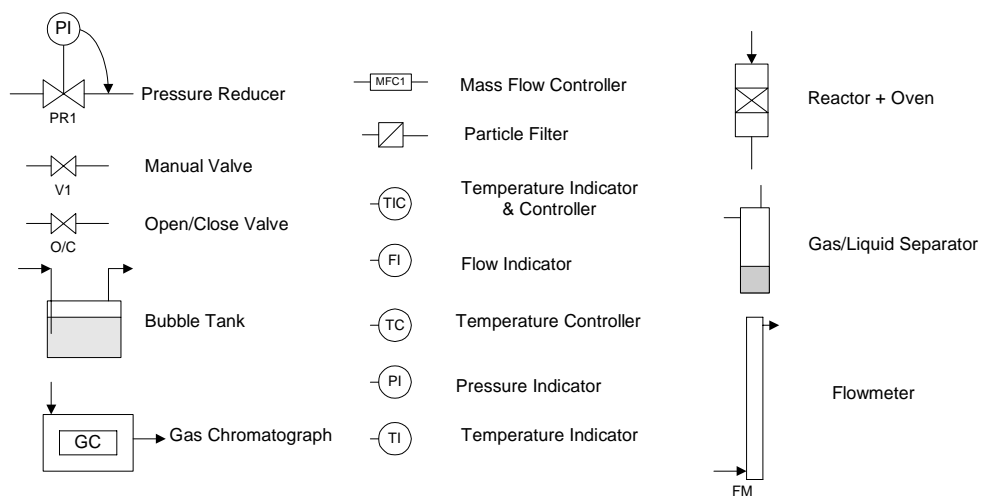
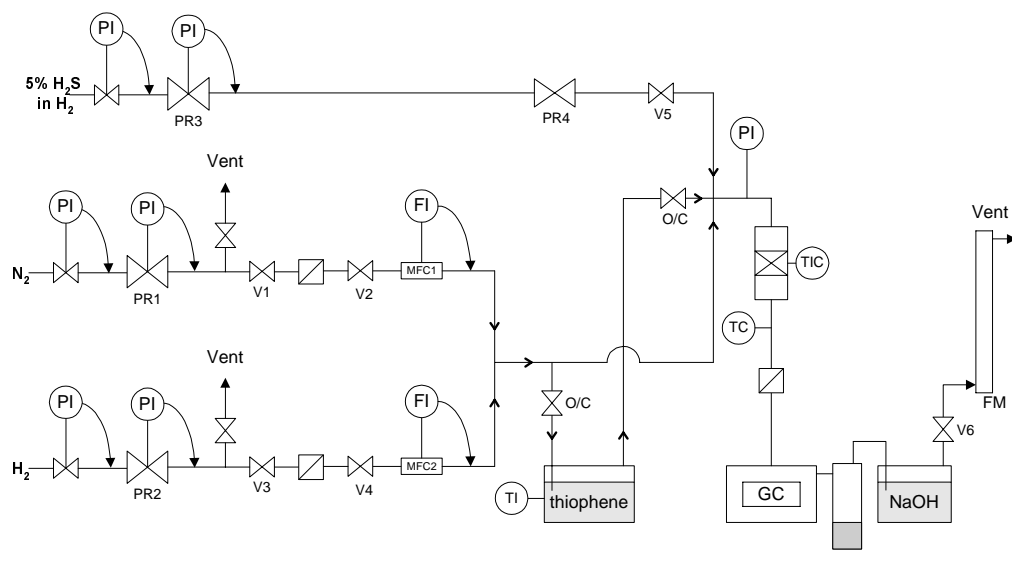


Figure 3-4 Experimental setup for thiophene HDS.

positioned in a metal tube in the reactor directly below the catalyst bed. The offgas stream passed through a bubble tank containing a 5M NaOH (pellets, extra pure, Merck) solution with the indicator Indigo Carmine (Merck), where H_2S was captured by forming Na_2S . The bubble tank for capturing the offgas was used in the same manner as was presented in chapter 3.2.2.

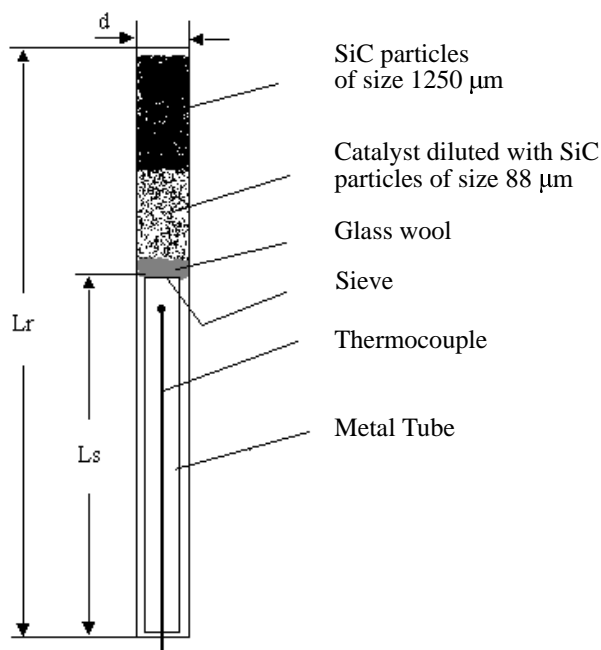


Figure 3-5 Drawing of the reactor (i.d. = 1 cm, L_r = 45 cm, L_s = 20 cm).

3.3.3 Procedures

Activation of the commercial catalysts based on molybdenum was done by transforming the metallic oxides to their corresponding sulfided phases. The sulfiding of the catalysts was carried out by passing a 5% $\text{H}_2\text{S}/\text{H}_2$ (60 ml/min) mixture through the reactor. The temperature was kept at 25 °C for 30 min and then the reactor was heated up to the sulfiding temperature 407 °C at a heating rate of 10 °C/min. After one hour at the constant sulfiding temperature, the reactor was cooled down to the desired reaction temperature under the flow of the $\text{H}_2\text{S}/\text{H}_2$ gas mixture. The same procedure was used for one series of experiments with the Pt/Y-zeolite catalyst. The second series of experiments with the Pt/Y-zeolite catalyst was performed on the reduced catalyst without sulfiding and the third series on the Pt/Y-zeolite catalyst without any activation at all. The Pt/Y-zeolite catalyst was calcined prior to use. The calcination step was done *off situ* in air by the following procedure: the temperature was increased with the heating rate of 1 °C/min from 20 °C

to 180 °C, kept at 180 °C for 3 hours, then increased by 1 °C/min to 400 °C and kept there for 9.5 hours. The flow of air during calcining was 290.7 cm³/min and the amount of the powdered catalyst was approximately 1 gram. After the calcination step the Pt/Y-zeolite catalyst was ready for activation treatment. The reduction of Pt/Y-zeolite was performed *in situ*. The catalyst was first dried in 200 ml/g_{cat}/min of N₂. The temperature was increased by 0.8 °C/min to 240 °C and kept there for 4 hours. Then N₂ was switched to H₂ (200 ml/g_{cat}/min), the temperature was increased to 409 °C at a heating rate of 10 °C/min, and kept there for 2 hours. After the reduction procedure the catalyst was cooled down to the reaction temperature under the H₂ flow.

Immediately after the pretreatment step and after the desired reaction temperature was reached, the reaction was started by passing the H₂/thiophene mixture (molar ratio = 37) through the reactor. Gaseous thiophene was added to the H₂ gas stream by bubbling through liquid thiophene in a glass saturator kept at a constant temperature of 0 °C in a water bath with ice. The vapor pressure of thiophene at these conditions according to the Antoine equation is 2484.9 Pa (Equation (2-8)) and the reaction mixture flow was 100 ml/min during all the experiments. The reaction temperature was between 200 and 400 °C for all catalysts studied and the pressure was 0.1 MPa. The system was left to stabilize overnight. The mixture of products at the given temperature was analyzed by on-line GC until the steady state was observed. The steady state was usually reached in about 6 hours. Then three consecutive analyses for the evaluation were taken and the reaction temperature was increased by 25 °C to the next experimental point. At this temperature the steady state was reached again, analyses taken, and the same procedure was repeated until the reaction temperature was 400 °C. Because of the observed lower activity of the Pt/Y-zeolite catalyst, these series did not follow all the temperature points of the “standard” experiments. The temperatures of performed experiments are given in the results section in Table 4-VII.

Each of the catalyst series was concluded by the repetition of the experiment at one of the lower temperatures to have an insight about the deactivation of the catalyst during the experimental period.

3.3.4 Analysis

The reaction products were analyzed on-line using a Chrompac CP 9000 gas chromatograph equipped with a WCOT fused silica column (100 m x 0.25 mm x 0.25 μm) with a CP-Sil 2 CB

coating. The oven temperature program was optimized during the experiments for the best peak resolution and the chromatograph was equipped with FID detector, which was heated to 250 °C. Injection temperature was 250 °C and He was used as a carrier gas. For NiMo/ γ -Al₂O₃ in the temperature region of 200 - 375 °C the following temperature program was used for the analysis: initial temperature 40 °C was kept for 1 minute, then increased by the heating rate of 5 °C/min to 175 °C and kept there for 2 minutes. The total time of analysis was 27 minutes, but the peak resolution of the products was not very good, thus for all other experiments at all catalysts the temperature program was changed to the following multirise program: initial temperature of 35 °C was kept for 9 minutes, then increased by 5 °C/min to 60 °C, then increased by 10 °C/min to 175 °C and kept there for 2 minutes. The total time of analysis was 28 minutes with reasonably good resolution of the product peaks. The main products were identified according to the Chrompack reference book [250], the relevant page from which is in Appendix A1.

3.4 High-pressure studies of dibenzothiophene HDS and the “matrix effect”

3.4.1 Materials

In this part of work only a commercial NiMo/ γ -Al₂O₃ catalyst was used. The fresh catalyst was supplied in extrudate form. Prior to use, the extrudates were crushed and sieved to obtain a catalyst particle size in the range of 75-125 μ m. The solution of 0.1 wt% of dibenzothiophene (pure, Fluka Chemika) in n-heptane (HPLC grade, Rathburn Chemicals Ltd.) was used as a feed for this study. The matrix effect studies were done with dimethyldisulfide (>98%, Fluka Chemika), thiophene (99+% without benzene, Acros Organics), toluene (p.a., Prolabo), and naphthalene (Merck). Cyclohexylbenzene (98%, Acros Organics), biphenyl (Merck), and bicyclohexyl (99%, Acros Organics) were used for the identification of the reaction products.

3.4.2 Apparatus

The apparatus used in this part of work is shown in Figure 3-6. The reactions were carried out in a stainless steel tube microreactor with inserted metal tube with a steel mesh supporting the catalyst, as presented in Figure 3-5. To avoid hot spots in the catalyst bed, 0.1 g of the catalyst diluted with SiC (88 μ m) in a weight ratio 1:10 was used. An empty run without a catalysts was

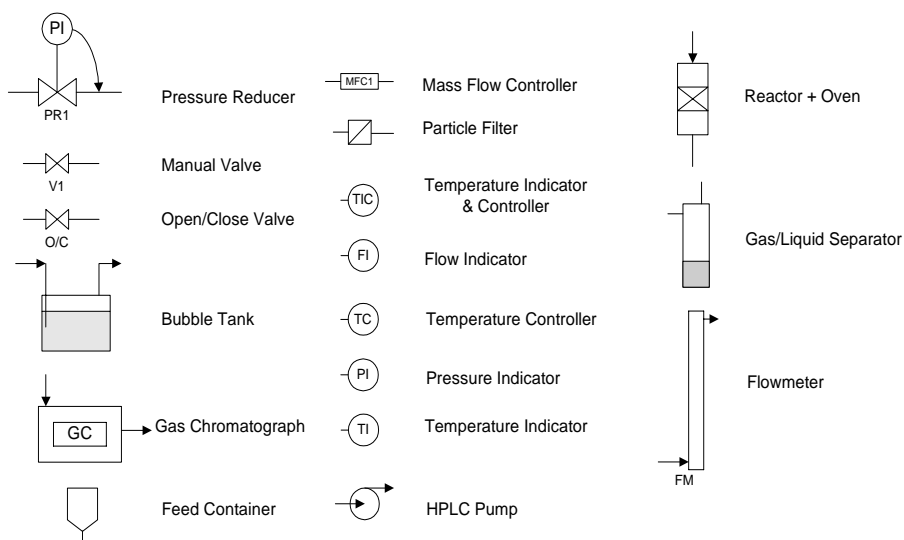
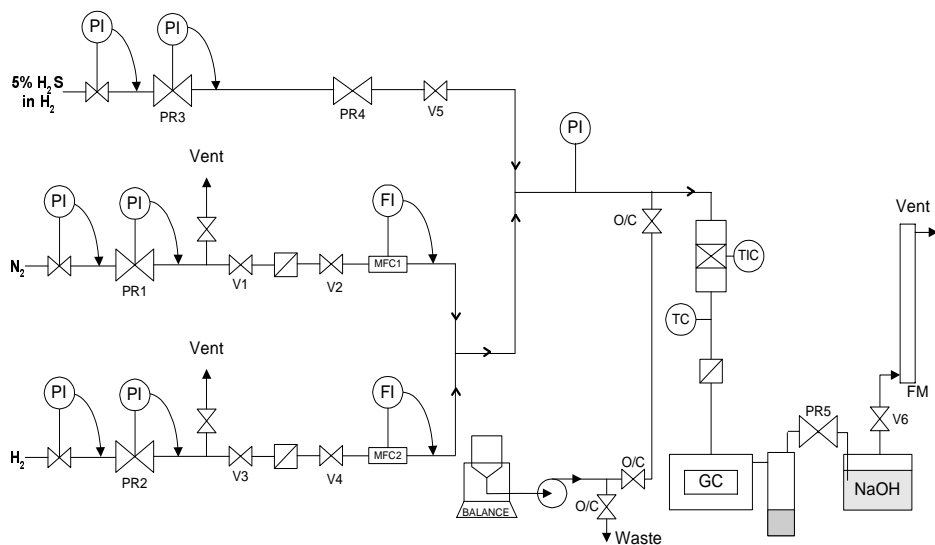


Figure 3-6 Apparatus for a high-pressure study of DBT HDS and matrix effect.

performed as well. The glass wool was placed below the catalyst bed to prevent the loss of fine particles of the catalyst by the flow of the reaction mixture. Above the catalyst bed, coarse SiC particles (1250 μm , ~ 20 g) were placed to obtain an even temperature profile in the reaction mixture flow before the catalyst bed was reached. The reactor was heated using a programmable temperature controller and the temperature was monitored by a thermocouple positioned in a metal sheet in the reactor directly below the catalyst bed. The liquid product mixture was collected in the liquid-gas separator, which was emptied regularly. All lines from the reactor to the separator were heated to approximately 250 $^{\circ}\text{C}$ to avoid condensation in the lines. The back pressure valve was positioned downstream of the separator. The offgas stream passed through a bubble tank containing a 5M NaOH (pellets, extra pure, Merck) solution with the indicator Indigo Carmine (Merck), where H_2S was captured by forming Na_2S . The bubble tank for capturing the offgas was used in the same manner as was presented in chapter 3.2.2.

3.4.3 Procedures

The sulfiding of $\text{NiMo}/\gamma\text{-Al}_2\text{O}_3$ was done by the same process as described in chapter 3.3.3. After the sulfiding procedure the reactor was cooled down to the desired reaction temperature under N_2 flow.

Immediately after the pretreatment step and after the desired reaction temperature was reached, the reaction was started by passing a $4 \cdot 10^4$ molar ratio of H_2 to dibenzothiophene (DBT) through the reactor. DBT was dissolved in n-heptane and the solution was pumped by a HPLC pump into the top of the reactor, where it was mixed with H_2 . The liquid flow rate was controlled by keeping the liquid reservoir on a balance. The system was left to stabilize overnight before the data were measured. The mixture of products at the given temperature was analyzed by on-line GC. A steady state was usually reached in about 6 hours. Then three consecutive analyses for the evaluation were taken and the conditions were changed. The steady state was reached again, analyses taken, and the same procedure was repeated.

Based on initial experiments, the conditions chosen for the study of the matrix effect were: $P = 2$ MPa, $T = 200$ $^{\circ}\text{C}$, $\text{LHSV} = 21.4$ h^{-1} , and the ratio of H_2 and DBT + n-heptane mixture = 203 Nm^3/Nm^3 . The main solvent used for DBT was n-heptane, but for the study of the matrix effect also other compounds were used in the mixture as an inhibitor or co-solvent. The compositions of

the feeds used in this study are presented in Table 3-II. The molar ratio between H_2 and DBT was kept constant.

After the results were obtained for the given feed mixture of DBT/n-heptane with an inhibitor, the feed was changed back to the pure 0.1 wt% DBT in n-heptane and the system was left to reach the same steady state conversion as before the introduction of the new feed. This is demonstrated in Appendix A2, where one can see that the steady-state was reached after approximately 6 hours. By this procedure it was ensured that the inhibition (matrix) effect study was performed every time on the same state of the catalyst (non-inhibited, non-deactivated).

Table 3-II: The compositions of the feed for DBT experiments

Reactants	Solvent	Characteristics of feed
<i>DBT^a</i>	<i>n-heptane</i>	<i>0.02 wt% S</i>
DBT+DMDS	n-heptane	0.10 wt% S
DBT+DMDS	n-heptane	0.07 wt% S
DBT+DMDS	n-heptane	0.04 wt% S
DBT+Thiophene	n-heptane	0.10 wt% S
DBT+Thiophene	n-heptane	0.07 wt% S
DBT+Thiophene	n-heptane	0.04 wt% S
DBT	n-heptane + toluene	50 wt% aromatics
DBT	n-heptane + toluene	25 wt% aromatics
DBT	n-heptane + toluene	10 wt% aromatics
DBT	n-heptane + naphthalene	10 wt% aromatics

^a Standard solution used throughout the whole study.

The experiments had to be stopped for a period of 10 days during this study and the catalyst was “conserved” in the reactor for this period of time under the temperature of 200 °C and pressure 2 MPa. The procedure of “conservation” was following: The feed to the reactor was changed to pure n-heptane and the H_2 flow was increased to remove sulfur species from the catalytic system. The removal of sulfur compounds was confirmed by the chromatographic analysis. After about 3 hours under the described conditions, when the removal of sulfur species was confirmed, the liquid feed to the reactor was stopped. After the next 2 hours the H_2 flow was decreased to the value which assured the pressure in reactor to stay 2 MPa. The experiments after the “conservation” showed no effect of this treatment on the activity of the catalyst.

3.4.4 Analysis

The analysis of the products was done by the same means as in the case of thiophene HDS described in chapter 3.3.4. The chromatograph was equipped with a flame ionization detector kept at 250 °C. The injection temperature was 250 °C and He was used as the carrier gas. The only change was that of the temperature program for the column, because of the heavier compounds. The following temperature program was used for the analysis: initial temperature 120 °C was kept for 10 minutes, then increased by a heating rate of 5 °C/min to 200 °C and kept there for 35 minutes. The total time of analysis was 53 minutes with reasonably good resolution of product peaks. The products were identified using their boiling points and standards.

4. RESULTS

4.1 High-pressure HDS of light gas oil

4.1.1 Use of GC-AED for analysis of light gas oil

A light gas oil (LGO) was hydrotreated over a commercial NiMo catalyst in the upflow reactor described in chapter 3.1.

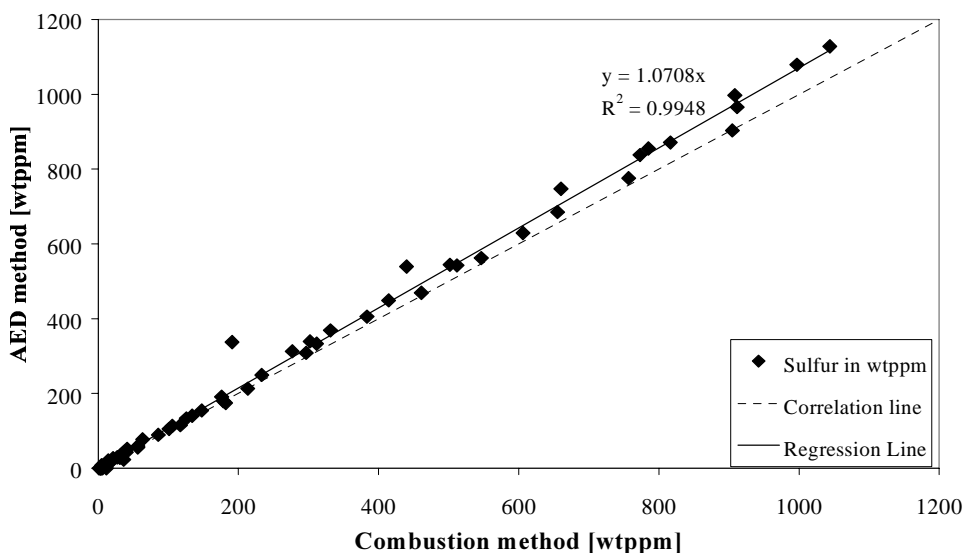


Figure 4-1 Correlation of GC-AED and a standard combustion analysis used for obtaining total amount of sulfur. Every GC-AED chromatogram in this analysis was evaluated as a single peak.

To ensure the relevance of the GC-AED method for analysis, several samples with a wide range of sulfur contents were analyzed. Figure 4-1 shows that the total amount of sulfur in samples obtained by the quantitative evaluation of GC-AED chromatograms is in very good agreement with the sulfur amount obtained by a standard combustion method. To achieve this agreement, the quantitative evaluation of chromatograms includes computer integration of the

whole spectrum as one peak (in a restricted retention time range determined by the lowest and highest retention time of sulfur components in the feed (Appendix A3) and the calculation of the amount of sulfur according to Equation (4-1),

$$wtppm = \frac{A_S \cdot 10000}{A_{C_{tot}} \cdot RF} \cdot 100 \quad (4-1)$$

where A_S is an area of the whole sulfur spectrum in the sulfur 181 nm AED, $A_{C_{tot}}$ is an area of the whole spectrum in the carbon 179 nm AED, and RF is a response factor for the used chromatographic system determined from the processing of standard samples. Only a few selected sulfur components can be analyzed individually, since the number of sulfur peaks is large and resolution is insufficient to allow separation of each peak. A large proportion of the total

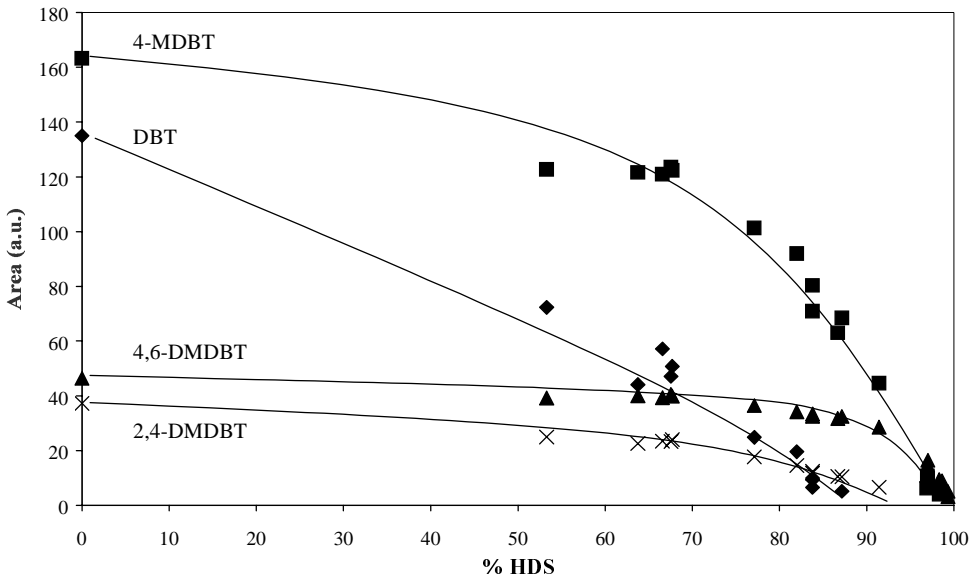


Figure 4-2 Behavior of selected sulfur components of light gas oil at several levels of HDS reaction. NiMo catalyst, pressure 4 MPa, $H_2/oil = 200 \text{ Nm}^3/m^3$. DBT: dibenzothiophene; 4-MDBT: 4-methyldibenzothiophene; 2,4-DMDBT: 2,4-dimethyldibenzothiophene; 4,6-DMDBT: 4,6-dimethyldibenzothiophene.

sulfur in the untreated fraction appears as an unresolved background envelope in the middle boiling-point range of the oil (Appendix A3).

4.1.2 Hydrodesulfurization activity of NiMo/ γ -Al₂O₃

The conditions for this study were chosen to be industrially relevant (total pressure 4 MPa, temperature range 250 - 400 °C, and the space velocity was varied to achieve a range of sulfur conversions).

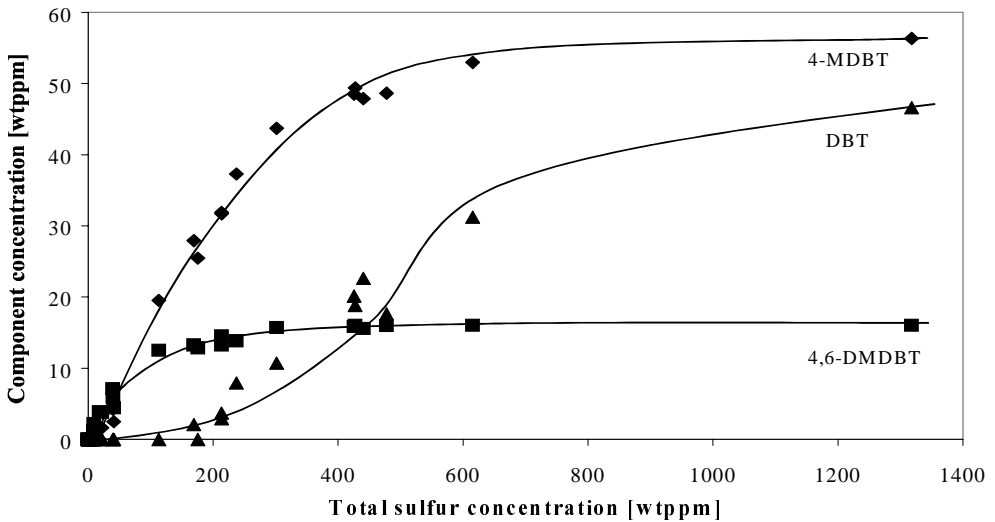


Figure 4-3 Concentration of individual sulfur components as a function of the total concentration of sulfur in the treated oil. NiMo catalyst, pressure 4 MPa, H_2 /oil = 200 Nm³/m³. DBT: dibenzothiophene; 4-MDBT: 4-methyldibenzothiophene; 4,6-DMDBT: 4,6-dimethyldibenzothiophene.

Figure 4-2 shows the difference in behavior of selected components of the oil fraction as a function of the total HDS conversion. The area on the Y-axis represents the integrated peak of selected sulfur component in each chromatogram. It is evident that certain substituted dibenzothiophenes, especially 4,6- and 2,4-dimethyldibenzothiophene (4,6- and 2,4-DMDBT,

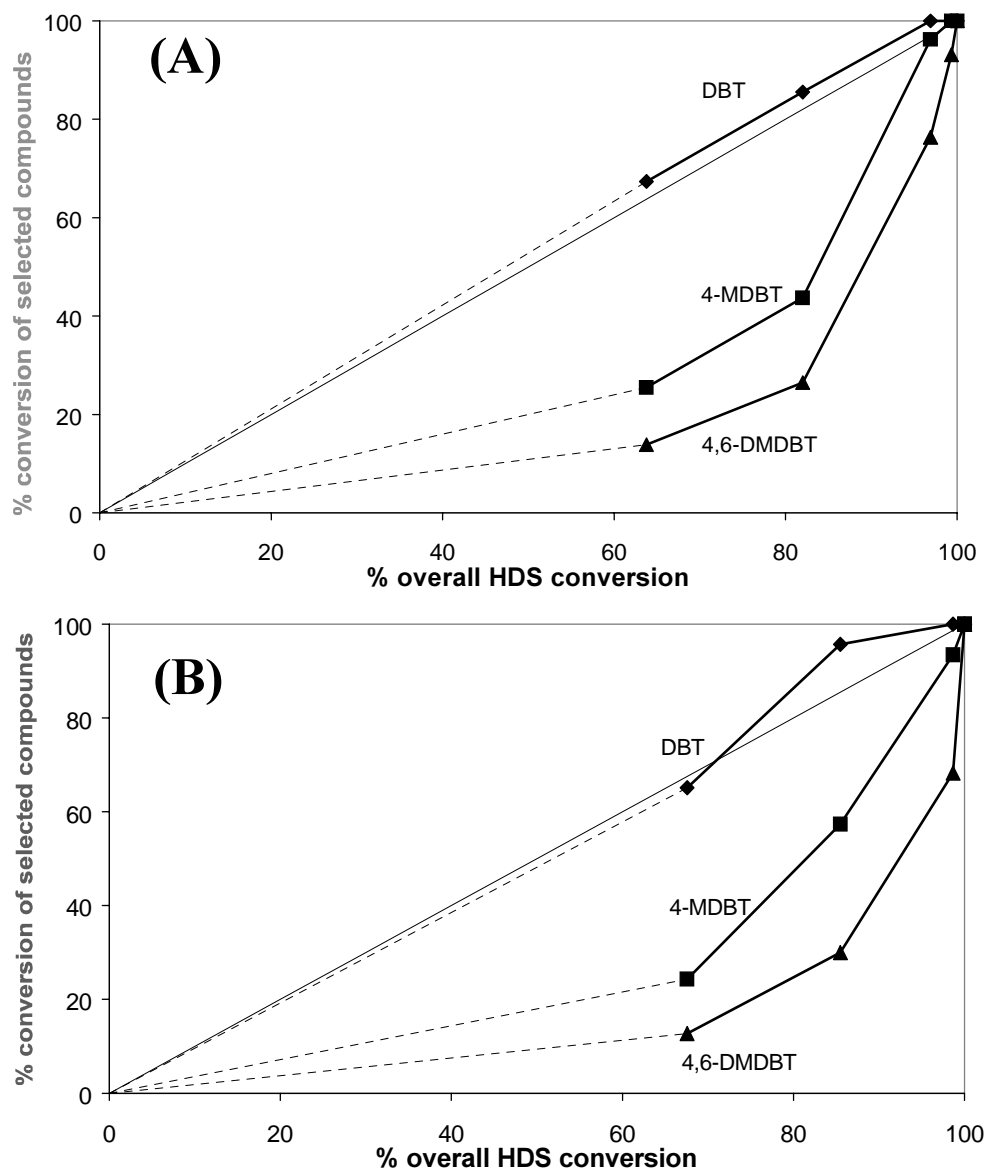


Figure 4-4 The correlation between the overall HDS conversion and the conversions of selected individual compounds. NiMo catalyst, LHSV = 1 h⁻¹ (A) and 2 h⁻¹ (B), pressure 4 MPa, H₂/oil = 200 Nm³/m³. DBT: dibenzothiophene; 4-MDBT: 4-methyldibenzothiophene; 4,6-DMDBT: 4,6-dimethyldibenzothiophene.

respectively), are the most resistant sulfur compounds in the mixture and that all of them show very similar behavior. It was found that it is easier to remove 4-methyldibenzothiophene (4-MDBT) but there is still a large difference between the reactivity of this compound and that of unsubstituted dibenzothiophene (DBT). The only exception is one unidentified DMDBT (not shown in the figure) at 250 °C, which can be speculated to be 2,8-DMDBT in accordance with other studies in the literature [189][190]. This compound seems to be even more reactive than DBT, but this behavior was not observed at higher temperatures.

Figure 4-3 shows the removal of individual sulfur compounds as a function of the total desulfurization over the NiMo catalyst. DBT disappears first and is followed by 4-MDBT, which starts to react in the region of 450 wtppm of total product sulfur amount. The concentration of 4,6-DMDBT is not significantly reduced before the total amount of sulfur in the product is ca. 150 wtppm.

The correlation between the overall HDS conversion and the conversions of the selected individual compounds is presented in Figure 4-4 for two studied space velocities. Results from the other two studied LHSV, 0.5 h⁻¹ and 4 h⁻¹, are shown in Appendix A4 (A) and (B), respectively. It shows again that DBT is the most reactive of the single compounds identified here. From the comparison of the figures for different LHSVs one can see that at certain conditions (temperature, pressure, LHSV, studied gas oil), the behavior of DBT closely resembles the overall behavior of the oil fraction, which can be used with advantages for further studies.

4.1.3 Kinetic studies

Equations used for the kinetic calculations were presented in chapter 2.1. Kinetic plots of DBT, 4-MDBT, and 4,6-DMDBT at 275 °C are shown in Figure 4-5. The focus will be mainly held on 275 °C, because the data obtained at this temperature were the only data set suitable for kinetic analysis. Kinetic plots for temperatures 250 °C and 300 °C are presented in Appendix A5 (A) and (B), respectively. The experiments at higher temperatures (the region 300 - 400 °C) lead to almost 100 % conversion of all the studied components and thus it was not possible to obtain the data for kinetic analysis. The hydrodesulfurization of each component was treated as a pseudo-first-order reaction (in accordance with literature, see e.g. Letourneur *et al.* [252]) and an approximate linear relationship was observed for each component. Rate constants obtained at different reaction temperatures were calculated from the regression lines and are listed in Table 4-I.

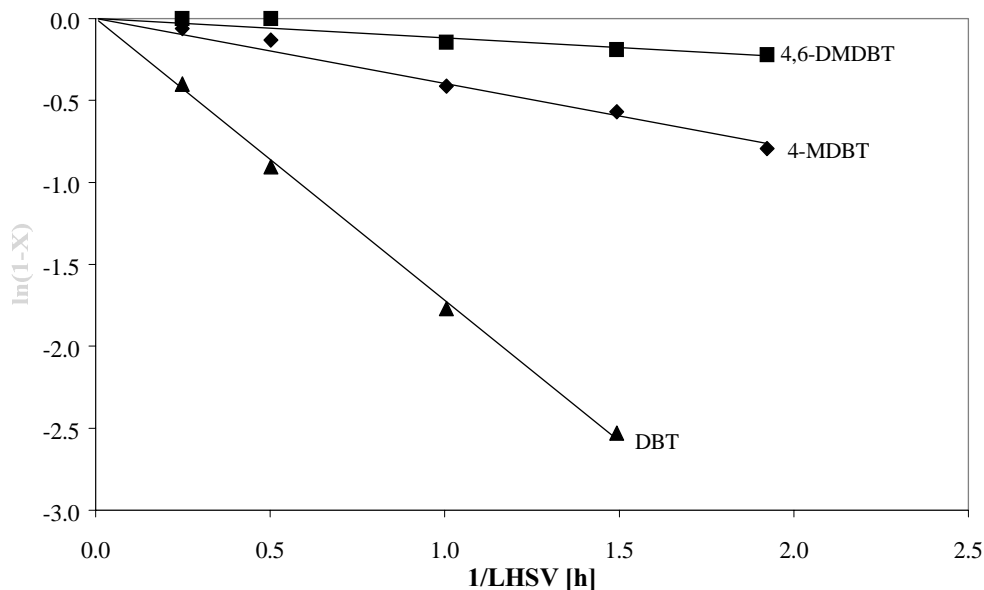


Figure 4-5 Pseudo-first-order plots of dibenzothiophene (DBT), 4-methyldibenzothiophene (4-MDBT), and 4,6-dimethyldibenzothiophene (4,6-DMDBT). NiMo catalyst, reaction temperature 275 °C, pressure 4 MPa, $H_2/oil = 200 \text{ Nm}^3/m^3$.

The calculated rate constants support the qualitative observations made above. The rate of disappearance of DBT is at all temperatures studied here much higher than that of the other two components. Table 4-I contains the rate constants of HDS at different temperatures and relative ratio of the rate constants for selected components based on the rate constant of 4,6-DMDBT. The

Table 4-I: Pseudo-first-order rate constants of desulfurization of DBTs at different temperatures over a NiMo catalyst, pressure 4 MPa, $H_2/oil = 200 \text{ Nm}^3/m^3$

Temperature	250 °C		275 °C		300 °C	
	k [s ⁻¹]	Ratio	k [s ⁻¹]	Ratio	k [s ⁻¹]	Ratio
DBT	$1.5 \cdot 10^{-4}$	57.7	$4.8 \cdot 10^{-4}$	14.6	$1.6 \cdot 10^{-3}$	7.4
4-MDBT	$2.7 \cdot 10^{-5}$	10.4	$1.1 \cdot 10^{-4}$	3.4	$5.6 \cdot 10^{-4}$	2.5
4,6-DMDBT	$2.6 \cdot 10^{-6}$	1.0	$3.3 \cdot 10^{-5}$	1.0	$2.2 \cdot 10^{-4}$	1.0

difference in relative reactivity of the DBTs studied here changes drastically with changing temperature. While at 250 °C the ratio of rate constants of DBT, 4-MDBT, and 4,6-DMDBT was found to be 57.7 : 10.4 : 1.0, respectively, the same ratio at 300 °C was 7.4 : 2.5 : 1.0. It is necessary to mention that some data obtained at 250 °C and especially at 300 °C show quite a big scattering, but the trend is still very clear: At higher temperatures the difference in reactivity is smaller.

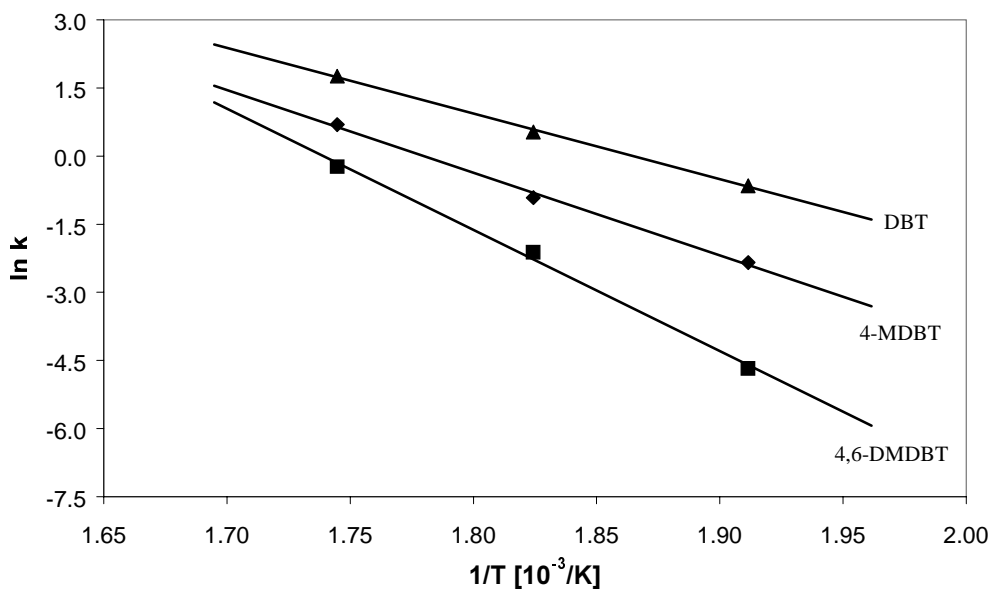


Figure 4-6 Arrhenius plots of dibenzothiophene (DBT), 4-methyldibenzothiophene (4-MDBT), and 4,6-dimethyldibenzothiophene (4,6-DMDBT). NiMo catalyst, pressure 4 MPa, $H_2/oil = 200 \text{ Nm}^3/\text{m}^3$.

Arrhenius plots of DBT, 4-MDBT, and 4,6-DMDBT, based on pseudo-first-order rate constants calculated from the slopes of straight lines plotted through experimental points at kinetic plots (Figure 4-5) for different temperatures, are presented in Figure 4-6. The activation energies calculated from the slopes of the straight lines for DBT, 4-MDBT, and 4,6-DMDBT are 120, 151, and 222 kJ/mol, respectively.

A more detailed look at the behavior of these components with temperature reveals some interesting differences. By isolating experiments at fixed space velocity, it is evident that 4,6-

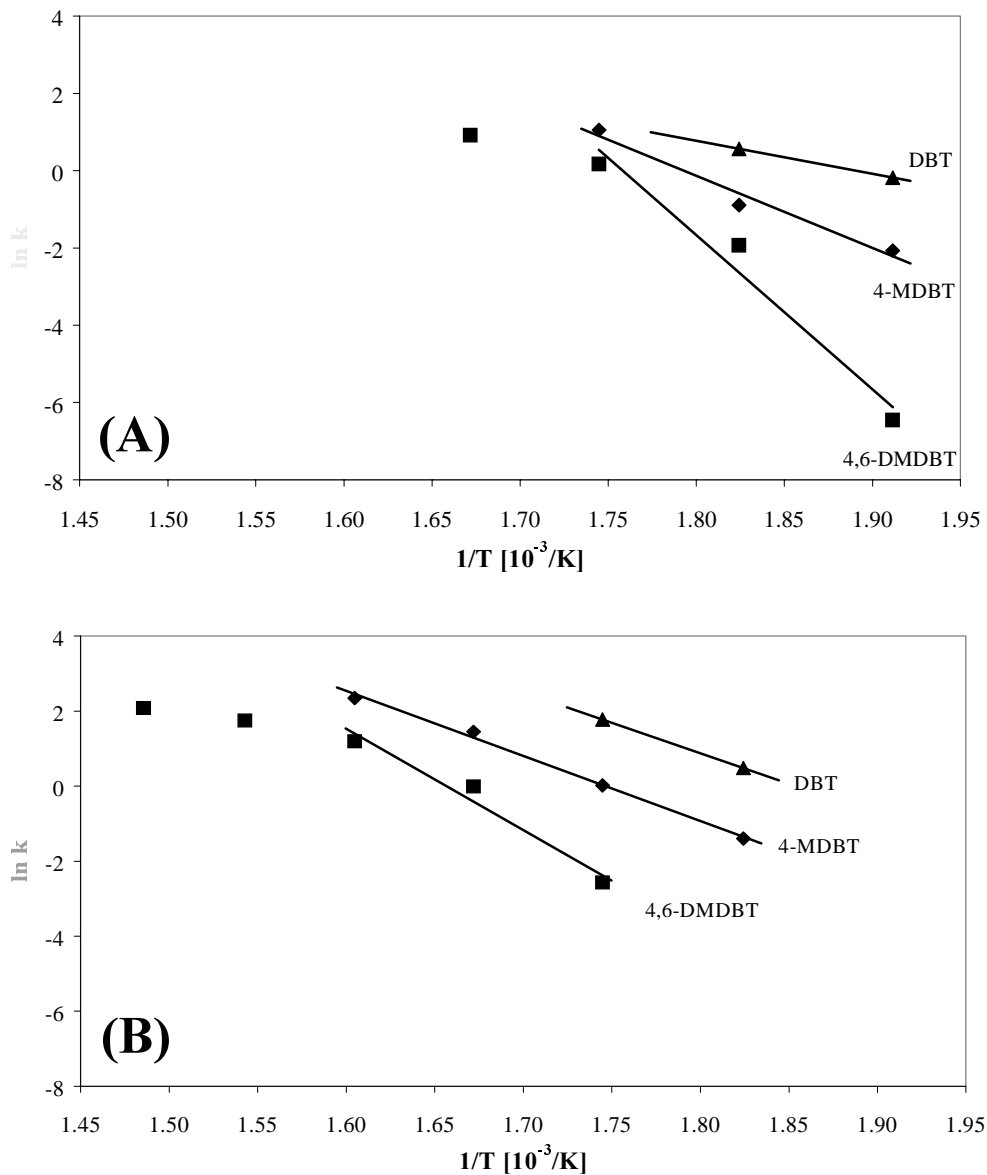


Figure 4-7 Arrhenius plots of dibenzothiophene (DBT), 4-methyldibenzothiophene (4-MDBT), and 4,6-dimethyldibenzothiophene (4,6-DMDBT) based on Equation (4-2). LHSV 1 h⁻¹ (A) and 4 h⁻¹ (B), NiMo catalyst, pressure 4 MPa, H₂/oil = 200 Nm³/m³.

DMDBT shows a different behavior compared to other compounds. Arrhenius plots of pseudo-first-order rate constants of DBT, 4-MDBT, and 4,6-DMDBT calculated from the Equation (4-2) at LHSV 1 h^{-1} and 4 h^{-1} are presented in Figure 4-7. Experimental results from LHSV 0.5 h^{-1} and 2 h^{-1} are shown in Appendix A6. Experimental points for DBT and 4-MDBT at higher temperatures are not shown since the conversion of these compounds was complete at the given conditions.

$$k = LHSV \cdot \ln \frac{ppm_{feed}}{ppm_{product}} \quad (4-2)$$

The activation energies were calculated from the slopes of the straight lines (selected points in the lower temperature range) indicated in the figure and are presented in Table 4-II for all studied LHSVs. A very high reactivity and thus a high conversion of DBT at the conditions used here makes it very difficult to follow the kinetics of DBT. The reported results (Table 4-II) are based only on two experimental points, and should therefore be treated with some caution. Nevertheless, the trends are similar and the absolute numbers agree quite well with the activation energies obtained from the data in Figure 4-6.

Table 4-II: Apparent activation energies of desulfurization of DBTs at different LHSVs over NiMo catalyst, pressure 4 MPa, $\text{H}_2/\text{oil} = 200 \text{ Nm}^3/\text{m}^3$

LHSV [h^{-1}]	E_a [kJ/mol]			
	0.5	1.0	2.0	4.0
DBT ^a	N.D.	71	129	136
4-MDBT	157	155	162	144
4,6-DMDBT	240	332 ^b	N.D.	224 ^c

N.D.: not determined.

^a Activation energies of DBT calculated from two obtained experimental points.

^b Activation energy of 4,6-DMDBT using experimental points only up to $300 \text{ }^\circ\text{C}$.

^c Activation energy of 4,6-DMDBT using experimental points only up to $350 \text{ }^\circ\text{C}$.

4.2 Deactivation studies during thiophene HDS at atmospheric pressure

4.2.1 Initial deactivation behavior

Conversions of thiophene as a function of time on stream (TOS) for molybdenum catalysts are presented in Figure 4-8. At 400 °C, the Mo catalyst prepared by a standard impregnation method shows slightly higher activity towards thiophene HDS than the Mo catalyst prepared with nitrilotriacetic acid (NTA) as a chelating agent. The shape of the deactivation curve is the same for both catalysts and the activity (measured as the conversion of thiophene) is approximately halved after four hours on stream. The initial deactivation is very fast, but after approximately two hours on stream the deactivation rate decreases considerably. At 300 °C, the standard Mo catalyst shows no change in activity during two and half hours on stream.

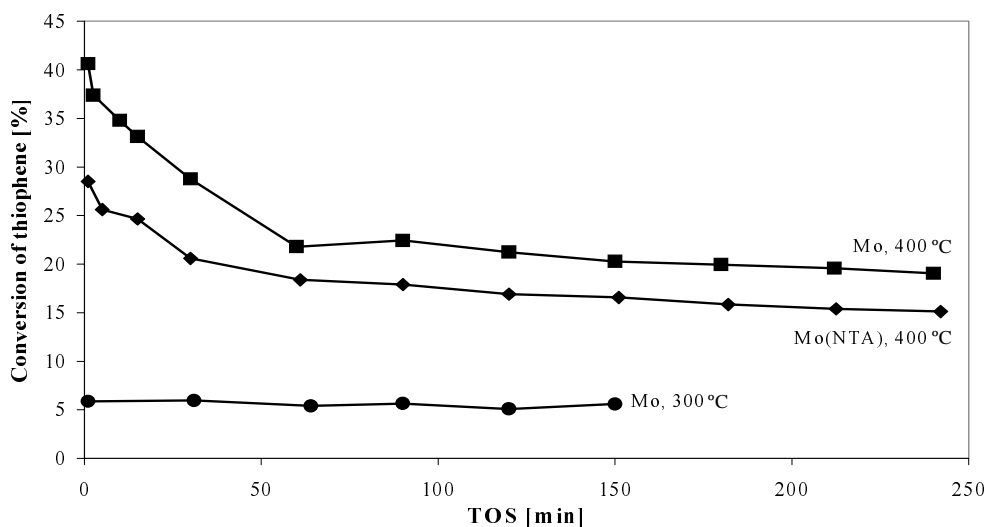


Figure 4-8 Comparison of the deactivation behavior of molybdenum catalysts prepared by the standard impregnation method and by the reaction with complexing agent NTA. Pressure 0.1 MPa, reaction temperatures 300 °C and 400 °C.

The activity of the NiMo catalyst prepared by the standard impregnation method is about 20 % higher than that of the NTA based NiMo catalyst at 300 °C, as presented in Figure 4-9. For NiMo,

a fast initial deactivation, seen as a loss of approximately 15 % of the initial conversion, is observed during the first 30 min on stream. After that time, the deactivation rate decreases and the conversion drops a further 5 % of the activity in the subsequent 210 minutes on stream. The deactivation of the NiMo (NTA) is less severe and a "steady-state" is reached already after ca. 15 min with a loss of activity of about 8 %.

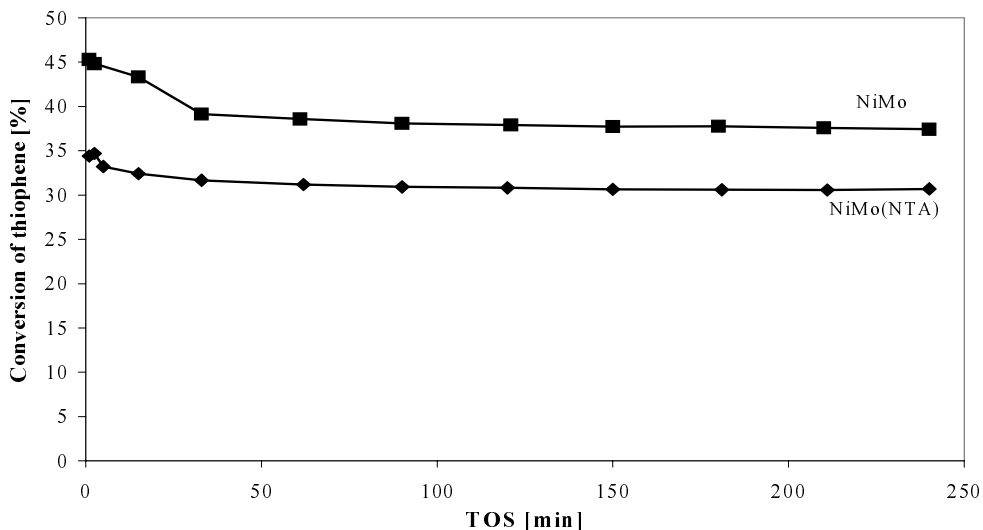


Figure 4-9 Comparison of the deactivation behavior of NiMo catalysts prepared by the standard impregnation method and by the reaction with complexing agent NTA. Pressure 0.1 MPa, reaction temperature 300 °C.

Results from experiments with a smaller amount of the standard NiMo catalyst (0.1g) and twice the flow rate of hydrogen (200 ml/min) at reaction temperatures 300 and 400 °C are presented in Figure 4-10. At 300 °C, the catalyst behaves similarly as during the experiments with standard reaction conditions, but the deactivation is slightly more severe. The decrease in conversion during the initial 30 minutes is about 20 % and the total loss after 240 minutes on stream is nearly 25 %. At 400 °C, the overall activity is much higher and the deactivation behavior resembles that of the Mo catalyst. The activity decreases considerably during the first 60-90 minutes on stream and the "steady-state" is not reached, even after 240 min on stream. The total decrease in conversion is nearly 50 %.

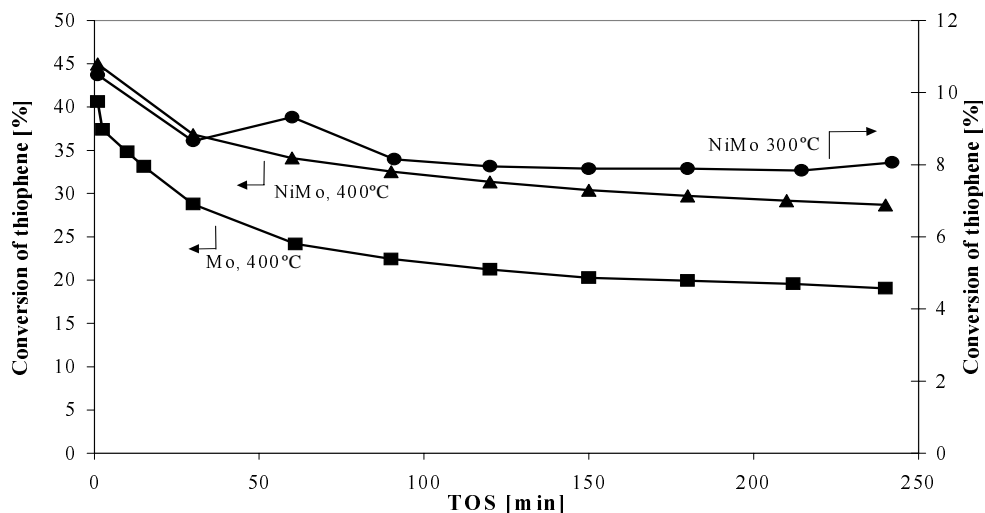


Figure 4-10 Deactivation behavior of the standard NiMo catalyst at different reaction conditions (0.1g of catalyst, flow rate of $H_2 = 200$ ml/min) compared to standard experiment with the Mo catalyst (0.5g of catalyst, flow rate of $H_2 = 100$ ml/min). Pressure 0.1 MPa, reaction temperatures 300 °C and 400 °C.

In Figure 4-11, a comparison of the deactivation behavior of two NiMoP catalysts with different metal loading at 300 °C is presented. NiMoP (A) has a lower Mo and P content and a higher Ni loading than NiMoP (B) and the metal content of both NiMoP catalysts is twice as high as that of NiMo catalysts (see Table 3-I). The conversion of thiophene over NiMoP (A) is about 5 % higher than over NiMo, while the activity of NiMoP (B) is virtually the same as that of NiMo. Deactivation curves of both NiMoP catalysts are similar to those of NiMo catalysts and a loss of activity is in the same range of about 20 %. Again, the fast initial deactivation followed by the "steady-state" is observed.

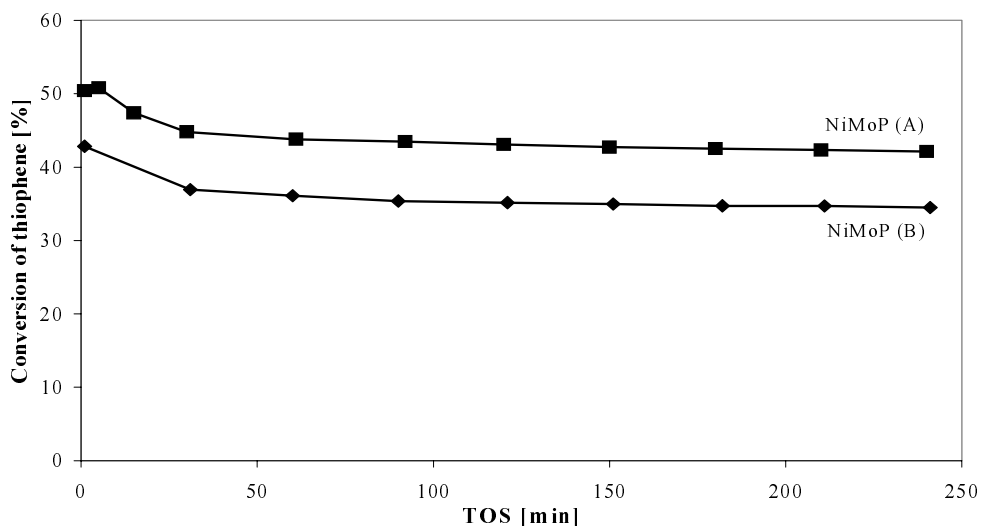


Figure 4-11 Comparison of deactivation behavior of NiMoP catalysts with different metal loading (for more details see Table 3-I). Pressure 0.1 MPa, reaction temperature 300 °C.

4.2.2 Reactivation experiments

Treatment of the Mo catalyst with the standard sulfiding mixture (10% H₂S in Ar + H₂) for 60 minutes after 90 minutes on stream was performed at reaction temperatures of 350, 375, and 400 °C. Resulting leads to a recovery of the considerable part of the lost activity as one can see from the top part of Figure 4-12. One can also see that the deactivation of the standard Mo catalyst is more severe at higher temperatures (see the bar termed “steady-state”). The loss of activity increases with increasing reaction temperature, while the relative gain of activity, calculated as a ratio between the activity after and before resultfiding, is almost constant.

Similar experiments were performed with the standard NiMo catalyst at reaction temperatures 250, 275, 300, and 350 °C and results are presented in the lower part of Figure 4-12. The catalyst was again treated with the standard sulfiding mixture for 60 minutes after 120 minutes on stream. This treatment of the NiMo catalyst leads to a close to total recovery of the initial activity and after thiophene is re-introduced, the behavior of the resultfided catalyst follows closely that of a

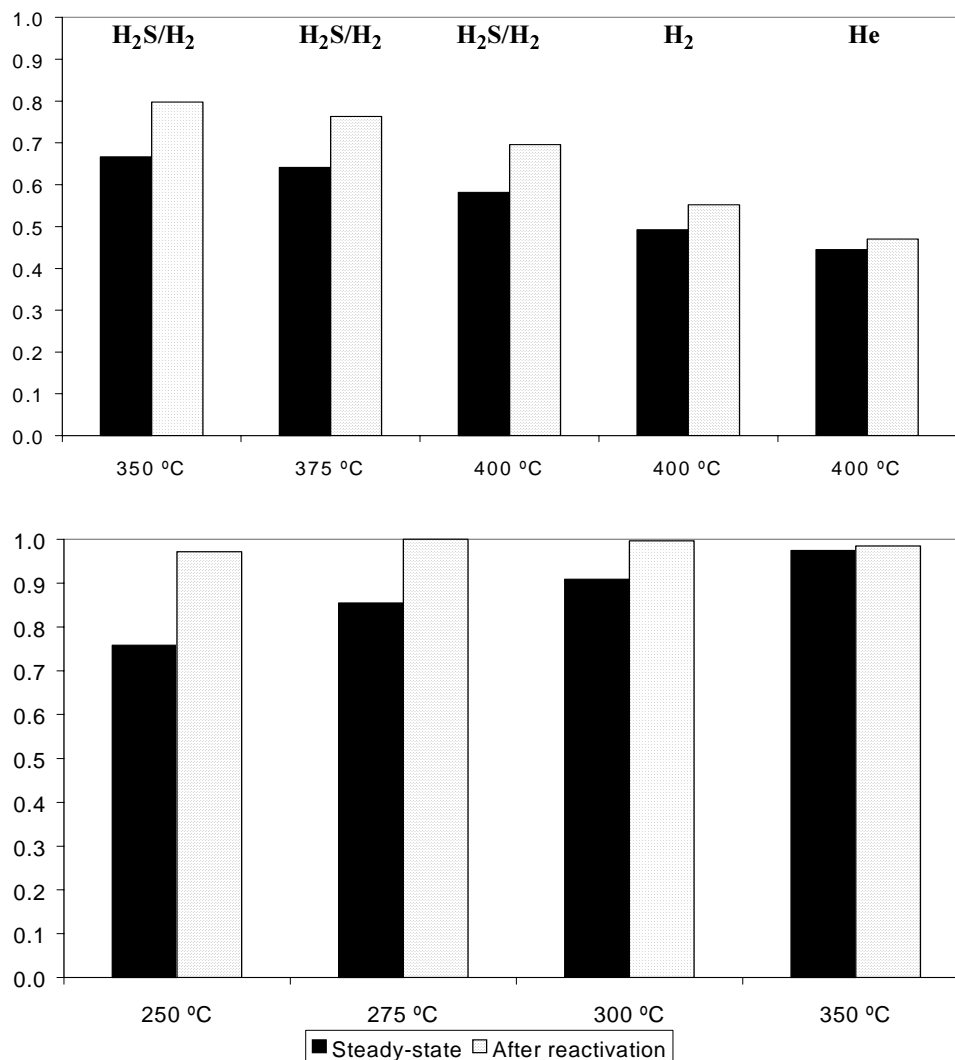


Figure 4-12 Reactivation of Mo (top) and NiMo (bottom) catalysts at atmospheric pressure by resulfiding, and additionally for Mo by pure H₂ and inert (He). “Steady-state” = relative activity before the reactivation, “After reactivation” = relative activity immediately after the reactivation. The relative activity at the start of the experiment is equal to 1.

freshly sulfided catalyst, as can be seen in Figure 4-13. For NiMo, the loss of activity decreases with increasing temperature (see the bar called “steady-state”) and the relative gain of activity follows the same trend. This is in direct contrast to the behavior of the Mo catalyst.

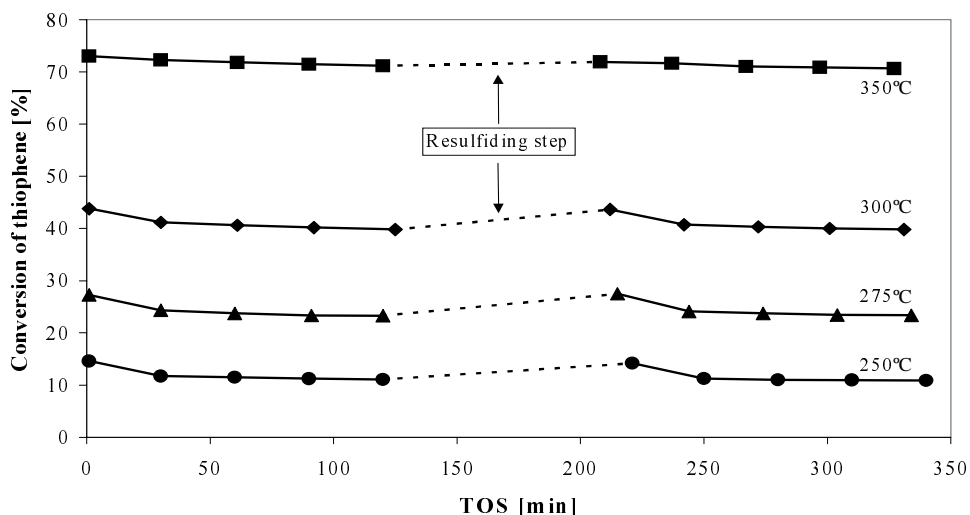


Figure 4-13 Resulfiding of NiMo catalyst. Pressure 0.1 MPa, reaction temperatures: 250 °C to 350 °C.

In the top part of Figure 4-12, two additional experiments (both at 400 °C) are presented. Mo was reactivated either by a pure H₂ flow or with an inert flow (pure He), without introducing H₂S to the catalyst. The H₂ or He flow was the same as the flow of H₂ during standard sulfiding, but due to the absence of H₂S, the total flow over the catalyst was half of that of the previous experiments. The reactivation lasted for 60 minutes and was performed after 120 min on stream for the H₂ experiment and after 240 min on stream for He experiment. Treatment either with H₂ or with He leads to a certain recovery of the activity, but it is not as effective as resulfiding.

4.2.3 Diluted flow of H₂ with inert (He)

Results of experiments with H₂ flow diluted by He in ratio 1:1 for Mo and NiMo are presented in Figure 4-14 and Figure 4-15, respectively.

In Figure 4-14, five deactivation curves are shown. The curve named "H₂" represents a standard experiment at 400 °C with H₂ flow without any He dilution, and "H₂/He" represents an experiment at 400 °C, where the H₂:He ratio was kept 1:1 during the whole run. The deactivation pattern is the same in both cases with the only difference being the lower activity (about 50 %) observed for the latter case, which shows the kinetic effect of H₂. The next two curves represent experiments, where the ratio was changed once ("H₂, H₂/He") or twice ("H₂, H₂/He, H₂") during the run. The results show that it is actually possible to "switch" from one deactivation curve to another and back again just by changing the dilution of the H₂ flow. And finally the last curve shows a double change in the H₂:He ratio at 300 °C. The same effect as at 400 °C is observed and the only difference is a lower activity, which is related to a lower temperature.

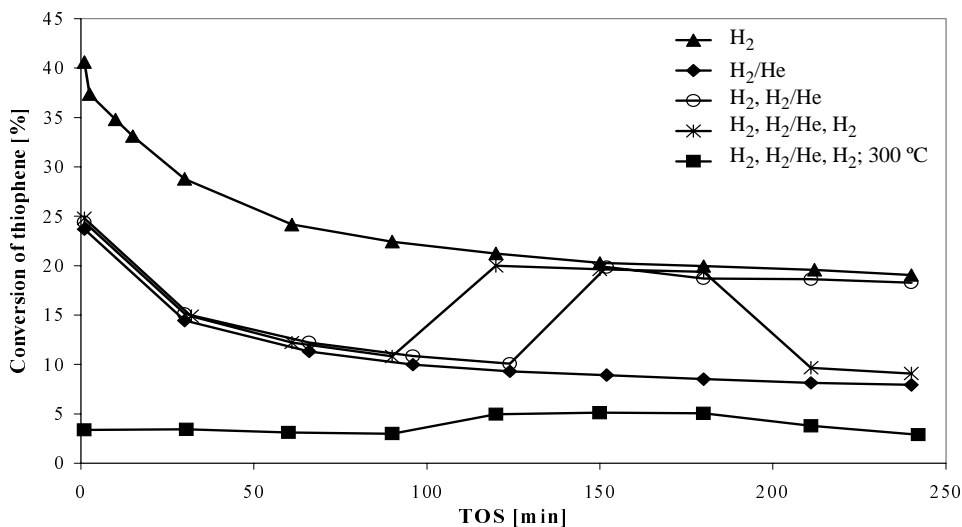


Figure 4-14 Effect of the dilution of the H₂ flow by He on the deactivation behavior of the Mo catalyst. Pressure 0.1 MPa, reaction temperatures 300 °C and 400 °C.

An experiment with a diluted flow of H₂ by He for the NiMo catalyst is presented in Figure 4-15. Curves show the same fast initial deactivation followed by the "steady-state" for both cases. The catalyst activity in the conversion of thiophene measured in the run with diluted H₂ flow is ca. 30 % lower than in the case of the non-diluted experiment.

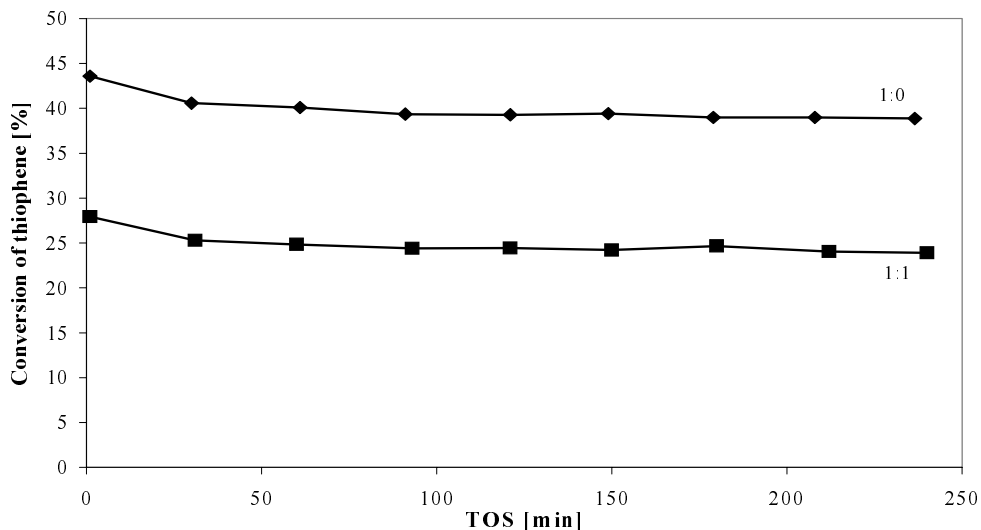


Figure 4-15 Effect of the dilution of the H₂ flow by He on the deactivation behavior of the NiMo catalyst. Pure H₂ flow (1:0) and H₂:He (1:1). Pressure 0.1 MPa, reaction temperature 300 °C.

From Figure 4-14 and Figure 4-15 one can see that both Mo and NiMo are affected in the same way by the dilution of the hydrogen flow by helium.

4.2.4 Hydrodesulfurization of thiophene: Reaction products selectivity

Figure 4-16 shows the product selectivity of the HDS of thiophene for all catalysts studied. The main products are trans-2-butene, cis-2-butene, 1-butene, and n-butane. Small amounts of byproducts were observed as well, but their sum was 2-5 % and they were not further identified. The selectivity towards the main products does not change during the run, except for the Mo catalyst, as will be described below. For all the catalysts, trans-2-butene has the highest yield, followed by cis-2-butene and n-butane together with 1-butene. On the Mo catalyst, the selectivity for n-butane and 1-butene changes after 60 min on stream. For NiMo, n-butane has the lowest selectivity. Product distribution for the NTA catalysts Mo (NTA) and NiMo (NTA) shows that in contrast to the standard Mo and NiMo catalysts the lowest selectivity is now observed towards 1-butene. And finally both NiMoP catalysts show the same product distribution as the NTA

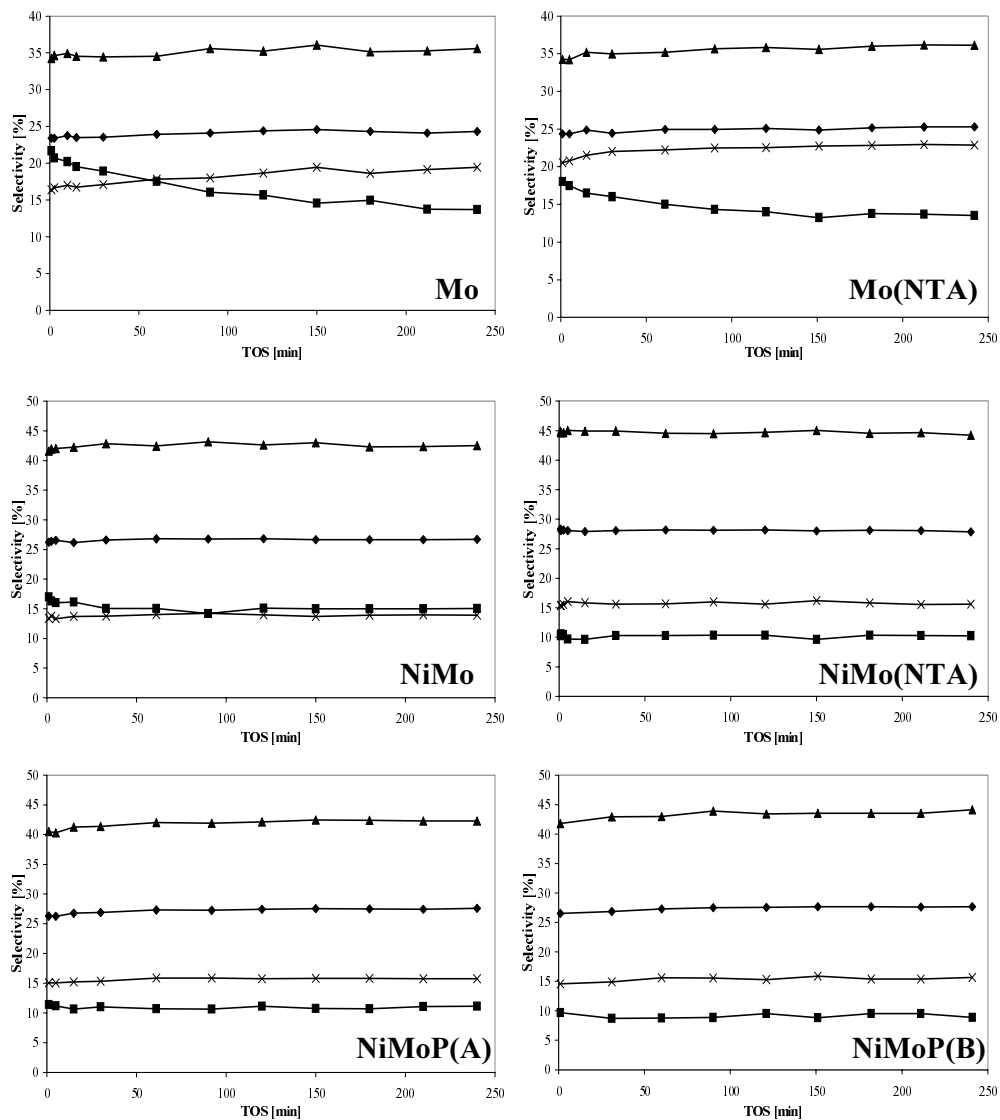


Figure 4-16 Product distribution from thiophene HDS for all studied catalysts. 1-butene (square), n-butane (cross), trans-2-butene (triangle), and cis-2-butene (diamond). Pressure 0.1 MPa, reaction temperature 400 °C (Mo catalyst) and 300 °C (NiMo and NiMoP catalysts).

catalysts. The only difference between the catalysts with and without phosphorus was the considerably higher amount of unidentified side products due to cracking over the NiMoP catalysts.

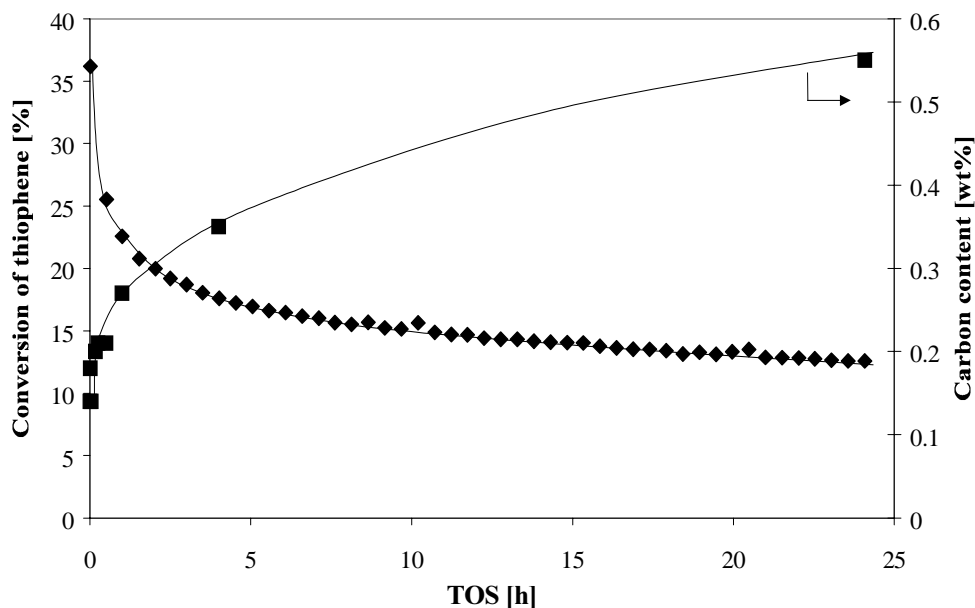


Figure 4-17 Carbon content and conversion of thiophene over a standard Mo catalyst as a function of time on stream. Pressure 0.1 MPa, reaction temperature 400°C.

4.2.5 Characterization of spent catalysts

4.2.5.1 Carbon and sulfur analysis

Data from carbon and sulfur analyses for standard Mo catalyst are presented in Table 4-III. A small amount of carbon is already present on the catalyst after the sulfiding step. With increasing time on stream, the amount of deposited carbon then increases together with the decrease in the thiophene conversion, as presented in Figure 4-17. After a few hours on stream, the rate of the carbon build-up is slightly higher than the decrease in the conversion of thiophene. In Figure 4-18, another experiment with shorter reaction time is shown and comparing these two figures

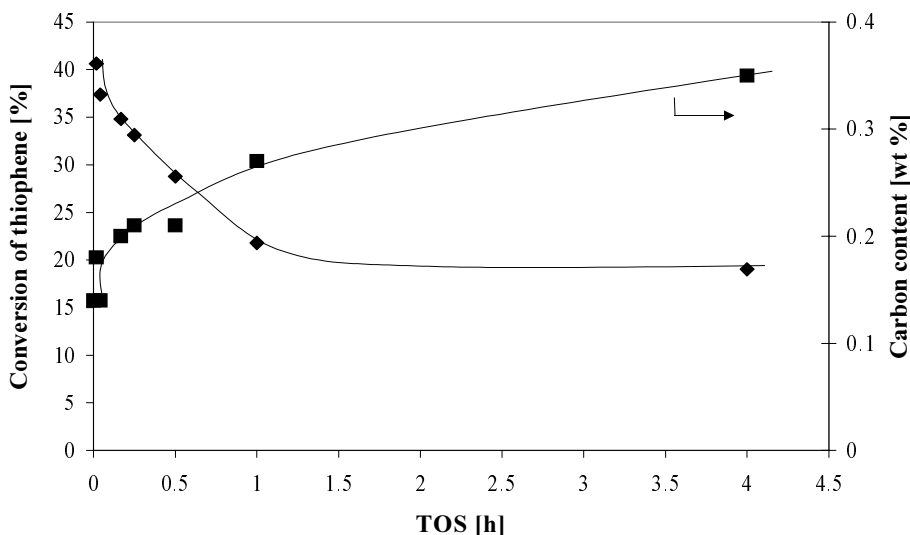


Figure 4-18 Carbon content and conversion of thiophene over a standard Mo catalyst as a function of time on stream for 240 min. Pressure 0.1 MPa, reaction temperature 400 °C.

shows very good reproducibility of experiments. Figure 4-19 shows the amount of carbon present on the standard Mo catalyst after the reaction at 400 °C together with one data point measured at 300 °C, which lies very close to the 400 °C trendline. In the same graph results are shown from experiments in which the catalyst was not flushed with He after the end of the reaction. Hence, the actual time on stream (catalyst exposed to residual thiophene in the setup) was much longer for these experiments. The lines for both types of experiments have similar shape with only difference being the total amount of deposited carbon, which is lower in the case of the He flushed samples.

Table 4-III shows the carbon and sulfur content of all standard Mo catalyst samples after the indicated time on stream. It is evident that the reactivation with H₂ or the resultfiding of catalyst at reaction temperature of 400 °C, followed by the thiophene reaction, does not affect the amount of carbon deposited on catalyst. With the decreasing reaction temperature (of resultfiding experiments) the amount of carbon decreases. During the experiment under the H₂ flow diluted by He, a 20 % higher amount of carbon deposited on catalyst. This amount decreases if the diluted

Table 4-III: Carbon and sulfur analysis data for the standard molybdenum catalyst at given reaction temperatures after the indicated time on stream; Experimental procedures are indicated in the column “conditions”, standard experiments are in the first nine rows

Conditions	TOS [min]	Carbon [wt%]	Sulfur [wt%]
only sulfided	0	0.14 ± 0.02	4.3 ± 0.1
400 °C	1	0.18 ± 0.02	4.1 ± 0.1
400 °C	2.5	0.14 ± 0.02	4.3 ± 0.1
400 °C	10	0.20 ± 0.02	4.3 ± 0.1
400 °C	15	0.21 ± 0.02	4.3 ± 0.1
400 °C	30	0.21 ± 0.02	4.3 ± 0.1
400 °C	60	0.27 ± 0.02	4.3 ± 0.1
400 °C	240	0.35 ± 0.02	4.3 ± 0.1
400 °C	1445	0.55 ± 0.05	4.3 ± 0.1
400 °C, reactivated with H ₂	277	0.37 ± 0.02	4.2 ± 0.1
400 °C, resulfided	240	0.35 ± 0.02	4.2 ± 0.1
375 °C, resulfided	251	0.30 ± 0.02	4.2 ± 0.1
350 °C, resulfided	261	0.26 ± 0.02	4.4 ± 0.1
400 °C, H ₂ :He (1:1)	240	0.45 ± 0.02	4.1 ± 0.1
400 °C, H ₂ :He (1:1 to 1:0 to 1:1)	240	0.39 ± 0.02	4.2 ± 0.1
400 °C, H ₂ :He (1:1 to 1:0)	240	0.36 ± 0.02	4.3 ± 0.1
300 °C	150	0.28 ± 0.02	4.2 ± 0.1
300 °C, H ₂ :He (1:1 to 1:0 to 1:1)	242	0.34 ± 0.02	4.3 ± 0.1

flow is changed to pure H₂ during the experiment. If the experiment is stopped during the diluted flow of H₂, the amount of carbon is higher. When ending the experiment under the non-diluted H₂ flow, an amount of carbon similar to that of the standard deactivation experiments is observed. A dilution experiment at 300 °C gives results similar to the rest of the experiments. For standard Mo catalyst, the amount of sulfur is not affected by the reaction or the special treatments and stays almost unchanged from the case of the sulfided catalyst, to which no thiophene was introduced.

The results of carbon and sulfur analyses for the standard NiMo catalyst are presented in Table 4-IV. During the standard deactivation experiments, the amount of carbon deposited on the

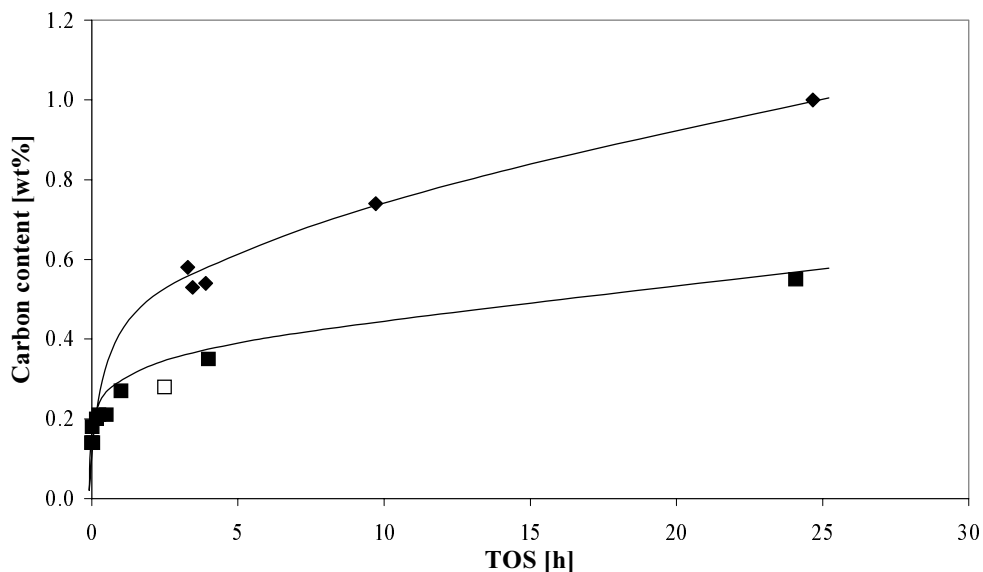


Figure 4-19 Carbon content on the standard Mo catalyst. Cooling down with (squares) or without (diamonds) He flushing. Pressure 0.1 MPa, reaction temperatures 400 °C and 300 °C (empty square).

catalyst does not change with time on stream and the carbon was already present after the sulfiding procedure. The amount of carbon is slightly lower than for the standard Mo catalyst.

Results from experiments with the resulfiding procedure in Table 4-IV show that the amount of carbon increases with decreasing reaction temperature, which is different from the standard Mo catalyst. The experiment at 250 °C gives the highest observed amount of carbon. Very close to that amount is the result of experiment with diluted H₂ flow and this is similar to experiments with the Mo catalyst. The amount of sulfur is approximately 20 % higher than that for the Mo catalyst and it does not change significantly with TOS or during the resulfiding.

Results from carbon and sulfur analyses for NTA based Mo and NiMo catalysts are presented in Table 4-V. The amount of carbon deposited on Mo (NTA) is about 3-4 times higher in comparison to the standard Mo catalyst. The main difference between these two types of catalyst is the development of the carbon build-up. While in case of the standard Mo catalyst the amount of carbon increases with TOS, the amount of carbon observed on Mo (NTA) after sulfiding stays

Table 4-IV: Carbon and sulfur analysis data for the standard NiMo catalyst at given reaction temperatures after the indicated time on stream; Experimental procedures are indicated in the column “conditions”, standard experiments are in the first four rows

Conditions	TOS [min]	Carbon [wt%]	Sulfur [wt%]
only sulfided	0	0.15 ± 0.02	4.6 ± 0.1
300 °C	1	0.20 ± 0.02	5.0 ± 0.1
300 °C	60	0.15 ± 0.02	5.0 ± 0.1
300 °C	240	0.20 ± 0.02	5.0 ± 0.1
350 °C, resulfided	327	0.19 ± 0.02	5.4 ± 0.1
300 °C, resulfided	331	0.23 ± 0.02	5.0 ± 0.1
275 °C, resulfided	334	0.24 ± 0.02	4.8 ± 0.1
250 °C, resulfided	340	0.29 ± 0.02	5.0 ± 0.1
300 °C, H ₂ :He (1:1)	240	0.27 ± 0.02	4.9 ± 0.1

constant during the entire experiment (4 hours). The amount of sulfur does not change and it is the same for both Mo catalysts. Over NiMo (NTA), amount of carbon is 4-5 times higher compared to the standard NiMo and the amount increases with TOS. The amount of sulfur is fairly constant and it is the same for both types of catalyst. Again, almost all of the observed carbon was already present on the catalyst directly after the sulfiding step. In Table 4-V, one experiment over NiMo (NTA) with a faster heating rate during sulfiding is also presented. The amount of deposited carbon is slightly higher than that on the catalyst prepared by the standard method (heating rate 2 °C/min). The observed deactivation behavior (Appendix A7) showed only small differences between these two catalysts.

Results from carbon and sulfur analyses for NiMoP (A) are also given in Table 4-V. The amount of sulfur is approximately 50 % higher as compared to the other catalysts investigated here. This is due to the higher metal loading of the NiMoP catalyst. Again, the sulfur amount does not change significantly during the time on stream. As for the carbon analysis, a build-up similar to that on the standard Mo catalyst is observed. A small amount of carbon is present on the catalyst already after the sulfiding step and this amount increases with increasing TOS. It reaches its maximum value after approximately 30 minutes and does not change thereafter. The absolute values lie between the amounts observed on standard and NTA catalysts.

Table 4-V: Carbon and sulfur analysis data for Mo (NTA), NiMo (NTA), and NiMoP (A) catalysts at given reaction temperatures after the indicated time on stream

Catalyst	Conditions	TOS [min]	Carbon [wt%]	Sulfur [wt%]
Mo (NTA)	only sulfided	0	1.00 ± 0.05	4.3 ± 0.1
	400 °C	1	0.99 ± 0.05	4.1 ± 0.1
	400 °C	15	0.97 ± 0.05	4.2 ± 0.1
	400 °C	61	1.04 ± 0.05	4.1 ± 0.1
	400 °C	242	0.95 ± 0.05	4.0 ± 0.1
NiMo (NTA)	only sulfided	0	0.85 ± 0.05	4.6 ± 0.1
	300 °C	1	0.87 ± 0.05	4.8 ± 0.1
	300 °C	15	1.00 ± 0.05	4.8 ± 0.1
	300 °C	60	1.00 ± 0.05	5.0 ± 0.1
	300 °C	240	0.95 ± 0.05	5.1 ± 0.1
	300 °C ^a	240	1.20 ± 0.05	5.0 ± 0.1
NiMoP (A)	only sulfided	0	0.21 ± 0.05	8.4 ± 0.1
	300 °C	1	0.30 ± 0.05	8.4 ± 0.1
	300 °C	30	0.52 ± 0.05	8.6 ± 0.1
	300 °C	60	0.47 ± 0.05	8.5 ± 0.1
	300 °C	240	0.49 ± 0.05	7.7 ± 0.1

^a Experiment with the sulfiding rate of 10 °C/min.

4.2.5.2 BET and Hg intrusion results

Results from N₂ physisorption and Hg intrusion porosimetry are presented in Table 4-VI. A loss of about 10 % in surface area is observed during the sulfiding of standard Mo and NiMo catalysts, and about 30 % in the case of the NiMoP catalyst. Note that the catalyst gains weight due to the transformation from oxide to sulfide. On the other hand, the surface area of Mo (NTA) and NiMo (NTA) catalysts increases by sulfiding. The increase is about 70 % in the case of Mo (NTA) and almost 100 % in the case of NiMo (NTA). For all the catalysts, in the presence of thiophene, the surface area does not change with increasing time on stream.

Table 4-VI: BET analysis and Hg intrusion porosimetry data for all catalysts studied at given reaction temperatures after the indicated time on stream

Catalyst	Conditions	TOS [min]	Surface area ^a [m ² /g]	Pore volume ^b [cm ³ /g]
Mo	fresh	-	257	0.57
	only sulfided	0	237	0.54
	400 °C	1	231 ± 2	0.51 (0.55)
	400 °C	240	235 ± 2	0.53 (0.54)
	400 °C	1480	232 ± 2	0.53
	400 °C, reactivated with H ₂	277	236	0.53
	300 °C	150	236 ± 2	0.54 (0.45)
NiMo	fresh	-	242	0.55
	only sulfided	0	231	0.51
	300 °C	1	222 ± 2	0.49 (0.48)
	300 °C	240	228 ± 2	0.50 (0.49)
Mo (NTA)	fresh	-	150	0.40
	only sulfided	0	N.A.	N.A.
	400 °C	1	215	0.52
	400 °C	242	240	0.54
NiMo (NTA)	fresh	-	120	0.30
	only sulfided	0	220	0.50
	300 °C	1	220	0.50
	300 °C	240	215	0.50
NiMoP (A)	fresh	-	195	0.48
	only sulfided	0	N.A.	N.A.
	300 °C	1	130	0.40
	300 °C	240	145	0.47

^a Surface area was determined by the BET analysis.

^b Pore volume from N₂ physisorption, in parenthesis data from Hg intrusion porosimetry (if available).

For Mo and NiMo catalysts, the decrease in pore volume is again observed only during the sulfiding step and it remains unchanged during the run. In the case of the NTA catalysts, the pore volume increases by approximately 50 %, but it is constant with the increasing time on stream. For the NiMoP catalyst, the decrease in pore volume during the sulfiding is observed, but with the increasing TOS, pore volume increases again. The pore volume distribution remains unchanged during all experiments for all analyzed catalysts. The average pore size for standard Mo catalyst is about 6-10 nm.

4.2.5.3 IR and Raman spectroscopy analysis

The infrared analysis of eight spent standard Mo catalyst samples (Table 4-III) is shown in Figure 4-20. The samples were taken at different times on stream and Figure 4-20 shows that there are no major differences visible. The band region above 3000 cm^{-1} , where the interesting

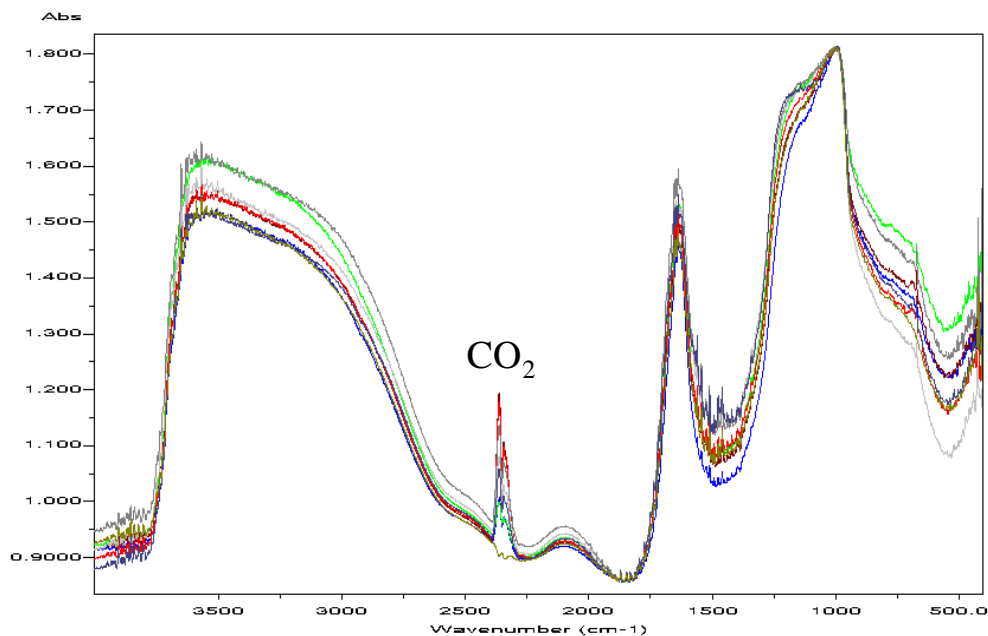


Figure 4-20 IR spectra of eight spent standard Mo catalysts. CO₂ peak is assigned according to standard IR database (Appendix A8).

information about the type of coke could be revealed, is hidden in the signal of water, which was impossible to eliminate. In the fingerprint region for carbonaceous materials ($1200\text{-}1700\text{ cm}^{-1}$) several features can be distinguished but the intensity of the bands does not follow the TOS and is random between the samples. The conclusion is that this kind of analysis is not useful for our purpose.

On the other hand, Raman spectroscopy was found to be a helpful tool in the determination of the distribution of the metals and NTA throughout the catalyst particle, after the impregnation and drying. Figure 4-21 shows the Mo and NTA profiles throughout the catalyst particle. The curves are fitted using the second order polynomial (parabolic) and both are very similar, indicating the ratio of Mo and NTA to be equal throughout the particle.

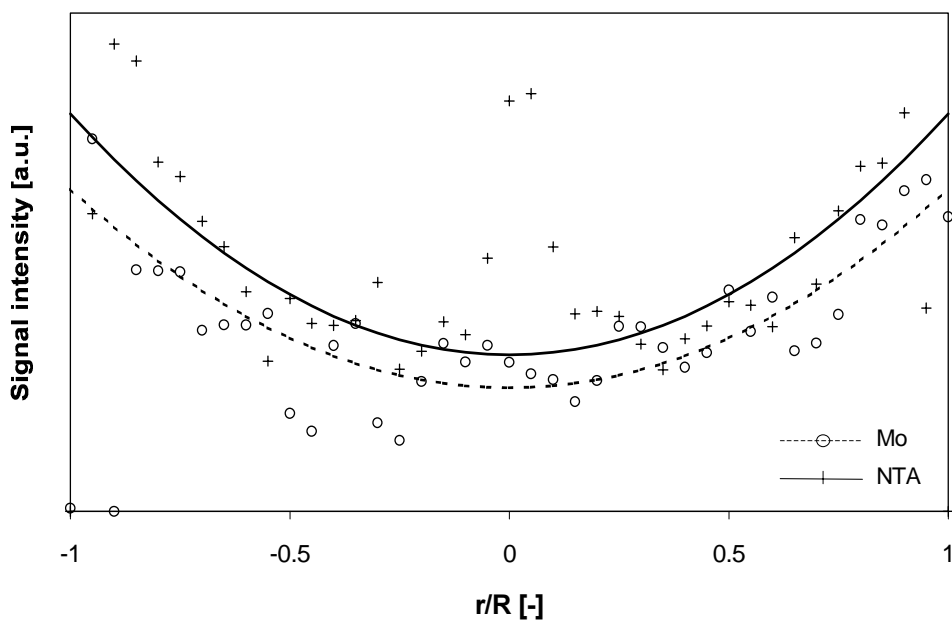


Figure 4-21 Raman spectroscopy profile throughout the particle of Mo (NTA) catalyst.

4.3 Steady state kinetics of thiophene HDS at atmospheric pressure

4.3.1 Kinetic behavior

The conversion of thiophene over all the investigated catalysts is presented in Figure 4-22. The total HDS conversion was slightly different from the thiophene conversion because of one detected compound, which was assumed to contain sulfur. The (+) sign represents the HDS conversion over the NiMo catalyst and it is possible to see that the difference is very small. A difference of the same magnitude was found for all catalysts and is not highlighted in Figure 4-22. For Ni and Co promoted catalysts, one can see that the conversion follows a “S”-curve, represented by a slow increase in conversion at low and high temperatures and steeper increase in the temperature range of 230 - 350 °C. At high temperatures, NiMo catalyst gives total conversion of thiophene, while the deactivation of the CoMo catalyst was observed. In comparison with molybdenum based catalysts, the Pt/Y-zeolite catalyst seems to have a very low activity towards the thiophene HDS and there was no effect of the pretreatment of the catalyst. The Pt/Y-zeolite

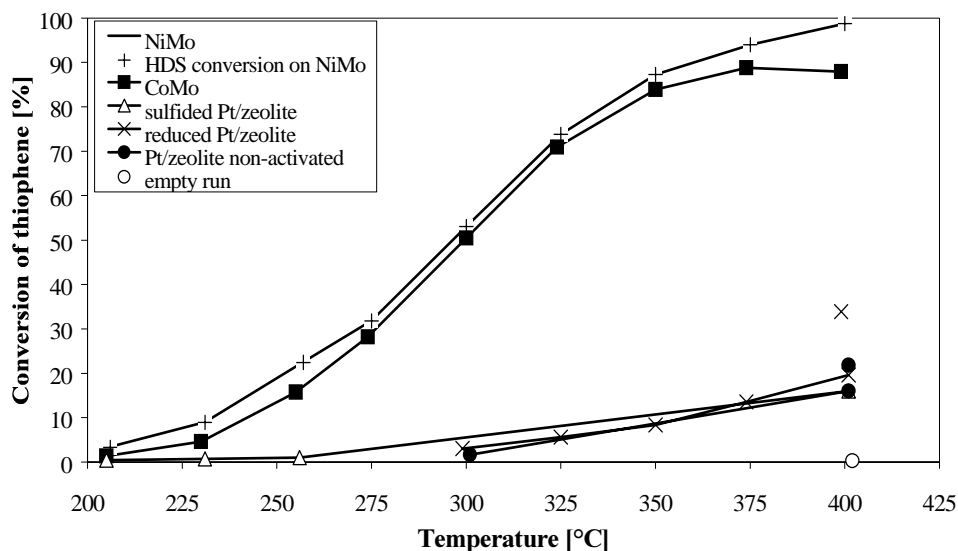


Figure 4-22 Conversion of thiophene over the studied catalysts at pressure 0.1 MPa.

catalyst also showed very fast deactivation. The cross (x) at 400 °C outside the line in Figure 4-22 is the conversion at the start of the experiment and the cross at 400 °C on the line is the conversion after two days on stream. The same is true for the non-activated Pt/Y-zeolite (full circles). This is in contrast to the high stability of Mo based catalysts.

First order reaction constants for the hydrodesulfurization of thiophene over NiMo/ γ -Al₂O₃, CoMo/ γ -Al₂O₃, and Pt/Y-zeolite catalysts in the temperature interval 200 - 400 °C were calculated from Equation (2-6) and are presented in Table 4-VII. The calculated constants are based on the mass of catalyst.

Table 4-VII: First order rate constants for hydrodesulfurization of thiophene

	NiMo	CoMo	Pt/Y-zeolite (sulfided)	Pt/Y-zeolite (non-activated)	Pt/Y-zeolite (reduced)
Temperature	k [m ³ /(g _{cat} ·s)]				
206 °C	1.17·10 ⁻⁷	4.76·10 ⁻⁸	1.49·10 ⁻⁸	N.A.	N.A.
231 °C	3.17·10 ⁻⁷	1.58·10 ⁻⁷	2.41·10 ⁻⁸	N.A.	N.A.
257 °C	8.55·10 ⁻⁷	5.72·10 ⁻⁷	3.48·10 ⁻⁸	N.A.	N.A.
275 °C	1.28·10 ⁻⁶	1.11·10 ⁻⁶	N.A.	N.A.	N.A.
300 °C	2.53·10 ⁻⁶	2.34·10 ⁻⁶	N.A.	5.83·10 ⁻⁸	1.09·10 ⁻⁷
325 °C	4.49·10 ⁻⁶	4.13·10 ⁻⁶	N.A.	N.A.	2.02·10 ⁻⁷
350 °C	6.92·10 ⁻⁶	6.09·10 ⁻⁶	N.A.	N.A.	3.04·10 ⁻⁷
374 °C	9.44·10 ⁻⁶	7.30·10 ⁻⁶	N.A.	N.A.	5.06·10 ⁻⁷
400 °C	1.47·10 ⁻⁵	7.07·10 ⁻⁶	5.85·10 ⁻⁷	6.00·10 ⁻⁷	7.60·10 ⁻⁷

N.A. - not available

Table 4-VII shows the expected increase in the rate constant with the temperature and quite similar activities for the molybdenum based catalysts. On the Pt/Y-zeolite catalyst, the low Pt loading and thus a very low activity at lower temperatures led to the selection of only a few experimental conditions and thus it was not possible to obtain reaction rates for the same temperature range as for Mo based catalysts. Low values of rate constants for the Pt/Y-zeolite catalyst compared to molybdenum-based ones correspond to the observed lower activity of the Pt/Y-zeolite catalyst shown in Figure 4-22.

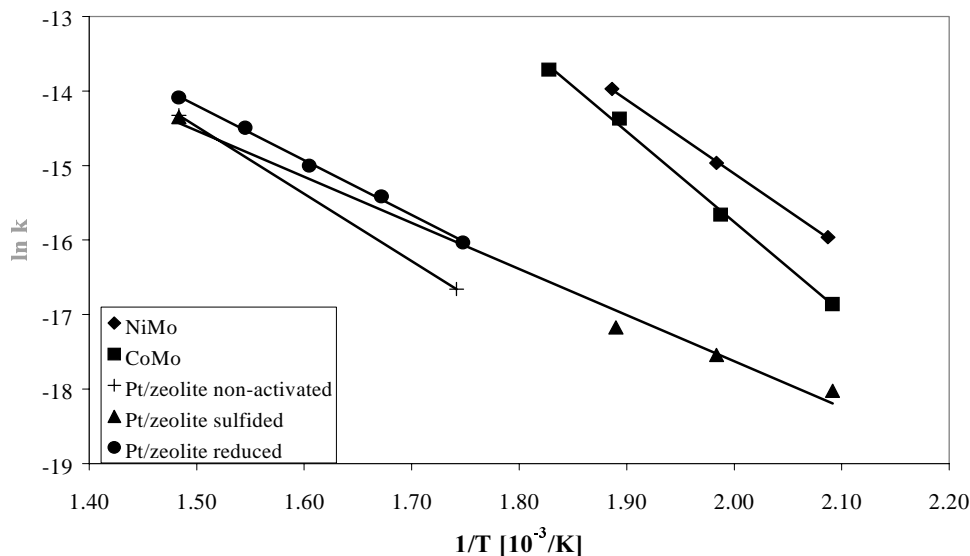


Figure 4-23 Arrhenius plots for the studied catalysts at pressure 0.1 MPa.

Activation energies for the thiophene HDS over the studied catalysts (Table 4-VIII) were obtained from Arrhenius plots for the temperature region where the reaction is assumed to be governed by the surface reaction.

Table 4-VIII: Activation energies for hydrodesulfurization of thiophene

Catalyst	E_a [kJ/mol]
NiMo/ γ -Al ₂ O ₃	82
CoMo/ γ -Al ₂ O ₃	101
Pt/Y-zeolite sulfided	51
Pt/Y-zeolite non-activated	75
Pt/Y-zeolite reduced	61

The activation energy for molybdenum based catalysts are higher than for Pt/Y-zeolite. On Pt/Y-zeolite, it is possible to see a small effect of pretreatment on the HDS activity. Sulfiding leads to the lowest activation energy, while the non-activated Pt/Y-zeolite catalyst has an activation energy very close to that of the NiMo catalyst. However, the difference in activation energies is not very significant.

4.3.2 Selectivity of reaction products of thiophene hydrodesulfurization

Figure 4-24 shows the product selectivity of the HDS of thiophene for all studied catalysts. The main products are trans-2-butene, cis-2-butene, 1-butene, and n-butane. A certain amount of unidentified products was observed as well, but the sum of their selectivities was below 3 % and with the exception of two peaks they were not further studied. A peak at low retention time (RT)

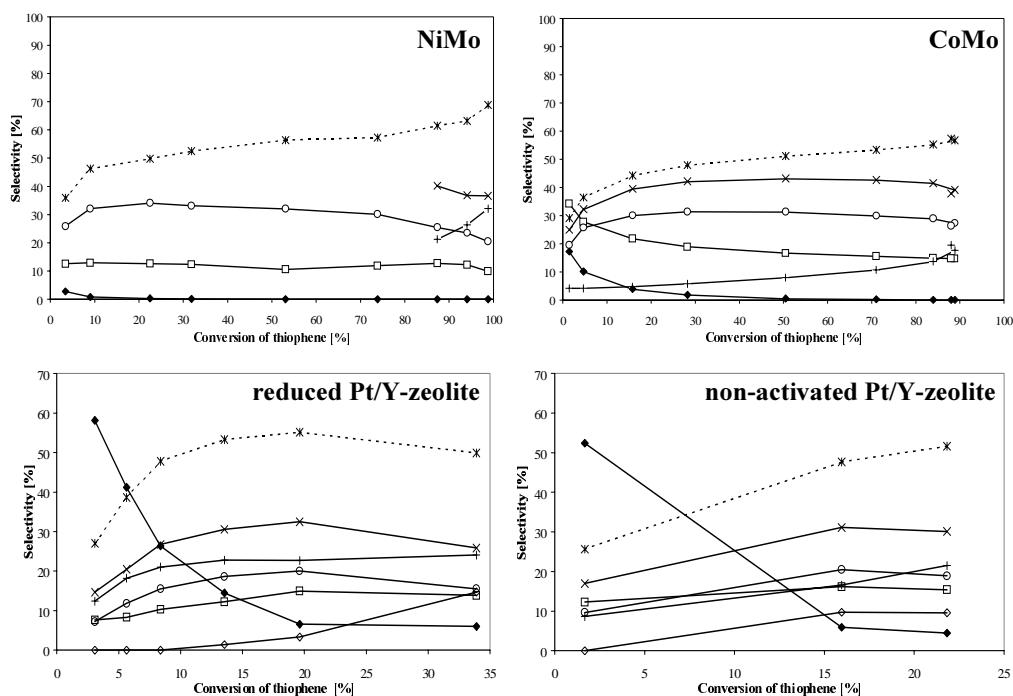


Figure 4-24 Product selectivity for studied catalysts. 1-butene (squares), n-butane (+), trans-2-butene (x), cis-2-butene (o), unidentified high RT component (diamonds), unidentified low RT component (empty diamonds), and unseparated n-butane with trans-2-butene (stars).

appeared at all chromatograms at higher reaction temperatures (observed, but not presented on the figure for NiMo and CoMo). A high boiling point component (with respect to thiophene) was observed on the chromatograms for all catalysts at all temperatures. Especially on Pt/Y-zeolite catalyst, the high boiling point component had a very high selectivity at low thiophene

conversions, while on molybdenum based catalysts the selectivity at higher temperatures was negligible. The analytical method applied during the low conversions of thiophene on the NiMo catalyst made it impossible to separate peaks of n-butane and trans-2-butene and those two compounds eluted in one peak. It is represented by a dashed line and stars in Figure 4-24. The resolution was improved for further studies, but the sum of two mentioned peaks is presented in the figure for the other catalysts as well to facilitate the comparison with the NiMo catalyst.

In Figure 4-24, the selectivities of products for thiophene HDS over Pt/Y-zeolite catalyst are also presented. The selectivities are slightly different from the molybdenum based catalysts. Two unidentified peaks were observed here as well - one at a low retention time and one at the higher retention times. The very low conversion and thus no detectable product peaks (with an exception of traces of butene) at low temperatures made it impossible to determine selectivities for sulfided Pt/Y-zeolite. The only exception was the experiment at 400 °C and the calculated selectivities fitted exactly to the plot of selectivities over the non-activated Pt/Y-zeolite.

In summary, on NiMo and CoMo catalysts, two isomers of 2-butene had the highest selectivity and they were followed by 1-butene and n-butane. At low conversions, an unknown high retention time component showed a high selectivity. On Pt/Y-zeolite catalyst, trans-2-butene had the highest selectivity and was followed by n-butane. 1-butene and cis-2-butene had approximately the same selectivity as in the previous cases, the unknown high boiling point component had very high selectivity at very low conversions of thiophene, while at higher conversion a low retention time peak started to show relatively high selectivity.

4.4 High-pressure steady-state kinetics of DBT HDS and study of “matrix effect”

4.4.1 DBT in n-heptane

Preliminary experiments with 0.1 wt% DBT in n-heptane were done at pressure of 2 MPa, $LHSV = 21.4 \text{ h}^{-1}$ and in the temperature region 150 - 250 °C. The conversion of DBT as a function of the reaction temperature is shown in Figure 4-25. First order reaction rate constants were calculated using Equation (2-6) and are presented in Table 4-IX. They are based on the mass of the catalyst. The Arrhenius plot for hydrodesulfurization of DBT based on the kinetic data from Table 4-IX indicated a change in the rate determining step around 170 °C. The calculated activation energies for the low and high temperature regions are 17 and 100 kJ/mol, respectively.

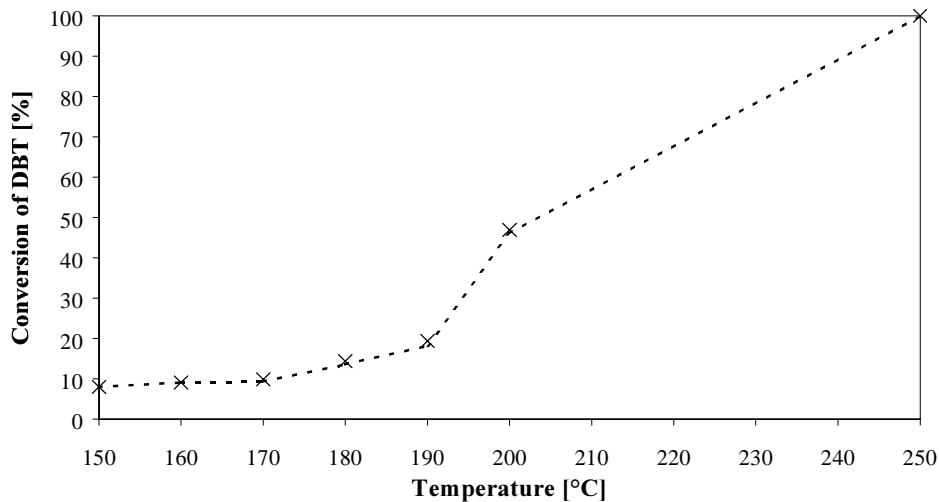


Figure 4-25 Conversion of DBT (x) and the overall HDS conversion (dashed line) as a function of the reaction temperature. NiMo/ γ -Al₂O₃, LHSV = 21.4 h⁻¹, pressure 2 MPa.

Table 4-IX: First order rate constants for hydrodesulfurization of DBT

Reaction temperature [°C]	k [m ³ /(g _{cat} ·s)]
150	7.36·10 ⁻¹⁰
160	8.46·10 ⁻¹⁰
170	9.17·10 ⁻¹⁰
180	1.38·10 ⁻⁹
190	1.90·10 ⁻⁹
200	5.59·10 ⁻⁹
250	N.D.

N.D. : Not determined because of the total conversion

Based on the results from this series and other preliminary experiments the conditions chosen to study the effect of co-solvents and inhibitors were: $P = 2 \text{ MPa}$, $T = 200 \text{ }^\circ\text{C}$, $LHSV = 21.4 \text{ h}^{-1}$ and the ratio of H_2 and DBT + n-heptane mixture of $203 \text{ Nm}^3/\text{Nm}^3$. This gave a DBT conversion of approximately 57 % and a range of conversions when other compounds were added.

4.4.2 Inhibition effect of sulfur compounds on the hydrodesulfurization of DBT

The effect of other sulfur compounds on the hydrodesulfurization of dibenzothiophene was studied by the addition of dimethyldisulfide (DMDS) and thiophene to the feed mixture. Detailed information on the feed compositions is given in Table 3-II.

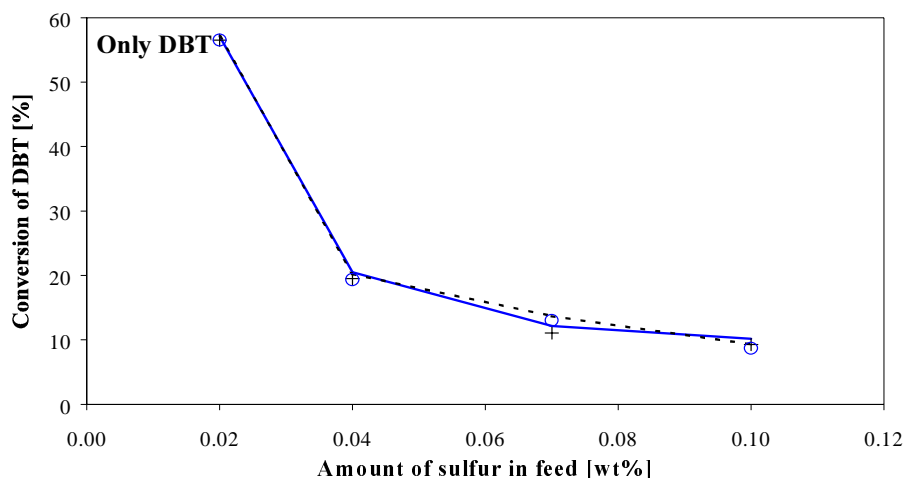


Figure 4-26 Conversion of DBT and the overall HDS conversion as a function of the amount of sulfur in the feed. DBT+DMDS (full line), DBT+thiophene (dashed line), HDS conversion in DBT+DMDS solution (o), and HDS conversion in DBT+thiophene solution (+).

The comparison of conversions of DBT and the overall HDS conversions in the reactions with different amount of sulfur is presented in Figure 4-26. Both the HDS and DBT conversions are affected in the same way. The more total sulfur in the feed, the lower is the conversion of DBT. There was no significant difference between the effect of DMDS and thiophene on the conversions.

Rate constants for the hydrodesulfurization of DBT inhibited by either DMDS or thiophene were calculated according to Equation (2-14) and are listed in Table 4-X. The constants are based on the mass of the catalyst. The reaction order with respect to the inhibitor H₂S (assuming that the added sulfur compound is converted to H₂S) was determined from the plot of logarithm of reaction rate versus logarithm of the concentration of H₂S (Appendix A9 (A)). From the slope of the regression line, the reaction order with respect to H₂S was determined and is presented in Table 4-X.

Table 4-X: Rate constants for the hydrodesulfurization of DBT with the addition of DMDS, thiophene, and toluene and reaction orders with respect to the sulfur or aromatics concentration

Feed mixture	Reaction order with respect to S or aromatics	Rate constant [m ³ /(g _{cat} ·s)]
DBT in n-heptane	-	$(6.5 \pm 1.3) \cdot 10^{-9}$
DBT in n-heptane + DMDS	-0.58	$(1.7 \pm 0.1) \cdot 10^{-12}$
DBT in n-heptane + thiophene	-0.62	$(1.1 \pm 0.1) \cdot 10^{-12}$
DBT in n-heptane + toluene	-0.18	$(1.4 \pm 0.2) \cdot 10^{-9}$

4.4.3 Inhibition effect of aromatics on the hydrodesulfurization of DBT

The effect of aromatics on the hydrodesulfurization of dibenzothiophene was studied by the addition of either naphthalene or toluene to the feed mixture. The detailed information on the feed compositions is given in Table 3-II.

The comparison of conversions of DBT and the overall HDS conversions in the reactions with different amount of naphthalene and toluene is presented in Figure 4-27. Both the HDS and DBT conversions are affected in the same way, but there is a significant difference between the effect of the two compounds studied. A small addition of toluene slightly decreases the conversion and the inhibition effect is getting stronger with the increasing amount of aromatics. On the other hand, naphthalene addition has much stronger effect, it decreased the conversion of DBT already at very low concentrations. Moreover, the addition of naphthalene led to rapid deactivation of the catalyst, presumably due to coking. This made it impossible to run continuing series of experiments with increasing concentration of naphthalene. When returning to the standard feed the activity was not recovered.

The rate constant for the hydrodesulfurization of DBT inhibited by toluene was calculated according to Equation (2-14) and is presented in Table 4-X. The reaction order with respect to toluene was determined (Appendix A9 (B)) and is presented in Table 4-X. Because of the lack of experiments with naphthalene, the kinetic data for these experiments were not obtained.

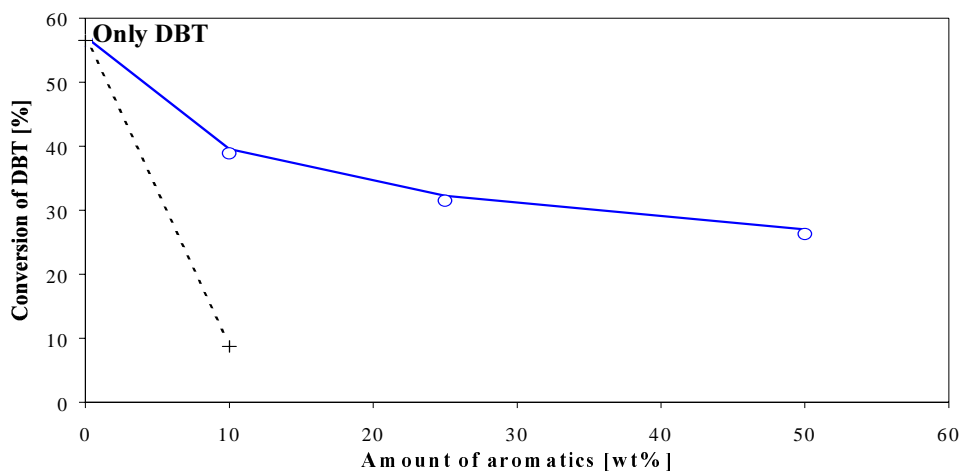


Figure 4-27 Conversion of DBT and the overall HDS conversion as a function of the amount of aromatics in the feed. DBT+ toluene (full line), DBT+naphthalene (dashed line), HDS conversion in DBT+toluene solution (o), and HDS conversion in DBT+naphthalene solution (+).

4.4.4 Selectivity of reaction products of hydrodesulfurization of DBT

The products observed during the hydrodesulfurization of DBT were identified as cyclohexylbenzene (CHB), biphenyl (BP), and tetrahydro-/hexahydrodibenzothiophene (THDBT/HHDBT). The observed products were the same for all performed experiments and the dependence of their selectivities on the DBT conversion is presented in Figure 4-28. During the experiments with DBT in n-heptane, biphenyl is a main product at low conversions of DBT. Other products start to appear with the increasing conversion of DBT. An increasing amount of cyclohexylbenzene and a maximum in the amount of THDBT/HHDBT is observed. At the total conversion of DBT, no THDBT/HHDBT is detected, while the selectivities of biphenyl and cyclohexylbenzene are 63 % and 37 %, respectively.

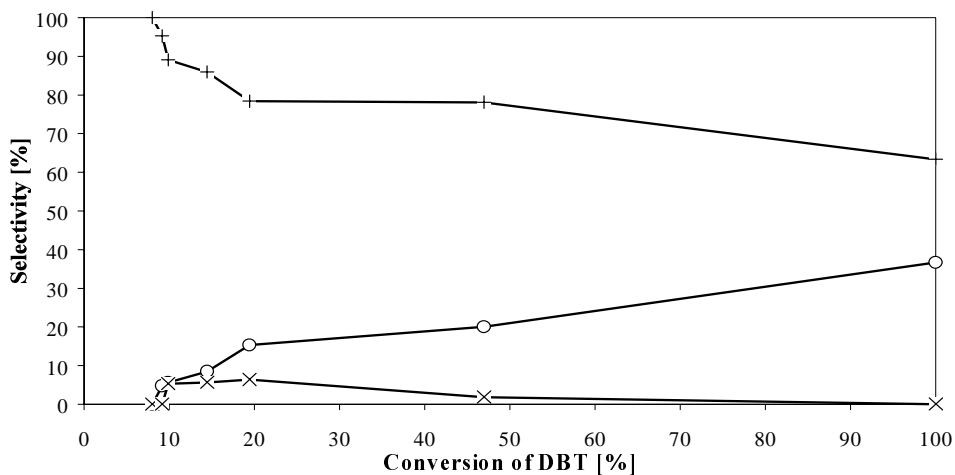


Figure 4-28 The dependence of the product selectivities on the conversion of DBT. BP (+), CHB (o), THDBT/HHDBT (x).

In the experiments with thiophene and DMDS, the selectivities of all products are affected, even if the effect is not very strong. With increasing amount of added thiophene, selectivity to BP increases (Figure 4-29 A), while the selectivity to CHB is decreasing (Figure 4-29 C). With DMDS, the effect on the selectivities is not so pronounced at its lower concentrations. On the other hand, at higher concentrations of added DMDS the selectivity to BP is going through a minimum value (Figure 4-29 A), while the selectivity towards CHB is decreased (Figure 4-29 C). The selectivity to THDBT/HHDBT is increasing in both cases with the increasing amount of added sulfur compound (Figure 4-29 B).

In the experiments with aromatics, the effect of added inhibitor is much more pronounced than in the case of sulfur compounds. With toluene, the selectivity towards BP sharply increases together with the sharp decrease in the selectivity to CHB (Figure 4-29 A and C, respectively). The effect of naphthalene is smaller and opposite when compared to toluene. The selectivity towards BP decreases and the selectivity towards CHB increases (Figure 4-29 A and C, respectively). Again, as in the case of sulfur compounds, the selectivity to THDBT/HHDBT is increasing in both cases with the increasing amount of added aromatics (Figure 4-29 B).

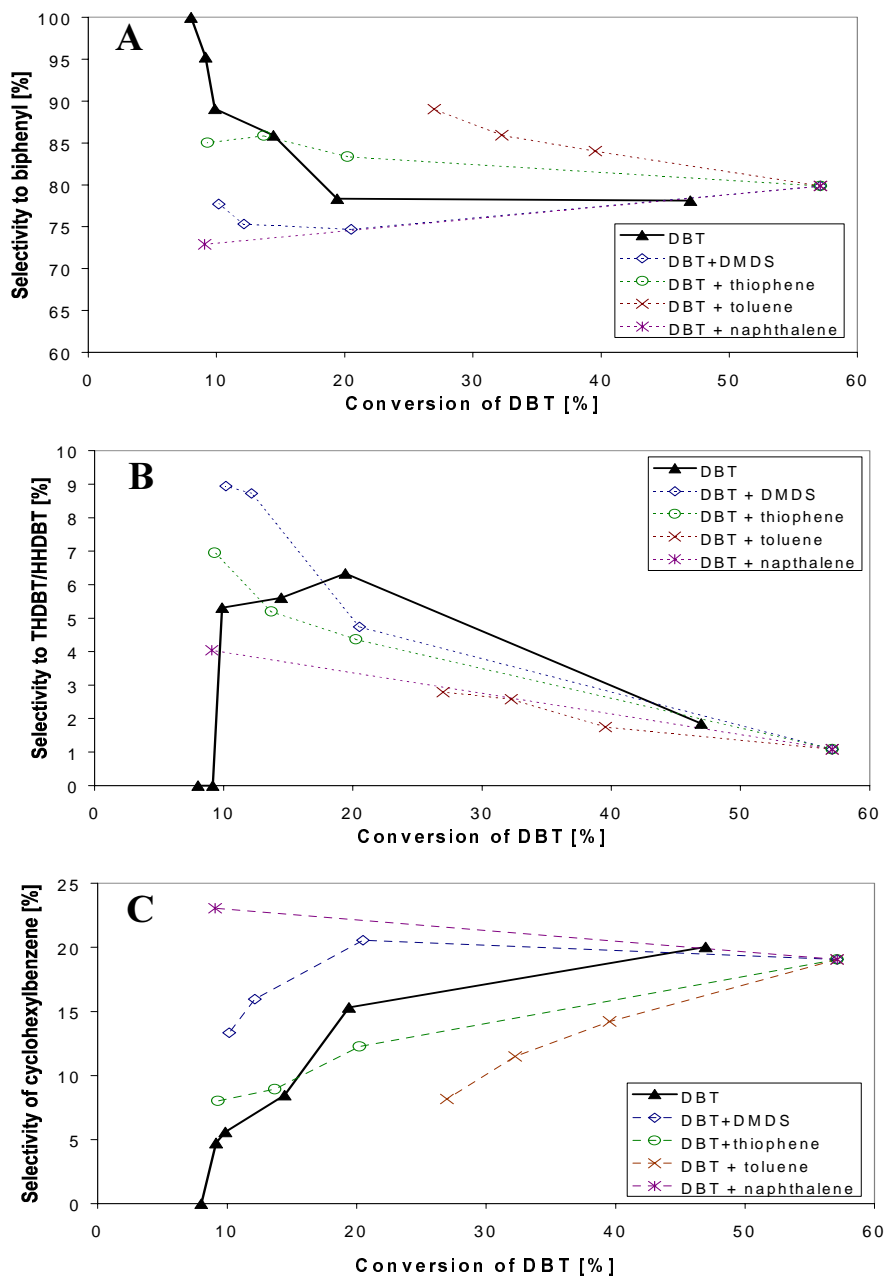


Figure 4-29 The dependency of selectivities of the products of DBT HDS on the conversion of DBT during the “matrix effect”. NiMo catalyst, pressure 2 MPa.

5. DISCUSSION

5.1 High-pressure HDS of light gas oil from the Statoil Mongstad refinery

The analytical method using a GC equipped with the atomic emission detector (AED) was found to be a very powerful tool for the detailed analysis of oil fractions before and after hydrotreating. The data presented in Figure 4-1 showed very good agreement between the results obtained from the standard combustion method with the new GC-AED method. Based on these results and studies published by others [91, 214, 240-249], the relevance of new method was accepted and GC-AED was used for further studies of light gas oil (LGO). Even if the resolution of the method in our case made it impossible to analyze most of the sulfur compounds, the least reactive ones (namely DBT, 4-MDBT, and isomers of DMDBT), which contribute the most to the residual sulfur in deeply hydroprocessed oils, were identified and studied.

The results in chapters 4.1.2 and 4.1.3 clearly point out that DBT is the most reactive sulfur compound from those identified and analyzed separately and that it is totally desulfurized already at about 85 % overall HDS conversion of LGO. Only one monosubstituted DBT, 4-MDBT, was found to be less reactive than DBT in the studied oil and this compound is not totally desulfurized until a total HDS conversion of approximately 95 % is reached. Several isomers of DMDBT were even less reactive and the least reactive one was found to be 4,6-DMDBT. 4-MDBT and 4,6-DMDBT are the only two sulfur compounds left in the oil at very high HDS conversions. 4,6-DMDBT is less reactive and the most refractory compound left in the oil. A similar study using both NiMo and CoMo catalysts has been done by Knudsen *et al.* [253] with similar results. It is very likely that the resistance of these substituted compounds towards the desulfurization is due to a steric hindrance (see Figure 1-7) preventing the interaction between the sulfur atom and the catalytic active site as has been suggested by several authors [8, 96, 185, 189, 198, 199, 254]. Simulation and experiments performed by Landau *et al.* [179] confirmed the idea that methyl groups screen the S atom from reaction. Thus in order to optimize the hydrodesulfurization process in the region of deep HDS (more than 95% conversion), one must focus on the most resistant sulfur components, represented by substituted dibenzothiophenes.

As was presented in Table 4-I, the difference in relative reactivity of the DBTs studied here changes drastically with changing temperature. While at 250 °C the ratio of rate constants of DBT, 4-MDBT and 4,6-DMDBT was found to be 57.7 : 10.4 : 1.0, respectively, the same ratio at 300 °C was 7.4 : 2.5 : 1.0. The reason for this behavior is most likely to be an increased reactivity of

substituted DBTs at elevated temperatures, but it could also be caused by different phase and equilibrium conditions at each of the studied temperatures. It is also interesting to note that in a model compound study over CoMo [132], presented in Table 5-II, the opposite trend was observed.

Apparent activation energies calculated from the slopes of the straight lines in Figure 4-6 are shown in Table 5-I, where a comparison of our results with data found in the literature is presented. There are some discrepancies in the absolute values, but the trends in the apparent

Table 5-I: Apparent activation energies [kJ/mol] of desulfurization of DBTs, conditions for our results: pressure 4 MPa, $H_2/oil=200 \text{ Nm}^3/m^3$

Source Catalyst	Our data NiMo	Ref. [185] NiMo	Ref. [205]: H-LGO ^a CoMo	Ref. [205]: SR-LGO ^a CoMo
DBT	120	100	92	113
4-MDBT	151	130	113	117
4,6-DMDBT	222	167	130	113

^a H-LGO = hydrotreated light gas oil, SR-LGO = straight-run light gas oil.

activation energies of selected compounds are similar to reports found in literature. In Table 5-I, the results of two LGOs, one straight-run (SR) and one hydrotreated (H) oil, are included (from ref. [205]). The SR-LGO shows higher apparent activation energies compared to H-LGO, indicating an effect of either the H_2S partial pressure or an effect of components in the oil, influencing the kinetics. Thus, differences in both activity and apparent activation energies of these components are linked with the composition of the reaction medium.

As was already mentioned in chapter 4.1.3, a more detailed look at the behavior of the studied components with temperature reveals some interesting differences. It was observed during the studies that 4,6-DMDBT shows a different behavior compared to other compounds. The lower apparent activation energy found for 4,6-DMDBT at temperatures above 350 °C at LHSV above 1 h^{-1} may be explained by an equilibrium limitation of the HDS reaction for this compound at elevated temperatures. This effect starts to be visible already at LHSV 1 h^{-1} , but this low space velocity allows us to achieve a high conversion of 4,6-DMDBT at lower temperatures where this equilibrium limitation is less pronounced. To explain the observed differences in the behavior, one has to look at the proposed mechanisms of the hydrodesulfurization of different sulfur

Table 5-II: Comparison with literature: Relative reactivity (r.a.) of sulfur compounds

Source	Catalyst	T [°C]	P [MPa]	r.a. of substituted DBTs DBT:4-MDBT:4,6-DMDBT
Our data	NiMo/ γ -Al ₂ O ₃	250	4	57.7 : 10.4 : 1
		275		14.6 : 3.4 : 1
		300		7.4 : 2.5 : 1
Kabe <i>et al.</i> [205]	CoMo/ γ -Al ₂ O ₃	330	2.94	24 : 4.5 : 1 (H-LGO) 11 : 4.1 : 1 (SR-LGO)
Meille <i>et al.</i> [198]	NiMo/ γ -Al ₂ O ₃	300	5	6 : 1.9 : 1 (without H ₂ S) 1.7 : 1.3 : 1 (with H ₂ S)
Kabe <i>et al.</i> [185] ^a	CoMo/ γ -Al ₂ O ₃	220	?	18.7 : 1.8 : 1
Farag <i>et al.</i> [132] ^a	CoMo/ γ -Al ₂ O ₃	300	2.9	2.0 : - : 1
		340		2.8 : - : 1
		380		5.4 : - : 1

^a Studies were done with single model compounds.

compounds. While DBT mainly reacts through the direct desulfurization route (cleavage of C-S bond as the first step), it is proposed in the literature that 4-MDBT and especially 4,6-DMDBT preferably react first by the hydrogenation way (the hydrogenation step is then followed by C-S bond cleavage) [179, 182, 198, 199, 253]. The hydrogenation route is probably even more favored on the NiMo catalyst, which has a higher hydrogenation activity. The cleavage of the C-S bond is irreversible while the hydrogenation step can, at certain conditions, be reversible. The equilibrium limitation of the hydrogenation reaction may become important at elevated temperatures and this may lead to the observed decrease of the activation energy at higher temperature. This can be supported by the fact that an apparent activation energy of 224 kJ/mol is obtained in the case of plotting experimental points for 4,6-DMDBT at LHSV 4 h⁻¹ only up to 350 °C. This value is fairly close to that one of the experiments performed at LHSV 0.5 h⁻¹. However, it should also be noted that transport limitations at higher temperatures cannot be excluded.

The comparisons of the observed relative reactivity and order of reactivity of sulfur compounds with the data from literature are shown in Table 5-II and Table 5-III, respectively. An inhibiting matrix effect, as proposed by Schulz *et al.* [210] and discussed also in the chapter 5.3, of the gas oil could be a part of the explanation of the observed inconsistencies in the relative reactivity found in the literature. A very strong inhibiting effect of components in the gas oil was

suggested. The effect was mainly caused by other sulfur compounds. This inhibition removes the differences in the relative reactivities of the sulfur compounds, as is clearly visible in the work of Kabe *et al.* [205] and Meille *et al.* [198]. It is also possible to see that with different catalysts the observed trend stays the same, only the ratio differs. The inhibiting effect makes it difficult to compare on the kinetic behavior of components of oils of different origin, because of composition and thus different matrix effects. From Table 5-II it is also clear that the difference in reactivity of individual components is strongly dependent on the temperature, which adds to the complexity of comparing different studies.

Table 5-III: Comparison with literature: Order of reactivity (o.r.) of sulfur compounds

Source	Catalyst	T [°C]	P [MPa]	o.r. of substituted DBTs ^a
Our data	NiMo/ γ -Al ₂ O ₃	250	4	4,6-DM <uid-DM< 4-M <uid-DM<2,4-DM< DBT <uid-DM
		275		4,6-DM <uid-DM< 4-M <rest of DM< DBT
		300		4,6-DM <rest of DM< 4-M < DBT
Schulz <i>et al.</i> [209]	CoMo/ γ -Al ₂ O ₃	277	5	all of DM < 4-M < DBT
Katti <i>et al.</i> [201]	NiMo/ γ -Al ₂ O ₃	355	11.9	4,6-DM < 4-M < DBT
Kilanowski <i>et al.</i> [189] ^b	CoMo/ γ -Al ₂ O ₃	350 - 450	0.1	4,6-DM < 4-M < DBT <2,8-DM
Houalla <i>et al.</i> [190] ^b	CoMo/ γ -Al ₂ O ₃	300	10.3	4,6-DM < 4-M <3,7-DM<2,8-DM< DBT

^a DM = dimethyl-DBT, M = methyl-DBT, uid = unidentified DBT.

^b Studies were done with single model compounds.

In spite of the difficulties this introduces, it is still possible to find a trend in the behavior of the studied components. 4,6-DMDBT is always the least reactive compound, 4-MDBT follows, and DBT has the highest reactivity of them. From the results in Table 5-III one can also see that a few of the disubstituted DBTs show even higher reactivity than unsubstituted DBT. We have not been able to identify with certainty these compounds, but 2,8-DMDBT is one example reported by others [189, 190] of such a compound belonging to the group of more reactive disubstituted DBTs. It is likely that this compound is represented by one peak in the group of unidentified DMDBTs. It is suggested that 2,8-DMDBT competes with DBT for the active sites and that 2,8-

DMDBT adsorbs more strongly on the catalyst surface thus inhibiting the desulfurization of DBT [190]. On the other hand, 4,6-DMDBT is weakly adsorbed and the steric hindrance comes into play. From the observed behavior of this compound it is possible to deduce that the reactivity of substituted DBTs is not affected only by steric effects but also electronic effects could be important factors influencing the desulfurization. A general view of the reaction is that the adsorption of the reactant molecule involves participation of delocalized π -electrons of aromatic rings as well as the sulfur atom [177, 190]. The stronger delocalization of electrons from the sulfur atom over an extensive π -system leads to a higher probability of the hydrogenation reaction to be the preferred step in the mechanism [191]. Thus the presence of methyl substituents in certain positions, 2 and 8 in this case, changes the electronic structure of the molecule and increases the strength of the adsorption on the active site of the catalyst. Further more, as Ma *et al.* [96] report, the hydrogenation of the aromatic ring then makes the molecule more susceptible to C-S bond cleavage by suppressing the conjugation of lone-pair electrons at the sulfur atom with π -electrons on the benzene ring. Thus the steric hindrance together with electronic effects have a strong influence on the reactivity of DBTs.

To conclude this chapter, all results presented here also show that at high conversions, the least reactive components, as 4,6-DMDBT, dominate the system. Improved catalysts for the deep HDS can therefore only be developed through further studies of the behavior of these components.

5.2 Hydrodesulfurization of thiophene at atmospheric pressure

5.2.1 Catalyst deactivation during thiophene HDS

5.2.1.1 Initial deactivation behavior

The initial deactivation behavior of several hydrotreating catalysts was studied. The catalysts were Mo/ γ -Al₂O₃, Mo(NTA)/ γ -Al₂O₃, NiMo/ γ -Al₂O₃, NiMo(NTA)/ γ -Al₂O₃, and two NiMoP/ γ -Al₂O₃ catalysts with different properties. Our results from these experiments are in agreement with the initial deactivation observed by Sarbak and Andersson [255] and they explain it by an initial coking of the catalyst. The discussion of our results in the following paragraphs will try to show that the similar behavior observed here can be explained by the same mechanism.

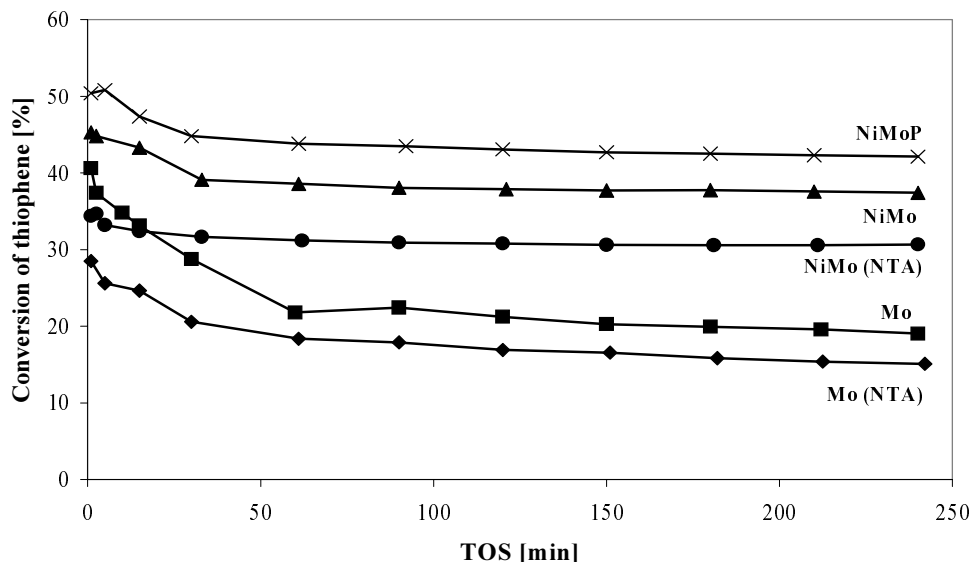


Figure 5-1 Deactivation curves for different catalysts. Pressure 0.1 MPa, reaction temperature 300 °C for NiMo, NiMo(NTA) and NiMoP catalysts, 400 °C for Mo and Mo (NTA) catalysts.

The first part of the discussion will be focused on the differences between the preparation methods. Results from this work, summarized in Figure 5-1, show no improvement of the activity by the method of preparation. Based on the literature (chapter 1.3.1.3), a larger difference between the standard and NTA based catalysts was expected. One of the possible explanations could be the fact that crushed extrudates were used in this study, while a powder catalyst was used in previous studies [64-66]. A strong interaction of the NTA based precursor of the active phase with the support could lead to an egg-shell catalyst in extrudates. However, Raman spectroscopy showed that the Mo/NTA ratio is constant throughout the extrudate (Figure 4-21). Our results are in agreement with the results of Cattaneo [63], who also failed to observe any enhancement of the activity. It is possible that in the present work the ratio between Ni and NTA was not optimal for the enhancing effect of the complexing agent and that is why no improvement of activity was observed. The catalysts were not prepared by ourselves and the Ni/NTA ratio is not known. Thus the apparent controversy between results from this work and [63] or papers by Coulier [256, 257] on one side and the results from [64-66] on the other side has to be further studied.

The differences between the promoted and unpromoted catalysts were however observed. The higher activity of NiMo catalysts as compared to Mo is in accordance with the literature ([8] and references therein). The promoting effect of Ni on the activity of molybdenum catalyst has been studied by many groups for a long time and is explained in the introduction chapter 1.3.1.2. The highest activity of NiMoP catalyst is logic since its metal loading is nearly twice that of the NiMo catalyst. However, when normalized to the amount of active phase, its activity was lower than of the NiMo catalyst. Only one set of experiments was done with NiMoP and thus the difference has to be treated with some caution. The difference in the activity was, however, confirmed by a significantly higher amount of by-products during the experiments with the phosphorus doped catalyst, which is closely related to the higher acidity of this catalyst.

Table 5-IV: Carbon content of catalysts after various times on stream

TOS [min]	0	1	60	240	1445
Mo ^a	0.14	0.18	0.27	0.35	0.55
Mo(NTA) ^b	1.00	0.99	1.04	0.95	N.A.
NiMo ^a	0.15	0.20	0.15	0.20	N.A.
NiMo(NTA) ^b	0.85	0.87	1.00	0.95	N.A.
NiMoP ^b	0.21	0.30	0.47	0.49	N.A.

^a Standard error is ± 0.02

^b Standard error is ± 0.05

N.A.: Not Available

All catalysts were analyzed for the amount of carbon and sulfur by combustion analysis and the summarized data from the result tables presented in Table 5-IV show that a small amount of carbon was already present directly after the sulfiding step. That is understandable for NTA catalysts, because the carbon containing molecule is used as a complexing agent during the preparation, but the carbon content after the sulfiding for non-NTA catalysts is surprising. The probable explanation is the presence of impurities in the tubes. The system is used for both sulfidation and thiophene HDS reactions, and traces of thiophene may be adsorbed on the tubings and desorb when a partial pressure of thiophene is low, as is the case of the sulfiding procedure. The experiments in Figure 4-19 show that the carbon deposition increases with time on stream with the carbon containing molecule at elevated temperatures, thiophene in this case. And the

experiment at 300 °C indicates that the carbon deposition is at our conditions less sensitive to the reaction temperature.

The observed carbon build-up on Mo catalyst correlates nicely with the initial decrease in thiophene conversion (Figure 4-17 and Figure 4-18). After several hours on stream, the difference between the rates of carbon deposition and the decrease of the thiophene conversion suggests that the carbon deposition is not the only factor influencing the activity of the catalyst. A similar behavior was observed for NiMoP, but the long TOS experiment was not done and thus the same conclusion as in the case of Mo catalyst cannot be drawn without uncertainties. The constant amount of deposited carbon on NiMo reflects the observed steady-state after about 30 minutes on stream. However, it does not explain clearly the initial decrease in activity, which seems to be independent of the carbon on the catalyst. As was mentioned in the case of the Mo catalyst, there has to be another factor influencing the activity of the catalyst here as well. The comparison of Mo and NiMo catalysts shows that the hydrogenation activity of nickel (discussed in more detail in chapter 5.2.2) could be the explanation for the lower equilibrium amount of carbon deposited. The higher carbon content of the NTA catalysts is most probably due to the preparation method, as was already mentioned. And there is a very small dependence of the activity of the catalyst on the sulfiding procedure, as is shown by the results of the carbon deposition and thiophene conversion in the experiment with the fast heating rate during the sulfiding mentioned in Table 4-V and Appendix A7. The constant amount of carbon (independent of the TOS), which equals for both Mo(NTA) and NiMo(NTA), indicates that there is no net carbon deposition during the reaction, even if the experiments were done at different temperatures. The shapes of the deactivation curves do not differ between standard and NTA catalysts, even though the carbon deposition follows a different pattern. This supports the idea that the carbon deposition causes only the fast initial decrease in the thiophene conversion, but there is also another factor working together with carbon deposition, which lowers the conversion of thiophene after longer TOS. The reason for the further lowering of the thiophene conversion could be the removal of the sulfur atoms from the surface of the catalyst. This topic will be addressed in more detail later on.

The amount of sulfur detected immediately after the sulfiding, where Mo catalysts have about 4 wt%, NiMo catalysts about 5 wt%, and NiMoP about 8 wt% of sulfur, shows that there is no difference between the standard and the NTA catalysts and that only the type and amount of promoter matters. The corresponding sulfur amount stays fairly constant during the whole TOS for all catalysts. The observed differences in the sulfur amounts after different times on stream are within the error of the detection method.

5.2.1.2 Reactivation experiments

The data from carbon analyses of the spent catalysts presented in the result section are summarized in Figure 5-2.

The reactivation of the Mo catalyst in H₂S/H₂ sulfiding mixture leads to the recovery of a significant part of the original activity and does not depend on the degree of deactivation. In pure H₂ only a slight recovery of the activity is found. Hence, a slight degree of desulfiding of the active phase under reaction conditions might occur and reactivation could be due to both restoration of desulfided sites and the removal of carbonaceous deposits from the active sites, in agreement with results of Elst *et al.* [234]. However, a certain degree of the surface desulfiding by the flow of H₂ cannot be totally excluded. The reactivation in pure He, being an inert gas, also recovered a small portion of the lost activity. This suggests that the reactivation mechanism also includes the restoration of active sites by the simple desorption of strongly adsorbed species. The paramount role among these species might be played by H₂S, a product of the thiophene hydrodesulfurization. However, the desorption of relatively light carbonaceous species or other reaction products might also be the reason for the observed minor recovery during He flow as well. A more detailed study is necessary to completely understand this process. Experiments at different reaction temperatures show that the deactivation of the Mo catalyst is more severe with increasing temperature, but in all cases the activity which can be recovered is almost the same. The carbon analysis data are in line with results from the HDS reaction. With increasing temperature and thus more severe deactivation, a larger amount of deposited carbon is observed. However, since the results from the standard deactivation experiments indicate that there is no direct connection between the decrease in the thiophene conversion and carbon deposition after longer TOS, the decrease in conversion is most probably not caused only by higher carbon deposition at higher temperatures. The desulfiding of the active phase of the catalysts together with the blocking of the active sites with produced H₂S then could be the cause of the observed decrease in thiophene conversion after long TOS.

The resulfiding experiments of the NiMo catalyst lead to a total recovery of original activity. In contrast with the Mo catalyst the activity loss decreases with increasing temperature. Moreover, after re-introducing thiophene, the behavior of the resulfided catalyst follows that of freshly sulfided catalyst. The carbon analysis data are again in line with the results from the HDS

reaction. With increasing temperature and thus less severe deactivation, a smaller amount of deposited carbon is observed. This is in contrast with Mo results as well.

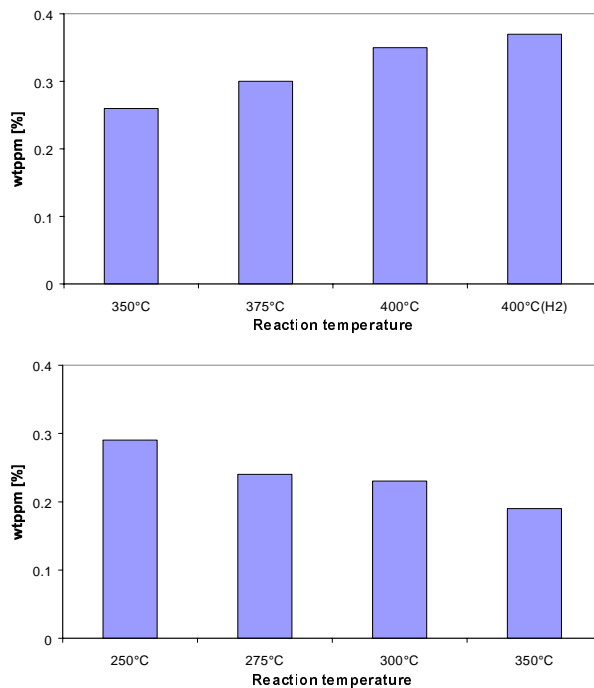


Figure 5-2 Carbon amounts deposited during the reactivation experiments.

The observed difference between Mo and NiMo catalysts suggests different relative rates of the individual steps (or parts) of the deactivation mechanism. The stronger deactivation of Mo catalyst with increasing reaction temperature is in accordance with the literature (see e.g. [8]), while the activity after reactivation shows that the lost active sites can only be restored partially. On the other hand, the decreasing deactivation at increasing reaction temperature for NiMo catalyst, as can be also inferred from their carbon content, is surprising. These results indicate that the NiMo catalyst has a higher activity for the hydrogenation reaction than the Mo catalyst, and that the activation energy for coke hydrogenation over NiMo is higher than for carbon deposition.

The reactivation experiments with different gas mixtures suggest that the reactivation of the Mo catalyst is a complex process consisting of three parts: the desorption of adsorbed species (mainly H₂S or reaction products), the removal of carbonaceous species by hydrogenation, and

restoring the sulfur active sites by resulfiding. The NiMo catalyst was not subjected to the same set of experiments, but the observed total recovery of the lost activity suggests the following: Thanks to the high hydrogenation activity of the NiMo catalyst the coke deposition has smaller negative effect on the catalyst activity and the main reasons for the deactivation are the other two processes, adsorption of reaction species and desulfiding of the catalyst surface. These two processes are then obviously reversible as has been shown with the activity of the catalyst after the reactivation step. This leads to the conclusion that in contrast with the NiMo catalyst, a main reason for the deactivation of the Mo catalyst is the carbon deposition on the active sites. The low hydrogenation activity of the Mo catalyst then makes it impossible to recover all of the activity, in contrast to what was observed for the NiMo catalyst.

5.2.1.3 Diluted flow of H_2 with inert (He)

Results from the dilution experiments of Mo and NiMo catalysts were presented in chapter 4.2.3. As can be seen, the system behaves reversibly; it “switches” from one deactivation curve to another and back again. The results from carbon analyses of the spent catalysts (chapter 4.2.5.1) show that the carbon content from experiments stopped with diluted H_2 is between 15 and 25 % higher than for those stopped under undiluted H_2 . Remarkably, the history seems to be much less important. Apparently, part of the carbon on Mo catalyst is deposited reversibly.

These experiments also show the influence of the H_2 pressure on the thiophene conversion and suggest that the order in H_2 is approximately one. The overall effect observed for H_2 contains two aspects. Primarily, the kinetic role in the thiophene HDS and secondly its role in the removal of carbon deposited on the catalyst surface.

Experiments with diluted H_2 over a NiMo catalyst produced similar results. Also the carbon analysis data show the same trend as in the case of Mo. The experiments with diluted flow led to the catalyst with more deposited carbon. The order in H_2 for NiMo catalyst was found to be different from the one for Mo catalyst, suggesting a slightly modified mechanism of thiophene HDS on different catalysts.

5.2.1.4 Surface area and porosity of studied catalysts

Results of the BET surface area analyses on standard catalysts (Mo, NiMo, and NiMoP) only show a difference between the oxidic catalyst precursors and the freshly sulfided catalysts. Standard spent catalysts show no changes in their surface area and a constant pore volume and pore size distribution, independent of the TOS as compared to their freshly sulfided counterpart.

For the NTA based catalysts, the observed changes are entirely different. Both fresh Mo (NTA) and NiMo (NTA) catalysts have a relatively low surface area and also the pore volume is much lower when compared to the standard catalysts. However, this is changed during the sulfiding and both the surface area and pore volume of the NTA catalysts increase to the levels of their standard counterparts. The explanation might be that the low values for the surface area and pore volume on the fresh NTA catalysts are caused by the presence of the complexing agent. NTA probably blocks the pores and decreases the surface area of the catalyst in its oxidic state, but during the sulfiding process NTA is decomposed and at least partly removed (as was explained earlier, NTA should help only during the preparation method to obtain more active catalyst). Some NTA is then transformed to the carbon deposited on the catalyst. This corresponds with the high amounts of the deposited carbon observed on the NTA catalysts and mentioned in chapter 5.2.1.1. By those two processes, the removal and the transformation, the surface properties of the NTA catalysts become the same as if no complexing agent was used. And again, spent NTA catalysts show no change in the surface area and pore volume with increasing time on stream.

Based on the observations it can be concluded that the deactivation of the catalysts is not caused by the changes of the surface structure of the catalyst, but that the main reasons for the deactivation are the ones already presented in chapter 5.2.1.2: blocking of the active sites, desulfiding, and the deposition of the carbonaceous species (but not causing the structural change).

5.2.2 Steady state kinetics of thiophene HDS at atmospheric pressure

In this part of work, data obtained for the thiophene HDS over commercial NiMo/ γ -Al₂O₃ and CoMo/ γ -Al₂O₃ and non-conventional Pt/Y-zeolite catalysts will be discussed with emphasis on steady state properties and differences in activity, deactivation, and selectivity of the catalysts.

5.2.2.1 Commercial molybdenum based catalysts

As was presented in Figure 4-22, where the conversion of thiophene is plotted as a function of reaction temperature, the conversion over commercial catalysts clearly increases with increasing temperature and follows a typical “S”-curve observed for the hydrodesulfurization reactions over different types of catalysts. An unexpected decrease in the thiophene conversion over CoMo catalyst at higher temperatures was assumed to be caused by the deactivation of CoMo catalysts at temperatures over 375 °C. The deactivation was confirmed by repeating an experiment at low temperature at the end of the experimental period and comparing it to the previously obtained data. A difference of 10 % between the compared results was found. The same experiment with NiMo catalysts showed a difference of about 1 %, which is within the margins of experimental error. A similar behavior of CoMo was reported by Qian *et al.* [163] during hydrodesulfurization of DBT. They observed a maximum in the conversion at about 325 °C and the same decrease at higher temperatures as was observed in our study. This was not the case for NiMo catalyst, where a total conversion of thiophene was reached at the highest reaction temperature of 400 °C. The behavior of the NiMo catalyst corresponds quite well with the results from the deactivation studies (chapter 5.2.1), where the deactivation of the catalyst decreased with increasing reaction temperature due to the continuous removal of coke by hydrogenation. The hydrogenation properties of NiMo catalyst thus make it less sensitive to coking at higher temperatures compared to cobalt-promoted catalysts.

Since neither the exact composition nor the preparation method of the commercial NiMo and CoMo catalysts used in this study was revealed by the supplier and the difference between them is not very significant, it is very difficult to make any conclusions about their order in the activity towards the thiophene HDS. The only reliable information thus could be obtained activation energy, which agrees very well with the literature data [258]. Comparison of both catalysts shows a stronger temperature dependence of the CoMo catalyst.

5.2.2.2 Non-conventional catalyst - Pt/Y-zeolite

As was mentioned in more detail in the introduction chapter 1.3.2, considerable effort is aimed at finding new types of catalysts for deep hydrodesulfurization. Noble metal catalysts are among these new types and zeolites as support have been studied quite thoroughly as well. Usually only one “part” of the catalyst (promoter or support) is changed from the conventional ones. In our

work, both promoter and support was different from the conventional ones and Pt/Y-zeolite catalyst used usually for hydrocracking [251] was tested in the thiophene hydrodesulfurization. The Pt/Y-zeolite catalyst was studied with three different pretreatments: non-activated, sulfided, and reduced.

A similar study on the noble metal catalyst supported on ZSM-5 and USY was done by Sugioka *et al.* [169, 173], respectively. The ZSM-5 studied had a higher Si/Al ratio and is thus more acidic than the Y-zeolite used here, so there has to be a careful screening of the results to make a correct comparison of our data to the literature. But ultrastable Y-zeolite (USY) is similar to our catalyst support. Sugioka studied thiophene hydrodesulfurization over calcined and reduced Pt/zeolite (Pt loading of 5 wt% and a high dispersion) at 400 °C and found it to be more active than the conventional CoMo/Al₂O₃ catalyst. They found a bifunctional activity of Pt/zeolite catalysts towards thiophene hydrodesulfurization, in which both Brönsted acid and platinum metal sites are active sites. The thiophene conversion was very high and slow deactivation was observed on Pt/USY. On the other hand, the stability of the zeolite catalysts was dependent on the SiO₂/Al₂O₃ ratio in the zeolite structure. On Pt/HZSM-5, with lower Si:Al ratio close to that of Y-zeolite and thus lower acidity of the catalyst, the activity towards thiophene HDS was stable. The deactivation was observed only at higher Si/Al ratios and was explained to be caused by the coking of strongly acidic active sites. Our catalyst similar to Pt/USY was deactivating much faster, but that could be linked to the very low amount of Pt in our study (0.03 %). However, the experimental periods were relatively short and it is not possible to make any conclusions about the stability of the catalyst during longer TOS. The same results are reported by Navarro *et al.* [168], where they used a low loading of Pt (0.72 wt%) on HY-zeolite for HDS of DBT. They mention a high initial deactivation possibly attributed to the zeolite support, followed by a slow decrease in the activity caused by the deactivation of active sites with increasing TOS. The fast initial deactivation of Pt/ultrastable Y-zeolite was also reported by Reinhoudt *et al.* [166]. In the case of Pt/HZSM-5 [169], the authors found no effect of pretreatment on the activity of the catalyst and a high robustness towards H₂S poisoning. Their proposed mechanism of the reaction, presented in Figure 5-3, involves thiophene activation on Brönsted active sites together with hydrogen activation on Pt metal sites and hydrogen spillover.

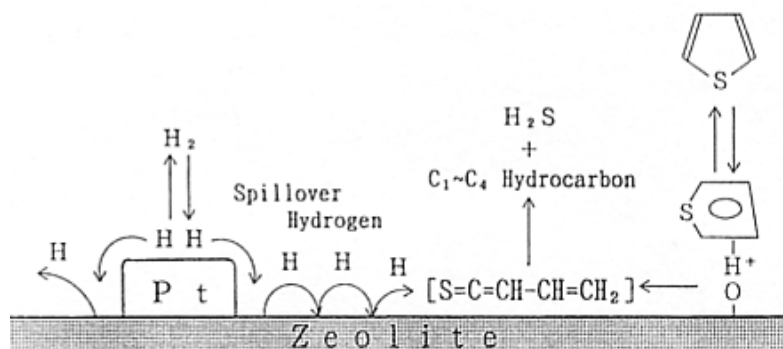


Figure 5-3 The possible mechanism of thiophene HDS by Sugioka *et al.* [169, 173].

Our results presented in Figure 4-22 show a quite different picture for the Pt/Y-zeolite catalyst when compared to conventional catalysts. The activity of the Pt/Y-zeolite catalyst is very low. Nevertheless, the conversion increases with increasing temperature, even if the increase is much less pronounced. However, if the rate constant is based on the amount of active promoter (Ni+Mo and Co+Mo against Pt), the activity of Pt/Y-zeolite catalysts reaches the same levels as the conventional catalysts, in a few cases even a higher activity. Thus the Pt/Y-zeolite catalyst with a higher Pt loading could be competitive in the thiophene HDS with conventional molybdenum based catalysts. A crude estimate indicates that a Pt loading of about 1.5 - 2.0 % would give similar activity as the conventional commercial catalysts. Hence, the high activity observed on a 5 % Pt/Y-zeolite catalyst in the work of Sugioka *et al.* [169, 173] is not surprising.

At the highest temperature, both the sulfided and non-activated Pt/Y-zeolite catalyst showed very low conversion and close to identical values. To rule out that this low conversion is not just thermal decomposition of thiophene without the help of a catalyst, a blank run with only inert (SiC) was done. A negligible conversion of thiophene (below 1 %) was observed, proving a catalytical behavior of Pt/Y-zeolite.

The identical values of the conversion at high temperatures for sulfided and non-activated catalyst was a quite interesting observation. Since the only difference between these two catalysts was the missing sulfiding step in the case of non-activated catalyst, the phenomenon can be explained by the *in situ* sulfiding of non-activated catalyst by the reaction mixture in the first few hours of the reaction. The quite high insensitivity of the catalysts to the way of sulfiding would then explain the identical values of the thiophene conversion after several hours on stream.

However, an exception from this is the first experiment with the reduced Pt/Y-zeolite, which gives ca. 35 % conversion of thiophene at 400 °C, about twice that of the other two pretreatments. Similar results were found by Reinhoudt *et al.* [166] using their Pt catalyst. However, upon repeating the experiment at exactly the same conditions after 145 hours on stream, the conversion is below 20 % and in the experiments between the same activity as the other two pretreated catalysts was found. Thus the effect of pretreatment is clearly important, but only for the initial activity of the catalyst. This indicates that metallic Pt as such is more active than the sulfidic or ionic form of the metal. However, the metal is susceptible to a rapid deactivation, probably due to partial or complete sulfidation. The observed deactivation is in agreement with Navarro *et al.* [168] and Reinhoudt [166]. The “deactivation test” was performed for all three types of pretreatment and at all cases the already low conversion was after a few days even lower, as was presented in Figure 4-22.

The activation energies for Pt catalysts were lower than the ones for molybdenum based catalysts for all pretreatment methods. The relatively high value of the activation energy for the non-activated catalyst has to be considered with some caution, because the value was obtained from only two experimental points.

To conclude, even if the activity of this catalyst might be comparable to the conventional types when sufficient loading of the metal is present, the fast deactivation due to coking of the active sites or the sintering of the metal particles makes this catalyst a less attractive alternative to conventional catalysts for hydrodesulfurization reactions. But this type of catalyst can be used as the catalyst in the second stage, downstream of a conventional catalyst, as was presented in the introduction.

5.2.2.3 Selectivity of reaction products of thiophene HDS

Chapters 4.2.4 and 4.3.2 describe the product selectivities during the initial deactivation experiments and during steady-state thiophene HDS, respectively. The main products of the reaction on all catalysts during all experiments were C₄ compounds: trans- and cis-2-butene, 1-butene, and n-butane. This corresponds well with the data reported in literature [258, 259]. The higher selectivity of trans-2-butene when compared to cis-2-butene suggests the shift of the isomerization equilibrium towards the more energetically stable and sterically less hindered

conformation of *trans*-2-butene. 1,3-butadiene was not observed and a few other products were detected at very low concentrations.

The product distribution and selectivity during the initial deactivation experiments over Ni promoted catalysts discussed in chapter 5.2.1 was not studied in such detail as in the case of steady-state kinetics. To summarize the main results, the four main C₄ products had (with the only exception in the case of the unpromoted Mo catalyst) similar selectivities over the different catalysts. That suggests the same mechanism of thiophene hydrodesulfurization over Ni promoted catalysts independent of the type or the preparation method of the catalyst. The comparison of the data for the NiMo catalyst from the initial deactivation studies (chapter 4.2.4) with the data for the same catalyst in the steady-state kinetics (chapter 4.3.2) shows no difference. A more detailed look on the differences in selectivities and product distribution between different types of catalysts during steady-state HDS of thiophene follows:

During steady-state HDS of thiophene, the lighter products (C₃ and lower) started to appear at about 300 °C and their amount was increasing with increasing reaction temperature. They were assigned to be products of the catalytic side-reactions, most probably products of acidic cracking at high temperature. However, these products were not clearly identified. On the other hand, the heavier products were observed at virtually all temperatures, but their amount was decreasing with increasing conversion of thiophene. One of these high retention time peaks had a quite high selectivity on NiMo and Pt/Y-zeolite catalysts at lower temperatures and based on the retention time this compound was assumed to be tetrahydrothiophene with a boiling point of 119 °C. This demonstrates an alternative route to thiophene HDS over catalysts with strong hydrogenation abilities (see HYD route in the reaction scheme in Figure 1-1).

There are also differences in the product selectivities between the molybdenum based catalysts and the Pt/Y-zeolite catalyst which will be examined in some more detail.

For all molybdenum based catalysts, the product selectivities were quite similar. The shape of the selectivity curves for unsaturated C₄ compounds suggests that these are the reaction intermediates, which are subsequently hydrogenated to *n*-butane. The selectivity of *n*-butane was observed to increase at high temperatures and corresponding to *n*-butane being the final product of thiophene hydrodesulfurization (Figure 1-1 and ref. [183, 192]). However, there is a difference between the catalysts in the selectivity towards *n*-butane at high conversions of thiophene. The selectivity is higher for NiMo catalysts, which corresponds to its higher hydrogenation activity when compared to CoMo (e.g. [183]). Since the hydrogenation is an exothermic process, one

would expect it to be less pronounced at higher temperatures. But this does not seem to be the case and the hydrogenation activity of NiMo catalyst increases at higher temperatures, so the reaction is most probably not governed by thermodynamics, but by kinetics. Hydrogenation proceeds on different active sites from desulfurization and the different ratio of these two types of active sites between the two catalysts may be part of the explanation of the observed phenomenon. Another difference was found to be the selectivity to 1-butene, which was about 12 % and stayed unchanged for the NiMo catalyst. On the CoMo catalyst 1-butene was the main product at low temperatures (35 %) and its selectivity decreased with increasing temperature (conversion of thiophene) to a level of about 15 %. This suggests slightly different relative rates of the steps in the mechanism of the hydrodesulfurization of thiophene (Figure 1-1) on those two catalysts. The selectivity towards cracking products was the same for both catalysts, suggesting an effect of temperature and no difference between the catalysts. This similarity indicates that this is cracking on acidic sites on the support. The selectivity to tetrahydrothiophene was very low over NiMo for all the temperatures, while it was relatively high at low temperatures at CoMo. If we assume this compound to be a reaction intermediate, then the observed phenomenon might be explained by the different reaction mechanisms of thiophene decomposition on the catalysts compared at low reaction temperatures.

On the Pt/Y-zeolite catalyst, some of the product selectivities depend on the pretreatment method. As was mentioned earlier, lack of experiments with the sulfided Pt/Y-zeolite made it impossible to generate the same plot as is presented in Figure 4-24. But the observed product selectivity over the sulfided Pt/Y-zeolite at 400 °C agree with the results from the non-activated Pt/Y-zeolite. This is in line with the idea of *in situ* sulfiding during thiophene HDS of the non-activated catalyst presented in chapter 5.2.2.2. Hence the discussion on the selectivities will be focused on the non-reduced and reduced catalyst. In both cases, the trend of selectivities of all three isomers of butene is the same as over molybdenum based catalysts. Also the selectivity to n-butane increases with increasing temperature. But the values of the selectivity to n-butane is different on reduced Pt/Y-zeolite. On the non-activated catalyst, the selectivity towards n-butane follows the same trend as in the case of conventional catalysts. But on the reduced Pt/Y-zeolite the n-butane selectivity is at all temperatures higher than the selectivities to cis-2-butene and 1-butene. This indicates that the Pt/Y-zeolite catalyst has a high initial hydrogenation activity, which is not surprising (see e.g. [168]). But this initial activity is lost upon extended exposure to sulfur.

Figure 4-24 also demonstrates a very high selectivity towards tetrahydrothiophene. Tetrahydrothiophene was observed over molybdenum based catalysts as well, but at much lower selectivities and it almost disappeared at higher conversions. On Pt/Y-zeolite catalyst, the selectivity to this product is also decreasing with higher temperatures to low values, but the selectivity at lower temperatures is still several times higher than over conventional catalysts. Obviously, the Pt/Y-zeolite catalyst at low conversions of thiophene favors another reaction pathway, which leads to tetrahydrothiophene. The scheme in Figure 5-3 illustrates the activation of thiophene and hydrogen on two different active sites and it is probable that both activated compounds will react to create a hydrogenated thiophenic ring before the C-S cleavage occurs. Navarro *et al.* [168] points out that the direct C-S cleavage route is preferred to the hydrogenation route on noble metal/zeolite catalysts at all temperatures, but the relative hydrogenation activity of the Pt/zeolite catalyst (compared to direct desulfurization) decreased significantly with increasing temperature. That is exactly the case observed during our experiments. But then again, the speculation that the hydrogenation of the thiophenic ring is important does not seem to be fully supported by the observation of selectivities over molybdenum based catalysts. If the hydrogenation properties play an important role in the reaction mechanism, one would expect it to be more pronounced on the NiMo catalyst. This is the case for the final reaction towards n-butane, but for tetrahydrothiophene the opposite is true, because the CoMo catalyst gives a higher selectivity at low temperatures. However, the article by Mijoin *et al.* [56] shows clearly that at all conditions the direct desulfurization (DDS) route is preferred to hydrogenation (HYD) on both NiMo and CoMo catalysts and that the ratio between DDS/HYD depends on the amount of active metal (Ni, Co) in the catalyst. Thus the difference in selectivity towards different reaction pathways is dependent on the catalyst composition, as is also presented in the work of Robinson *et al.* [67]. From the study of our catalysts it seems that the Ni : Mo ratio in the NiMo catalyst gives very low selectivity towards the initial hydrogenation route of the HDS of thiophene, while the different Co : Mo ratio in the CoMo catalyst slightly increases the selectivity towards the hydrogenation route when compared to NiMo. Another explanation could be the reaction rates of the formation and disappearance of the reaction intermediate. If the formation of the intermediate is higher on the NiMo catalyst when compared to CoMo and the subsequent reaction to C₄ products is faster on NiMo as well, then the observed difference in the selectivities on the catalysts can be understood. Nevertheless, this cannot be verified or displaced by evidence

without the detailed kinetic modelling of all the reaction steps and the knowledge of the exact composition of the studied catalysts.

According to scheme the presented by Blake *et al.* [260], tetrahydrothiophene can be desulfurized to 1,3-butadiene, which is immediately hydrogenated to form the observed final products.

Since HDS is defined as the removal of the sulfur atom from the organic compound, the presence of a sulfur-containing reaction intermediate would make the HDS conversion lower compared to the overall thiophene conversion. However, the concentration of this compound is very low and thus the difference between the two conversions is negligible (see Figure 4-22).

Over the Pt/Y-zeolite catalyst a low retention time peak was observed as well, but since it started to appear only at higher temperatures, it was assigned to be the product of cracking reaction at high temperatures.

5.3 High-pressure steady-state kinetics of DBT HDS and study of “matrix effect”

5.3.1 DBT in *n*-heptane

The kinetics of the hydrodesulfurization of dibenzothiophene (DBT) was studied in this part of work. The effect of other sulfur compounds and of aromatics on this reaction was studied as well and will be discussed in chapters 5.3.2 and 5.3.3, respectively. But first the focus will be given to the study of the hydrodesulfurization of pure DBT dissolved in *n*-heptane.

Figure 4-25 shows the conversion of DBT as a function of the reaction temperature. Three separate regions are visible. The first one with no change in the conversion, which is about 10 %, at temperatures 150 - 170 °C. The second region with a very small increase in the conversion in the temperature range 170 - 190 °C and the last one with a steep increase in the conversion at temperatures between 190 and 250 °C. The complete conversion of DBT was observed at 250 °C. The measurable, low, and apparently temperature-independent conversion of DBT at temperatures below 170 °C is very surprising. At present, no clear explanation of this phenomenon is available. The lack of a temperature response might indicate that this is an experimental artefact, e.g. due to inconsistencies in the mass balance. After reaching 170 °C, the reaction rate starts to increase and the activation energy in the temperature region 170 - 200 °C was found to be 101 kJ/mol, which is in quite good agreement with data found in the literature

[57, 185] and is also close to the range of activation energies found for DBT in the light gas oil in our previous studies (chapter 4.1.3).

The products of the hydrodesulfurization of DBT were presented in chapter 4.4.4. They were identified as biphenyl (BP), cyclohexylbenzene (CHB), and tetrahydro-/hexahydrodibenzothiophene (THDBT/HHDBT). Only the first two were identified by the injection of pure compounds. The maximum in the area of the peak eluting just shortly before DBT that is presented on the top of Figure 4-28 suggested that it is a reaction intermediate. According to observed retention time, selectivities, and a reaction scheme (Figure 1-6) it was thus assigned to THDBT/HHDBT. The bicyclohexyl (BCH) was not observed during our experiments suggesting that the hydrogenation step from CHB to BCH is very slow at our conditions and the reaction cannot yield detectable amount of BCH. A very similar product distribution was found in several papers presented in the literature, e.g. [182, 198, 200, 261].

BP as the main product at low conversions of DBT demonstrates that the direct desulfurization route (DDS) is preferred on the NiMo catalyst. This route is preferred to hydrogenation (HYD) followed by desulfurization at all temperatures, but at the same time the DDS/HYD ratio changes. In accordance with other studies [179, 261], the aromatic hydrogenation activity, defined as the ratio between the selectivities to CHB and BP¹, is increasing with increasing conversion of DBT. This can be explained by looking at the different active sites necessary for DDS and HYD. The DDS route is generally believed to require sulfur vacancies on the catalyst surface, where the cleavage of C-S bond and the formation of H₂S can occur. H₂S then most probably adsorbs strongly on these sites and affects the DDS path. The HYD route is believed to proceed through the activation of DBT on strong Brønsted acid active sites (see e.g. Nagai *et al.* [225]) followed by hydrogenation by activated H₂. Hence it seems that H₂S affects mainly the DDS route while HYD is inhibited much less and this is more pronounced with increasing temperature. The observed decrease in DDS/HYD ratio is then result of this effect.

-
1. One has to be very careful in the making conclusions about the BP/CHB ratio, since CHB is produced not only via the hydrogenation route from DBT, but in some extent also by the hydrogenating of BP produced via DDS (Whitehurst *et al.* [262]).

5.3.2 Effect of sulfur compounds on hydrodesulfurization of DBT

The effect of H_2S was presented by many authors and is a very important factor in the HDS reactions, but studies of the effect of other sulfur compounds are scarce. The strong inhibition effect of sulfur on the hydrodesulfurization of DBT over $\text{NiMo}/\gamma\text{-Al}_2\text{O}_3$ catalyst was observed in our work as well and it was not dependent on the type of sulfur compound. However, the way in which the reaction was affected at low concentrations of the added inhibitor was different. At the higher concentrations of the added sulfur compound the differences are diminishing and the effect of thiophene and DMDS was nearly the same. From the introduction it is clear that the studied model compound is very important in determining the H_2S effect on the HDS reaction [205]. With substituted DBTs, the HYD route is more affected, while during the HDS of unsubstituted DBT the DDS route is more inhibited [204, 213]. The results of our work agree with the H_2S data published in [215]: The addition of DMDS, which decomposes immediately to H_2S , inhibits the direct desulfurization route of DBT hydrodesulfurization leading to BP. At the same time the selectivity towards the CHB (hydrogenation route) is therefore slightly increased. On the other hand, the addition of thiophene (up to a certain amount) seems to have the opposite effect: The selectivity towards BP (DDS route) was increased and a decrease in the selectivity towards the hydrogenation route was observed. This suggests a different mechanism of the inhibition. While the effect of H_2S has been thoroughly studied and the mechanism is well known, the same is not true for thiophene. H_2S was found to adsorb more strongly on the active sites responsible for C-S bond breaking, compared to the hydrogenation sites. This causes the elimination of S from organic sulfur compounds to be inhibited and the selectivity towards DDS decreases. This is true in the case of DMDS, which is very unstable and immediately decomposes to form two molecules of H_2S . On the other hand, decomposition of thiophene gives only one molecule of H_2S and thiophene is a more stable molecule when compared to DMDS. The mechanism of inhibition by thiophene is then probably related to both the inhibition by H_2S and the competition of the HDS reaction between thiophene and DBT. It seems obvious that at low concentrations of thiophene its inhibiting effect is more pronounced than the effect of H_2S . The effect of thiophene can be explained by its higher activity compared to DBT, probably caused also by the easier and stronger adsorption on the catalyst active sites, which leads to the well known preference of the hydrodesulfurization of lighter thiophenic molecules before the DBT. At higher concentrations of

thiophene the increased amount of H_2S is produced and its inhibition of DBT hydrodesulfurization becomes stronger. The result of thiophene inhibition is then the same as was observed in the case of DMDS.

To conclude, the inhibition effect of both DMDS and thiophene is the same in the sense of the decrease of the DBT conversion. But at low concentrations, there are differences between the mechanisms of the inhibition between those two molecules. DMDS decomposes immediately to H_2S which inhibits the DDS route and thereby slightly increases the selectivity towards HYD. Thiophene at low concentrations inhibits the hydrogenation route, probably by the competitive adsorption on the active sites, while at higher concentrations the increased amount of H_2S has the same inhibition effect as is the case of DMDS. Obviously, the effect of H_2S inhibition is much stronger than that of thiophene.

5.3.3 *Effect of aromatics on hydrodesulfurization of DBT*

From the literature a strong inhibition effect of aromatics is well known. However, most of the work does not provide any clear conclusions regarding the inhibition of either the DDS or the HYD route. We have studied both toluene and naphthalene and a different inhibition behavior was observed. The addition of naphthalene decreased severely the total conversion of DBT. Both reaction pathways were suppressed, but the selectivity towards BP (DDS route) decreased, while the selectivity towards the hydrogenation of DBT increased. This seems to be in contrast with the results presented in the literature, where the preference of the hydrogenation of naphthalene to that of the sulfur compound is reported [188, 204, 218]. However, we also observed hydrogenation products of naphthalene, tetralin and decalin. Also the fact that the catalyst was almost totally deactivated already after one experiment with naphthalene might be of help in the explanation of the observed behavior. If the hydrogenolysis sites are susceptible to the deactivation by coke produced from naphthalene (and naphthalene is known as a perfect coke precursor), then the observed shift in the selectivity towards CHB could also be explained by the blocking of hydrogenolysis sites. This would inhibit the direct C-S cleavage and then the (not so severely inhibited) hydrogenation sites could continue in producing the hydrogenation products. Thus the interpretation could be as follows: Naphthalene is clearly a strong inhibitor of both the DDS and HYD reaction pathways during HDS of DBT. The observed decrease in selectivity to BP proves a much stronger effect of naphthalene on the DDS route. The presence of decalin and

tetralin, products of the hydrogenation of naphthalene, shows at the same time the competition between DBT and naphthalene for the hydrogenation sites on the catalyst. But the suppression of the DDS route is much larger than that of HYD route thanks to the deactivation and that is why we in the final picture observe seemingly controversial results: both hydrogenation of naphthalene and increase of selectivity for the HYD route in HDS of DBT. However, it is necessary to mention that due to the rapid deactivation we have done only a few experiments and the conclusion cannot be drawn without some uncertainty.

The experiments with toluene are easier to explain. The addition of toluene as a co-solvent affected the conversion of DBT much less and the selectivity ratio was affected in the opposite way than in the case of naphthalene. With increasing amounts of toluene in the solution the selectivity to BP increased and in the same time the produced amount of CHB decreased. The effect of toluene clearly seems to be a suppression of the hydrogenation properties of the catalyst. The deactivation of the hydrogenolysis sites does not play a paramount role here and it can be speculated that the competition between toluene and DBT for the hydrogenation sites governs the importance of the different HDS pathways. This leads to a decrease of the hydrogenation products of DBT reaction and to an increase in the observed selectivity to C-S cleavage.

The inhibition effect of aromatics is not so clear and well understood as was the case of the effect of H₂S. Fewer studies in the literature and insufficient data from our experiments, especially regarding heavier aromatics, make it impossible to draw strong conclusions and this part of the work should be pursued further.

6. CONCLUSIONS

GC-AED is a powerful tool in the detailed analysis of the individual sulfur compounds present in the light gas oil. By this method it is possible to obtain both qualitative and quantitative information about sulfur in the studied oil.

The difference in reactivities between individual sulfur compounds in the light gas oil exists. The order of reactivity of the identified sulfur compounds over a commercial NiMo/ γ -Al₂O₃ catalyst is DBT > 4-MDBT > 4,6-DMDBT. This agrees with the data found in the literature [189, 190, 201, 209]. The observed difference is changing with the changing reaction temperature - the difference is smaller at high reaction temperatures.

The catalyst preparation with the nitrilotriacetic acid (NTA) as a complexing agent did not improve the activity of the Mo/ γ -Al₂O₃ and NiMo/ γ -Al₂O₃ catalysts towards thiophene HDS. This is in contrast with the earlier observations found in the literature [64-67], but corresponds well with recent results [256, 257]. NTA does not have any effect on the deactivation behavior of the studied catalysts.

All studied catalysts (Mo/ γ -Al₂O₃, Mo(NTA)/ γ -Al₂O₃, NiMo/ γ -Al₂O₃, NiMo(NTA)/ γ -Al₂O₃, and two NiMoP/ γ -Al₂O₃) show a fast initial deactivation during thiophene HDS. This is more pronounced for the unpromoted catalysts, where the drop in the thiophene conversion is about 50 %. For the nickel-promoted catalysts the decrease is about 25-30 %. Nickel promoted catalysts are thus more robust and more resistant to the deactivation process. The presence of phosphorus slightly increases the activity of the nickel-promoted catalyst, but has no effect on the deactivation behavior in thiophene HDS at atmospheric pressure.

A significant difference between the Mo/ γ -Al₂O₃ and NiMo/ γ -Al₂O₃ catalysts was found during the reactivation experiments. The resulfiding of Mo/ γ -Al₂O₃ partly restored the activity lost during the HDS of thiophene and at all studied temperatures the percentage of the restored activity was the same. In the case of NiMo/ γ -Al₂O₃, a complete restoration of the activity lost during the HDS of thiophene was observed and it was independent on the reaction temperature as well. The behavior of the NiMo/ γ -Al₂O₃ catalyst after the resulfiding step closely resembled the

behavior of the fresh catalyst. The partial reactivation of Mo/ γ -Al₂O₃ with pure H₂ (without H₂S) and with pure inert (helium) indicates that the reactivation of the catalyst occurs through several mechanisms: Resulfiding leads to a restoration of the desulfided active sites, presence of H₂ leads to a hydrogenation and removal of the deposited carbonaceous species, and the flow of the gas leads to the desorption of the reactants and products from the active sites of the catalyst. The desorption of adsorbed species can occur with the flow of any gas or gas mixture (not only inert), but the hydrogenation of the carbonaceous species is connected with the presence of H₂, and the re-sulfiding of the catalyst can be observed only in the presence of H₂S.

For Mo/ γ -Al₂O₃, the deactivation of the catalyst is more pronounced with the increasing reaction temperature. The amount of the carbon deposited on the Mo/ γ -Al₂O₃ catalyst follows the same trend, it increases with the increasing temperature. However, for NiMo/ γ -Al₂O₃ the opposite behavior is observed. The amount of carbon and the degree of the deactivation is decreasing with the increasing temperature. This difference is attributed to the higher hydrogenation activity of nickel, which causes the faster removal of the deposited carbonaceous species. As was mentioned before, during the reactivation procedure all three causes of the deactivation are addressed and this leads to the conclusion that the desulfiding of the active sites and the adsorption of the reaction species is significantly less pronounced on the NiMo/ γ -Al₂O₃ catalyst.

Experiments with the H₂ flow diluted with helium indicate different reaction orders with respect to H₂. The Mo/ γ -Al₂O₃ catalyst is more sensitive to the partial pressure of H₂ when compared to NiMo/ γ -Al₂O₃. The “reversible coke” and a possibility to “switch” from the deactivation curve obtained during the diluted flow to the curve obtained during the normal conditions was observed on the Mo/ γ -Al₂O₃ catalyst.

Characterization studies of the spent catalysts show no change in the amount of sulfur present on the catalyst. The amount of carbon is increasing with the increasing time on stream for the Mo and NiMoP catalysts, while for the NTA-based catalysts and NiMo the amount stays constant. The higher amount of carbon deposited on the NTA-based catalysts corresponds to the presence of the carbon compound on the catalyst (NTA). For the standard catalysts, a decrease in the

surface area and pore volume was observed during the sulfidation step. It corresponds to the transformation of the oxidic state of the catalyst to the sulfidic one. On the other hand, an increase in the surface area and pore volume was observed during the sulfiding of the NTA-based catalysts. This was attributed to the removal of NTA from both the pores and the surface of the catalyst during the process. For all the catalysts, no change in the surface area and the pore volume with the increasing time on stream was observed indicating that the deactivation is not due to structural changes of the catalyst.

In the HDS of thiophene, CoMo and NiMo catalysts were found to be equally active. A Pt/Y-zeolite with low Pt-loading was tested in the reaction and the activity in thiophene HDS based on the amount of Pt was quite high. However, a very fast and strong deactivation was found in the case of the Pt/Y-zeolite catalyst, which makes it less suitable for the HDS process. Nevertheless, this type of catalyst could probably be applied in a two-stage hydrodesulfurization process.

The product selectivities during the HDS of thiophene were found to be the same for all standard catalysts, but slightly different for the Pt/Y-zeolite catalyst. The higher hydrogenation activity leads to higher selectivities of the hydrogenated products, especially the final product, n-butane. The selectivity to tetrahydrothiophene, the hydrogenated intermediate of thiophene was also dependent on the type of catalyst. Especially at low conversions (at low temperatures) there was a significant selectivity to this product over CoMo.

The inhibition effect of other sulfur compounds on the hydrodesulfurization of dibenzothiophene (DBT) was studied. Thiophene and DMDS have the same inhibiting effect on the total conversion of DBT, but the effect on the selectivities of the products is different at low concentrations of the inhibitor. DMDS, which immediately decomposes to two molecules of H₂S, affects the direct desulfurization route more, while thiophene affects the hydrogenation of DBT more. It is assumed that at low concentrations of thiophene a competitive adsorption of thiophene inhibits the HDS of DBT more than the presence of H₂S. However, at higher concentrations of the inhibitor both compounds affect the direct desulfurization pathway strongest. This indicates that the inhibiting effect of H₂S on the direct desulfurization route is stronger than the effect of thiophene on the hydrogenation pathway.

The inhibition effect of aromatics on the hydrodesulfurization of dibenzothiophene (DBT) was investigated using toluene and naphthalene. Both compounds affect the total conversion of DBT. Naphthalene was found to cause an irreversible deactivation of the catalyst and was thus observed to be a much stronger inhibitor. Naphthalene inhibits mainly the direct desulfurization pathway, while the hydrogenation route is more affected by the presence of toluene.

This work has addressed several important aspects of the hydrodesulfurization process: Kinetics of the individual components of the light gas oil, kinetics of the model compounds (thiophene and dibenzothiophene), and the effect of the other components of the oil on the conversion of the sulfur compounds (matrix effect). The initial deactivation of the hydrotreating catalysts was given significant attention as well. Future work should be focused mainly on the study of the matrix effect, because the inhibition by the other components in the oil is very closely related to the industrial operations and these effects are not evident from conventional kinetic studies of single components.

7. REFERENCES

- [1] S. F. Venner, *Hydrocarbon Process.* **79(5)** (2000) 51.
- [2] T. E. Swaty, J. L. Nocca, J. Ross, *Hydrocarbon Process.* **80(2)** (2001) 62.
- [3] J. Ancheyta-Juárez, E. Aguilar-Rodríguez, D. Salazar-Sotelo, G. Betancourt-Rivera, M. Leiva-Nuncio, *Appl. Catal. A* **180** (1999) 195.
- [4] G. Marroquín-Sánchez and J. Ancheyta-Juárez, *Appl. Catal. A* **207** (2001) 407.
- [5] J. Ancheyta, G. Betancourt, G. Marroquín, G. Centeno, L. C. Castaneda, F. Alonso, J. A. Munoz, Ma. T. Gómez, P. Rayo, *Appl. Catal. A* **233** (2002) 159.
- [6] H. R. Reinhoudt, R. Troost, A. D. van Langeveld, S. T. Sie, J. A. R. van Veen, J. A. Moulijn, *Fuel Process. Technol.* **61** (1999) 133.
- [7] S. T. Sie, *Fuel Process. Technol.* **61** (1999) 149.
- [8] H. Topsøe, B.S. Clausen, F.E. Massoth, *Hydrotreating Catalysis*, Springer-Verlag, Berlin Heidelberg, 1996, p. 114.
- [9] J. Laine and D. L. Trimm, *J. Chem. Tech. Biotechnol.* **32** (1982) 813.
- [10] E. Furimsky, *Appl. Catal. A* **171** (1998) 177.
- [11] M. Daage and R. R. Chianelli, *J. Catal.* **149** (1994) 414.
- [12] G. Alonso, M. Del Valle, J. Cruz, V. Petranovskii, A. Licea-Claverie, S. Fuentes, *Catal. Today* **43** (1998) 117.
- [13] L. Busetto, A. Iannibello, F. Pincolini, F. Trifiró, *Bull. Soc. Chim. Belg.* **90(12)** (1981) 1233.
- [14] M. Del Valle, J. Cruz-Reyes, M. Avalos-Borja, S. Fuentes, *Catal. Lett.* **54** (1998) 59.
- [15] Y. Iwata, K. Sato, T. Yoneda, Y. Miki, Y. Sugimoto, A. Nishijima, H. Shimada, *Catal. Today* **45** (1998) 353.
- [16] Y. Iwata, Y. Araki, K. Honna, Y. Miki, K. Sato, H. Shimada, *Catal. Today* **65** (2001) 335.

- [17] G. C. A. Schuit and B. C. Gates, *AIChE J.* **19(3)** (1973) 417.
- [18] P. Ratnasamy and S. Sivasanker, *Catal. Rev. - Sci. Eng.* **22(3)** (1980) 401.
- [19] P. Grange, *Catal. Rev. - Sci. Eng.* **21(1)** (1980) 135.
- [20] M. J. Ledoux, A. Peter, E. A. Blekkan, F. Luck, *Appl. Catal. A* **133** (1995) 321.
- [21] F. Maugé, J. Lamotte, N. S. Nesterenko, O. Manoilova, A. A. Tsyganenko, *Catal. Today* **70** (2001) 271.
- [22] Y. Sakashita, Y. Araki, H. Shimada, *Appl. Catal. A* **215** (2001) 101.
- [23] R. J. H. Voorhoeve and J. C. M. Stuiiver, *J. Catal.* **23** (1971) 228.
- [24] J. M. J. G. Lipsch and G. C. A. Schuit, *J. Catal.* **15** (1969) 163.
- [25] J. M. J. G. Lipsch and G. C. A. Schuit, *J. Catal.* **15** (1969) 174.
- [26] J. M. J. G. Lipsch and G. C. A. Schuit, *J. Catal.* **15** (1969) 179.
- [27] V. H. J. de Beer, T. H. M. van Sint Fiet, J. F. Engelen, A. C. van Handel, M. W. J. Wolfs, C. H. Amberg, G. C. A. Schuit, *J. Catal.* **27** (1972) 357.
- [28] R. J. H. Voorhoeve, *J. Catal.* **23** (1971) 236.
- [29] R. Huisman, R. de Jonge, C. Haas, F. Jellinek, *J. Solid State Chem.* **3** (1971) 56.
- [30] B. Delmon, *Bull. Soc. Chim. Belg.* **88(12)** (1979) 979.
- [31] D. Pirotte, J. M. Zabala, P. Grange, B. Delmon, *Bull. Soc. Chim. Belg.* **90(12)** (1981) 1239.
- [32] B. S. Clausen, H. Topsøe, R. Candia, J. Villadsen, B. Lengeler, J. Als-Nielsen, F. Christensen, *J. Phys. Chem.* **85(25)** (1981) 3868.
- [33] H. Topsøe, B. S. Clausen, R. Candia, C. Wivel, S. Mørup, *J. Catal.* **68** (1981) 433.
- [34] C. Wivel, R. Candia, B. S. Clausen, S. Mørup, H. Topsøe, *J. Catal.* **68** (1981) 453.
- [35] B. S. Clausen, B. Lengeler, R. Candia, J. Als-Nielsen, H. Topsøe, *Bull. Soc. Chim. Belg.* **90(12)** (1981) 1249.
- [36] H. Topsøe, B. S. Clausen, R. Candia, C. Wivel, S. Mørup, *Bull. Soc. Chim. Belg.* **90(12)** (1981) 1189.

- [37] N.-Y. Topsøe and H. Topsøe, *J. Catal.* **84** (1983) 386.
- [38] H. Topsøe and B. S. Clausen, *Catal. Rev. - Sci. Eng.* **26(3-4)** (1984) 395.
- [39] H. Topsøe, R. Candia, N.-Y. Topsøe, B. S. Clausen, *Bull. Soc. Chim. Belg.* **93(8-9)** (1984) 783.
- [40] L. S. Byskov, J. K. Nørskov, B. S. Clausen, H. Topsøe, *Catal. Lett.* **64** (2000) 95.
- [41] R. Candia, B. S. Clausen, H. Topsøe, *Bull. Soc. Chim. Belg.* **90(12)** (1981) 1225.
- [42] V. H. J. de Beer, T. H. M. van Sint Fiet, G. H. A. M. van der Steen, A. C. Zwaga, G. C. A. Schuit, *J. Catal.* **35** (1974) 297.
- [43] P. Chiplunker, N. P. Martinez, P. C. H. Mitchell, *Bull. Soc. Chim. Belg.* **90(12)** (1981) 1319.
- [44] A. N. Startsev, *J. Mol. Catal. A* **152** (2000) 1.
- [45] J. Grimblot, *Catal. Today* **41** (1998) 111.
- [46] B. R. G. Leliveld, J. A. J. van Dillen, J. W. Geus, D. C. Koningsberger, M. de Boer, *J. Phys. Chem. B* **101** (1997) 11160.
- [47] J. V. Lauritsen, S. Helveg, E. Lægsgaard, I. Stensgaard, B. S. Clausen, H. Topsøe, F. Besenbacher, *J. Catal.* **197** (2001) 1.
- [48] S. M. A. M. Bouwens, F. B. M. van Zon, M. P. van Dijk, A. M. van der Kraan, V. H. J. de Beer, J. A. R. van Veen, D. C. Koningsberger, *J. Catal.* **146** (1994) 375.
- [49] H. Topsøe, B. S. Clausen, N.-Y. Topsøe, J. Hyldtoft, J. K. Nørskov, *Prepr. - Am. Chem. Soc., Div. Petr. Chem.* **38(3)** (1993) 638.
- [50] H. Topsøe, N.-Y. Topsøe, O. Sørensen, R. Candia, B. S. Clausen, *Prepr. - Am. Chem. Soc., Div. Petr. Chem.* **28(5)** (1983) 1252.
- [51] H. Topsøe and B. S. Clausen, *Appl. Catal.* **25** (1986) 273.
- [52] C. G. Gachet, E. Dhainaut, L. de Mourgues, J. P. Candy, P. Fouilloux, *Bull. Soc. Chim. Belg.* **90(12)** (1981) 1279.

- [53] T. Kabe, W. Qian, A. Ishihara, *Catal. Today* **39** (1997) 3.
- [54] T. Kabe, A. Ishihara, W. Qian, M. Godo, *Catal. Today* **45** (1998) 285.
- [55] V. M. Kogan, N. N. Rozhdestvenskaya, I. K. Korshevets, *Appl. Catal. A* **234** (2002) 207.
- [56] J. Mijoin, V. Thévenin, N. Garcia Aguirre, H. Yuze, J. Wang, W. Z. Li, G. Pérot, J. L. Lemberon, *Appl. Catal. A* **180** (1999) 95.
- [57] W. Qian, Y. Hachiya, D. Wang, K. Hirabayashi, A. Ishihara, T. Kabe, H. Okazaki, M. Adachi, *Appl. Catal. A* **227** (2002) 19.
- [58] B. Canosa Rodrigo, H. Jeziorowski, H. Knözinger, X. Zh. Wang, E. Taglauer, *Bull. Soc. Chim. Belg.* **90(12)** (1981) 1339.
- [59] M. W. J. Crajé, V. H. J. de Beer, J. A. R. van Veen, A. M. van der Kraan, *Prepr. - Am. Chem. Soc., Div. Petr. Chem.* **39(4)** (1994) 538.
- [60] L. P. Nielsen, L. Ibsen, S. V. Christensen, B. S. Clausen, *J. Mol. Catal. A* **162** (2000) 375.
- [61] J. G. Kushmerick and P. S. Weiss, *J. Phys. Chem. B* **102** (1998) 10094.
- [62] M. Breyse, G. Berhault, S. Kasztelan, M. Lacroix, F. Maugé, G. Perot, *Catal. Today* **66** (2001) 15.
- [63] R. Cattaneo, F. Rota, R. Prins, *J. Catal.* **199** (2001) 318.
- [64] M. J. Vissenberg, Ph.D. dissertation, TU Delft, The Netherlands, 1999.
- [65] E. J. M. Hensen, Ph.D. dissertation, TU Delft, The Netherlands, 2000.
- [66] H. R. Reinhoudt, C. H. M. Boons, A. D. van Langeveld, J. A. R. van Veen, J. A. Moulijn, *Appl. Catal. A* **207** (2001) 25.
- [67] W. R. A. M. Robinson, J. A. R. van Veen, V. H. J. de Beer, R. A. van Santen, *Fuel Process. Technol.* **61** (1999) 89.
- [68] L. Coulier, V. H. J. de Beer, J. A. R. van Veen, J. W. Niemantsverdriet, *Topics Catal.* **13** (2000) 99.

- [69] T. Shimizu, K. Hiroshima, T. Honma, T. Mochizuki, M. Yamada, *Catal. Today* **45** (1998) 271.
- [70] A. M. Venezia, V. La Parola, G. Deganello, D. Cauzzi, G. Leonardi, G. Predieri, *Appl. Catal. A* **229** (2002) 261.
- [71] J. P. Janssens, A. D. van Langeveld, R. L. C. Bonné, C. M. Lok, J. A. Moulijn, *Prepr. - Am. Chem. Soc., Div. Petr. Chem.* **39(4)** (1994) 571.
- [72] J. Grimblot, P. Dufresne, L. Gengembre, J.-P. Bonnelle, *Bull. Soc. Chim. Belg.* **90(12)** (1981) 1261.
- [73] C. Glasson, C. Geantet, M. Lacroix, F. Labruyere, P. Dufresne, *Catal. Today* **45** (1998) 341.
- [74] C. Geantet, Y. Soldo, C. Glasson, N. Matsubayashi, M. Lacroix, O. Proux, O. Ulrich, J.-L. Hazemann, *Catal. Lett.* **73(2-4)** (2001) 95.
- [75] L. P. Nielsen, M. Schønning, S. V. Christensen, S. V. Hoffmann, Z. Li, P. Hofmann, F. Besenbacher, B. S. Clausen, *Catal. Lett.* **73(2-4)** (2001) 85.
- [76] W. Qian, A. Ishihara, Y. Aoyama, T. Kabe, *Appl. Catal. A* **196** (2000) 103.
- [77] F. P. Mertens, E. P. Dai, B. H. Bartley, L. D. Neff, *Prepr. - Am. Chem. Soc., Div. Petr. Chem.* **39(4)** (1994) 566.
- [78] C. Kwak, M. Y. Kim, K. Choi, S. H. Moon, *Appl. Catal. A* **185** (1999) 19.
- [79] R. de Back, F. Croonenberghs, P. Grange, Preparation of Catalysts VII, B. Delmon et al. (Eds.) Elsevier Science B. V., Amsterdam, 1998, p. 517.
- [80] P. Atanasova, T. Halachev, J. Uchytíl, M. Kraus, *Appl. Catal.* **38** (1988) 235.
- [81] A. Spojakina, S. Damyanova, L. Petrov, Z. Vit, *Appl. Catal.* **56** (1989) 163.
- [82] D. Chadwick, D. W. Aitchison, R. Badilla-Ohlbaum, L. Josefsson, in "Studies in Surface Science and Catalysis", Vol. 16, Preparation of Catalysts III, G. Poncelet, P. Grange, P. A. Jacobs (EDS), p. 323, Elsevier, Amsterdam (1983).

- [83] D. Chadwick, A. Oen, C. Siewe, *Catal. Today* **29** (1996) 229.
- [84] K. Hellgardt, A. Grutle, D. Chadwick, *Appl. Catal. A* **226** (2002) 79.
- [85] J. Cruz, M. Avalos-Borja, R. López Cordero, M. A. Banares, J. L. G. Fierro, J. M. Palacios, A. López Agudo, *Appl. Catal. A* **224** (2002) 97.
- [86] M. Yamamoto, O. Nishimura, T. Kotanigawa, *Appl. Catal. A* **174** (1998) 41.
- [87] R. Galiasso, W. Garcia, M. M. Ramirez de Agudelo, P. Andreu, *Catal. Rev. - Sci. Eng.* **26(3-4)** (1984) 445.
- [88] T. F. Kellett, A. F. Sartor, C. A. Trevino, *Hydrocarbon Process.* **59(5)** (1980) 139.
- [89] New 'toolkit' aids hydrotreating, *Hydrocarbon Process.* **81(6)** (2002) 32.
- [90] B. Seljestokken, Unpublished Statoil internal report, 1998.
- [91] T. Kabe, A. Ishihara, H. Tajima, *Ind. Eng. Chem. Res.* **31(6)** (1992) 1577.
- [92] T. Kabe, K. Akamatsu, A. Ishihara, S. Otsuki, M. Godo, Q. Zhang, W. Qian, *Ind. Eng. Chem. Res.* **36** (1997) 5146.
- [93] M. V. Landau, *Catal. Today* **36** (1997) 393.
- [94] A. Ishihara, H. Tajima, T. Kabe, *Chem. Lett.* (1992) 669.
- [95] Q. Zhang, A. Ishihara, H. Yashima, W. Qian, H. Tsutsui, T. Kabe, *J. Jpn. Petrol. Inst.* **40(1)** (1997) 29.
- [96] X. Ma, K. Sakanishi, T. Isoda, I. Mochida, *Prepr. - Am. Chem. Soc., Div. Petr. Chem.* **39(4)** (1994) 622.
- [97] X. Ma, K. Sakanishi, T. Isoda, I. Mochida, *Ind. Eng. Chem. Res.* **34** (1995) 748.
- [98] M. L. Ocelli and T. P. Debies, *J. Catal.* **97** (1986) 357.
- [99] M. Lewandowski and Z. Sarbak, *Fuel* **79** (2000) 487.
- [100] D. Li, T. Sato, M. Imamura, H. Shimada, A. Nishijima, *Appl. Catal. B* **16** (1998) 255.
- [101] Y.-W. Chen and M.-C. Tsai, *Ind. Eng. Chem. Res.* **36** (1997) 2521.
- [102] Y.-W. Chen and M.-C. Tsai, *Catal. Today* **50** (1999) 57.

- [103] C. Kwak, J. J. Lee, J. S. Bae, K. Choi, S. H. Moon, *Appl. Catal. A* **200** (2000) 233.
- [104] C. J. Song, C. Kwak, S. H. Moon, *Catal. Today* **74** (2002) 193.
- [105] Y. Okamoto, K. Ochiai, M. Kawano, K. Kobayashi, T. Kubota, *Appl. Catal. A* **226** (2002) 115.
- [106] K. Segawa, K. Takahashi, S. Satoh, *Catal. Today* **63** (2000) 123.
- [107] S. Yoshinaka and K. Segawa, *Catal. Today* **45** (1998) 293.
- [108] C. Pophal, F. Kameda, K. Hoshino, S. Yoshinaka, K. Segawa, *Catal. Today* **39** (1997) 21.
- [109] L. Coulier, J. A. R. van Veen, J. W. Niemantsverdriet, *Catal. Lett.* **79(1-4)** (2002) 149.
- [110] E. Olguin, M. Vrinat, L. Cedeno, J. Ramirez, M. Borque, A. López-Agudo, *Appl. Catal. A* **165** (1997) 1.
- [111] Z. B. Wei, W. Yan, H. Zhang, T. Ren, Q. Xin, Z. Li, *Appl. Catal. A* **167** (1998) 39.
- [112] E. Lecrenay, K. Sakanishi, T. Nagamatsu, I. Mochida, T. Suzuka, *Appl. Catal. B* **18** (1998) 325.
- [113] M. P. Borque, A. López-Agudo, E. Olguín, M. Vrinat, L. Cedeno, J. Ramírez, *Appl. Catal. A* **180** (1999) 53.
- [114] J. R. Grzechowiak, J. Rynkowski, I. Wereszczako-Zielinska, *Catal. Today* **65** (2001) 225.
- [115] S. K. Maity, M. S. Rana, S. K. Bej, J. Ancheyta-Juárez, G. Murali Dhar, T. S. R. Prasada Rao, *Catal. Lett.* **72(1-2)** (2001) 115.
- [116] F. P. Daly, H. Ando, J. L. Schmitt, E. A. Sturm, *Catalysis 1987*, J. W. Ward (Ed.), Elsevier Science Publishers B. V., Amsterdam, 1988, p. 553.
- [117] D. Sotiropoulou, C. Yiokari, C. G. Vayenas, S. Ladas, *Appl. Catal. A* **183** (1999) 15.
- [118] S. K. Maity, M. S. Rana, B. N. Srinivas, S. K. Bej, G. Murali Dhar, T. S. R. Prasada Rao, *J. Mol. Catal. A* **153** (2000) 121.
- [119] E. Lecrenay, K. Sakanishi, I. Mochida, T. Suzuka, *Appl. Catal. A* **175** (1998) 237.
- [120] S. Damyanova, L. Petrov, M. A. Centeno, P. Grange, *Appl. Catal. A* **224** (2002) 271.

- [121] N. G. Kostova, A. A. Spojakina, K. Jiratova, O. Solcova, L. D. Dimitrov, L. A. Petrov, *Catal. Today* **65** (2001) 217.
- [122] N.-Y. Topsøe and H. Topsøe, *Bull. Soc. Chim. Belg.* **90(12)** (1981) 1311.
- [123] J.-P. Janssens, A. D. van Langeveld, J. A. Moulijn, *Appl. Catal. A* **179** (1999) 229.
- [124] T. Chiranjeevi, P. Kumar, S. K. Maity, M. S. Rana, G. Murali Dhar, T. S. R. Prasada Rao, *Microporous Mesoporous Mater.* **44-45** (2001) 547.
- [125] T. Chiranjeevi, P. Kumar, M. S. Rana, G. Murali Dhar, T. S. R. Prasada Rao, *J. Mol. Catal. A* **181** (2002) 109.
- [126] T. Klimova, D. S. Casados, J. Ramírez, *Catal. Today* **43** (1998) 135.
- [127] M. Lewandowski and Z. Sarbak, *Appl. Catal. A* **168** (1998) 179.
- [128] T. Klicpera and M. Zdrzil, *Appl. Catal. A* **216** (2001) 41.
- [129] M. Breyse, B. A. Bennett, D. Chadwick, M. Vrinat, *Bull. Soc. Chim. Belg.* **90(12)** (1981) 1271.
- [130] H. Farag, D. D. Whitehurst, I. Mochida, *Ind. Eng. Chem. Res.* **37** (1998) 3533.
- [131] H. Farag, D. D. Whitehurst, K. Sakanishi, I. Mochida, *Catal. Today* **50** (1999) 9.
- [132] H. Farag, I. Mochida, K. Sakanishi, *Appl. Catal. A* **194-195** (2000) 147.
- [133] K. Sakanishi, T. Nagamatsu, I. Mochida, D. D. Whitehurst, *J. Mol. Catal. A* **155** (2000) 101.
- [134] J. L. Brito, F. Severino, N. N. Delgado, J. Laine, *Appl. Catal. A* **173** (1998) 193.
- [135] P. Vázquez, L. Pizzio, M. Blanco, C. Cáceres, H. Thomas, R. Arriagada, S. Bendezú, R. Cid, R. García, *Appl. Catal. A* **184** (1999) 303.
- [136] L. Kaluza and M. Zdrzil, *Carbon* **39** (2001) 2023.
- [137] B. Pawelec, R. Mariscal, J. L. G. Fierro, A. Greenwood, P. T. Vasudevan, *Appl. Catal. A* **206** (2001) 295.
- [138] K. M. Reddy, B. Wei, C. Song, *Catal. Today* **43** (1998) 261.

- [139] C. Song and K. M. Reddy, *Appl. Catal. A* **176** (1999) 1.
- [140] J. Ramírez, R. Contreras, P. Castillo, T. Klimova, R. Zárate, R. Luna, *Appl. Catal. A* **197** (2000) 69.
- [141] T. Klimova, E. Rodríguez, M. Martínez, J. Ramírez, *Microporous Mesoporous Mater.* **44-45** (2001) 357.
- [142] K. Kaneda, T. Wada, S. Murata, M. Nomura, *Energy Fuels* **12** (1998) 298.
- [143] Y. Okamoto, *Catal. Today* **39** (1997) 45.
- [144] S. Bendezú, R. Cid, J. L. G. Fierro, A. López Agudo, *Appl. Catal. A* **197** (2000) 47.
- [145] P. W. de Bont, M. J. Vissenberg, V. H. J. de Beer, J. A. R. van Veen, R. A. van Santen, A. M. van der Kraan, *Appl. Catal. A* **202** (2000) 99.
- [146] F. Bataille, J. L. Lemberon, G. Pérot, P. Leyrit, T. Cseri, N. Marchal, S. Kasztelan, *Appl. Catal. A* **220** (2001) 191.
- [147] T. Isoda, Y. Takase, K. Kusakabe, S. Morooka, *Energy Fuels* **14** (2000) 585.
- [148] W. J. J. Welters, V. H. J. de Beer, R. A. van Santen, *Appl. Catal. A* **119** (1994) 253.
- [149] Z. Sarbak, *Appl. Catal. A* **216** (2001) 9.
- [150] Z. Sarbak, *Appl. Catal. A* **207** (2001) 309.
- [151] Z. Sarbak, *Catal. Today* **65** (2001) 293.
- [152] N. Hermann, M. Brorson, H. Topsøe, *Catal. Lett.* **65** (2000) 169.
- [153] T. A. Pecoraro and R. R. Chianelli, *J. Catal.* **67** (1981) 430.
- [154] C. J. H. Jacobsen, E. Törnqvist, H. Topsøe, *Catal. Lett.* **63** (1999) 179.
- [155] R. Cowan, M. Høglin, H. Reinink, J. Jsebaert, D. Chadwick, *Catal. Today* **45** (1998) 381.
- [156] J. Raty and T. A. Pakkanen, *Catal. Lett.* **65** (2000) 175.
- [157] N. Escalona, J. Ojeda, R. Cid, G. Alves, A. López Agudo, J. L. G. Fierro, F. J. Gil Llambías, *Appl. Catal. A* **234** (2002) 45.
- [158] M. E. Grillo and P. Sautet, *J. Mol. Catal. A* **174** (2001) 239.

- [159] P. Pinto, M. J. Calhorda, T. Straub, V. Miikkulainen, J. Raty, M. Suvanto, T. A. Pakkanen, *J. Mol. Catal. A* **170** (2001) 209.
- [160] M. Wojciechowska, M. Pietrowski, B. Czajka, *Catal. Today* **65** (2001) 349.
- [161] M. Cattenot, C. Geantet, C. Glasson, M. Breysse, *Appl. Catal. A* **213** (2001) 217.
- [162] E. Dhainaut, H. Charcosset, C. Gachet, L. de Mourgues, *Appl. Catal.* **2** (1982) 75.
- [163] W. Qian, Y. Yoda, Y. Hirai, A. Ishihara, T. Kabe, *Appl. Catal. A* **184** (1999) 81.
- [164] L. I. Merino, A. Centeno, S. A. Giraldo, *Appl. Catal. A* **197** (2000) 61.
- [165] W. R. A. M. Robinson, J. A. R. van Veen, V. H. J. de Beer, R. A. van Santen, *Fuel Process. Technol.* **61** (1999) 103.
- [166] H. R. Reinhoudt, R. Troost, S. van Schalkwijk, A. D. van Langeveld, S. T. Sie, J. A. R. van Veen, J. A. Moulijn, *Fuel Process. Technol.* **61** (1999) 117.
- [167] M. Sugioka, L. Andalaluna, S. Morishita, T. Kurosaka, *Catal. Today* **39** (1997) 61.
- [168] R. Navarro, B. Pawelec, J. L. G. Fierro, P. T. Vasudevan, J. F. Cambra, M. B. Guemez, P. L. Arias, *Fuel Process. Technol.* **61** (1999) 73.
- [169] M. Sugioka, F. Sado, T. Kurosaka, X. Wang, *Catal. Today* **45** (1998) 327.
- [170] C. Song, *Chemtech* **29(3)** 1999 26.
- [171] C. Song and A. D. Schmitz, *Energy Fuels* **11** (1997) 656.
- [172] L. J. Simon, M. Rep, J. G. van Ommen, J. A. Lercher, *Appl. Catal. A* **218** (2001) 161.
- [173] M. Sugioka, F. Sado, Y. Matsumoto, N. Maesaki, *Catal. Today*, **29** (1996) 255.
- [174] T. Rades, V. Y. Borovkov, V. B. Kazansky, M. Polisset-Thfoin, J. Fraissard, *J. Phys. Chem.* **100** (1996) 16238.
- [175] L. Le Bihan and Y. Yoshimura, *Fuel* **81** (2002) 491.
- [176] B. C. Gates, J. R. Katzer, G. C. A. Schuit, *Chemistry of Catalytic Processes*, McGraw-Hill Book Company, 1979, p. 390-447.

- [177] M. Houalla, N. K. Nag, A. V. Sapre, D. H. Broderick, B. C. Gates, *AIChE J.* **24(6)** (1978) 1015.
- [178] W. S. O'Brien, J. W. Chen, R. V. Nayak, G. S. Carr, *Ind. Eng. Chem. Process Des. Dev.* **25** (1986) 221.
- [179] M. V. Landau, D. Berger, M. Herskowitz, *J. Catal.* **159** (1996) 236.
- [180] G. H. Singhal, R. L. Espino, J. E. Sobel, G. A. Huff, Jr., *J. Catal.* **67** (1981) 457.
- [181] B. H. Cooper and K. G. Knudsen, *Prepr. - Am. Chem. Soc., Div. Petr. Chem.* **46(4)** (2001) 338.
- [182] V. Lamure-Meille, E. Schulz, M. Lemaire, M. Vrinat, *Appl. Catal. A* **131** (1995) 143.
- [183] R. Shafi and G. J. Hutchings, *Catal. Today* **59** (2000) 423.
- [184] D. H. Broderick and B. C. Gates, *AIChE J.* **27(4)** (1981) 663.
- [185] T. Kabe and A. Ishihara, Q. Zhang, *Appl. Catal. A* **97** (1993) L1.
- [186] T. Isoda, X. Ma, I. Mochida, *Prepr. - Am. Chem. Soc., Div. Petr. Chem.* **39(4)** (1994) 584.
- [187] H. Farag, D. D. Whitehurst, K. Sakanishi, I. Mochida, *Catal. Today* **50** (1999) 49.
- [188] D. D. Whitehurst, H. Farag, T. Nagamatsu, K. Sakanishi, I. Mochida, *Catal. Today* **45** (1998) 299.
- [189] D. R. Kilanowski, H. Teeuwen, V. H. J. de Beer, B. C. Gates, G. C. A. Schuit, H. Kwart, *J. Catal.* **55** (1978) 129.
- [190] M. Houalla, D. H. Broderick, A. V. Sapre, N. K. Nag, V. H. J. de Beer, B. C. Gates, H. Kwart, *J. Catal.* **61** (1980) 523.
- [191] G. H. Singhal, R. L. Espino, J. E. Sobel, *J. Catal.* **67** (1981) 446.
- [192] I. A. Van Parijs and G. F. Froment, *Ind. Eng. Chem. Prod. Res. Dev.* **25** (1986) 431.
- [193] I. A. Van Parijs, L. H. Hosten, G. F. Froment, *Ind. Eng. Chem. Prod. Res. Dev.* **25** (1986) 437.
- [194] V. Vanrysselberghe and G. F. Froment, *Ind. Eng. Chem. Res.* **35** (1996) 3311.

- [195] V. Vanrysselberghe, R. Le Gall, G. F. Froment, *Ind. Eng. Chem. Res.* **37** (1998) 1235.
- [196] V. Vanrysselberghe and G. F. Froment, *Ind. Eng. Chem. Res.* **37** (1998) 4231.
- [197] D. Levaché, A. Guida, P. Geneste, *Bull. Soc. Chim. Belg.* **90(12)** (1981) 1285.
- [198] V. Meille, E. Schulz, M. Lemaire, M. Vrinat, *J. Catal.* **170** (1997) 29.
- [199] V. Meille, E. Schulz, M. Lemaire, M. Vrinat, *Appl. Catal. A* **187** (1999) 179.
- [200] M. J. Ledoux, C. P. Huu, Y. Segura, F. Luck, *J. Catal.* **121** (1990) 70.
- [201] S. S. Katti, D. W. B. Westerman, B. C. Gates, T. Youngless, L. Petrakis, *Ind. Eng. Chem. Process Des. Dev.* **23** (1984) 773.
- [202] F. van Looij, P. van der Laan, W. H. J. Stork, D. J. DiCamillo, J. Swain, *Appl. Catal. A* **170** (1998) 1.
- [203] L. Vradman, M. V. Landau, M. Herskowitz, *Catal. Today* **48** (1999) 41.
- [204] E. Lecrenay, K. Sakanishi, I. Mochida, *Catal. Today* **39** (1997) 13.
- [205] T. Kabe, K. Akamatsu, A. Ishihara, S. Otsuki, M. Godo, Q. Zhang, W. Qian, S. Yamada, *Sekiyu Gakkaishi* **42(3)** (1999) 236.
- [206] X. Ma, K. Sakanishi, I. Mochida, *Ind. Eng. Chem. Res.* **33** (1994) 218.
- [207] X. Ma, K. Sakanishi, I. Mochida, *Ind. Eng. Chem. Res.* **35** (1996) 2487.
- [208] J. Ancheyta, M. J. Angeles, M. J. Macías, G. Marroquín, R. Morales, *Energy Fuels* **16(1)** (2002) 189.
- [209] H. Schulz, W. Böhringer, F. Ousmanov, P. Waller, *Fuel Process. Technol.* **61** (1999) 5.
- [210] H. Schulz, W. Böhringer, P. Waller, F. Ousmanov, *Catal. Today* **49** (1999) 87.
- [211] J. Ancheyta-Juárez, E. Aguilar-Rodríguez, D. Salazar-Sotelo, G. Marroquín-Sánchez, G. Quiroz-Sosa, M. Leiva-Nuncio, *Appl. Catal. A* **183** (1999) 265.
- [212] M. Nagai and T. Kabe, *J. Catal.* **81** (1983) 440.
- [213] S. Kasahara, T. Shimizu, M. Yamada, *Catal. Today* **35** (1997) 59.

- [214] S. Shin, H. Yang, K. Sakanishi, I. Mochida, D. A. Grudoski, J. H. Shinn, *Appl. Catal. A* **205** (2001) 101.
- [215] T. Kabe, Y. Aoyama, D. Wang, A. Ishihara, W. Qian, M. Hosoya, Q. Zhang, *Appl. Catal. A* **209** (2001) 237.
- [216] J. Leglise, J. van Gestel, J.-C. Duchet, *Prepr. - Am. Chem. Soc., Div. Petr. Chem.* **39(4)** (1994) 533.
- [217] K. Hiroshi, T. Fujikawa, H. Tagami, K. Idei, *Prepr. - Am. Chem. Soc., Div. Petr. Chem.* **46(4)** (2001) 335.
- [218] T. Isoda, S. Nagao, X. Ma, Y. Korai, I. Mochida, *Appl. Catal. A* **150** (1997) 1.
- [219] H. Farag, K. Sakanishi, I. Mochida, D. D. Whitehurst, *Energy Fuels* **13** (1999) 449.
- [220] T. Koltai, M. Macaud, A. Guevara, E. Schulz, M. Lemaire, R. Bacaud, M. Vrinat, *Appl. Catal. A* **231** (2002) 253.
- [221] C. Kwak, J. J. Lee, J. S. Bae, S. H. Moon, *Appl. Catal. B* **35** (2001) 59.
- [222] G. C. Laredo S., J. A. De los Reyes H., J. L. Cano D., J. J. Castillo M., *Appl. Catal. A* **207** (2001) 103.
- [223] M. M. Ramírez de Agudelo, C. Galarraga, M. Pimentel, *Prepr. - Am. Chem. Soc., Div. Petr. Chem.* **38(3)** (1993) 700.
- [224] U. T. Turaga, G. Wang, X. Ma, C. Song, H. H. Schobert, *Prepr. - Am. Chem. Soc., Div. Petr. Chem.* **47(1)** (2002) 89.
- [225] M. Nagai, T. Sato, A. Aiba, *J. Catal.* **97** (1986) 52.
- [226] P. Zeuthen, K. G. Knudsen, D. D. Whitehurst, *Catal. Today* **65** (2001) 307.
- [227] A. N. R. Bos, L. Lefferts, G. B. Marin, M. H. G. M. Steijns, *Appl. Catal. A* **160** (1997) 185.
- [228] M. Absi-Halabi, A. Stanislaus, D. L. Trimm, *Appl. Catal.* **72** (1991) 193.
- [229] M. Marafi and A. Stanislaus, *Appl. Catal. A* **159** (1997) 259.

- [230] F. Diez, B. C. Gates, J. T. Miller, D. J. Sajkowski, S. G. Kukes, *Ind. Eng. Chem. Res.* **29** (1990) 1999.
- [231] S. M. Richardson, H. Nagaishi, M. R. Gray, *Ind. Eng. Chem. Res.* **35** (1996) 3940.
- [232] D. S. Thakur and M. G. Thomas, *Appl. Catal.* **15** (1985) 197.
- [233] V. L. S. T. da Silva, R. Frety, M. Schmal, *Ind. Eng. Chem. Res.* **33** (1994) 1692.
- [234] L. P. A. F. Elst, S. Eijsbouts, A. D. van Langeveld, J. A. Moulijn, *J. Catal.* **196** (2000) 95.
- [235] F. Pedraza, S. Fuentes, M. Vrinat, M. Lacroix, *Catal. Lett.* **62** (1999) 121.
- [236] E. Furimsky, *Catal. Rev. - Sci. Eng.* **22(3)** (1980) 371.
- [237] W. A. Dietz, *J. Gas Chromatogr.* **5** (1967) 68.
- [238] A. R. Katritzky, E. S. Ignatchenko, R. A. Barcock, V. S. Lobanov, *Anal. Chem.* **66** (1994) 1799.
- [239] R. Myrstad, J. S. Rosvoll, K. Grande, E. A. Blekkan, *Stud. Surf. Sci. Catal.*, **106** (1997) 437.
- [240] <http://www.chemistry.adelaide.edu.au/external/Soc-Rel/Content/aed.htm>
- [241] <http://www.chem.agilent.com/Scripts/Library.asp>
- [242] F. Augusto and A. L. P. Valente, *J. Chromatogr. A* **819** (1998) 85.
- [243] G. Becker and A. Colmsjö, *Anal. Chim. Acta* **376** (1998) 265.
- [244] B. D. Quimby, D. A. Grudoski, V. Giarrocco, *J. Chromatogr. Sci.* **36** (1998) 435.
- [245] A. Stumpf, K. Tolvaj, M. Juhász, *J. Chromatogr. A* **819** (1998) 67.
- [246] G. A. Depauw and G. F. Froment, *J. Chromatogr. A* **761** (1997) 231.
- [247] S. Inoue, T. Takatsuka, Y. Wada, S. Hirohama, T. Ushida, *Fuel* **79** (2000) 843.
- [248] T. Onaka, M. Kobayashi, Y. Ishii, K. Okumura, M. Suzuki, *J. Chromatogr. A* **903** (2000) 193.
- [249] T. Fujikawa, O. Chiyoda, M. Tsukagoshi, K. Idei, S. Takehara, *Catal. Today* **45** (1998) 307.

- [250] Chrompack Application Handbook, chromatographic separations.
- [251] H. Bergem, Ph.D. dissertation, NTNU Trondheim, Norway, 1997.
- [252] D. Letourneur, R. Bacaud, M. Vrinat, D. Schweich, I. Pitault, *Ind. Eng. Chem. Res.* **37** (1998) 2662.
- [253] K. G. Knudsen, B. H. Cooper, H. Topsøe, *Appl. Catal. A* **189** (1999) 205.
- [254] A. Milenkovic, M. Macaud, E. Schulz, T. Koltai, D. Loffreda, M. Vrinat, M. Lemaire, *Chemistry* **3** (2000) 459.
- [255] Z. Sarbak and S. L. T. Andersson, *Appl. Catal. A* **79** (1991) 191.
- [256] L. Coulier, Ph.D. dissertation, TU Eindhoven, The Netherlands, 2001.
- [257] L. Coulier, V. H. J. de Beer, J. A. R. van Veen, J. W. Niemantsverdriet, *J. Catal.* **197(1)** (2001) 26.
- [258] P. J. Owens and C. H. Amberg, *Advan. Chem. Ser.* **33** (1961) 182.
- [259] J. W. Benson, R. J. Angelici, G. L. Schrader, *Prepr. - Am. Chem. Soc., Div. Petr. Chem.* **39(4)** (1994) 553.
- [260] M. R. Blake, M. Eyre, R. B. Moyes, P. B. Wells, *Bull. Soc. Chim. Belg.* **90(12)** (1981) 1293.
- [261] T. C. Ho and J. E. Sobel, *J. Catal.* **128** (1991) 581.
- [262] D. D. Whitehurst, T. Isoda, I. Mochida, *Adv. Catal.* **42** (1998) 345.

APPENDIX

LIST OF APPENDICES

- A1. Page from the Chrompack reference book [250].
- A2. Stability of the DBT system after the change of conditions.
- A3. Chromatogram from the GC-AED showing the background envelope of the sulfur containing peaks.
- A4. The correlation between the overall HDS conversion and the conversions of selected individual compounds. NiMo catalyst, LHSV = 0.5 h⁻¹(A) and 4 h⁻¹(B), pressure 4 MPa, H₂/oil = 200 Nm³/m³.
- A5. Pseudo-first-order plots of DBT, 4-MDBT and 4,6-DMDBT. NiMo catalyst, reaction temperature 250 °C (A) and 300 °C (B), pressure 4 MPa, H₂/oil = 200 Nm³/m³.
- A6. Arrhenius plots of DBT, 4-MDBT and 4,6-DMDBT based on Equation (4-2). LHSV 0.5 h⁻¹ (A) and 2 h⁻¹ (B), NiMo catalyst, pressure 4 MPa, H₂/oil = 200 Nm³/m³.
- A7. Comparison of deactivation behavior of NiMo (NTA) catalysts with a different heating rate during sulfiding. Pressure 0.1 MPa, reaction temperature 300 °C.
- A8. Gas phase IR spectrum of CO₂ from the NIST database on internet.
- A9. Determination of the reaction order with respect to H₂S (A) and aromatics (B).



APPLICATION NOTE 121 - GC

Hydrocarbons C₁-C₆

The separation of saturated and unsaturated C₁-C₆ hydrocarbons

Technique : GC-capillary

Column : 25 m × 0.32 mm fused silica WCOT
CP-Sil 5 CB (1.2 μm) (Cat.no. 7760)

Temperature : 20°C

Carrier gas : He, 70 kPa (0.7 bar, 10 psi), 50 cm/s

Injector : Splitter, 100 ml/min

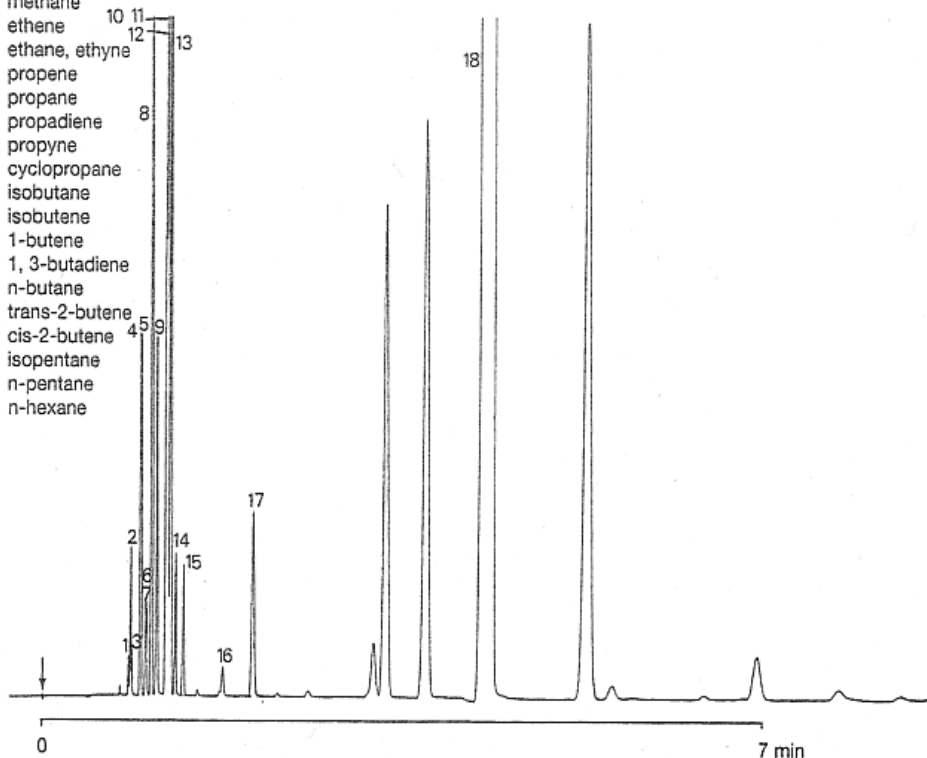
T = 200°C

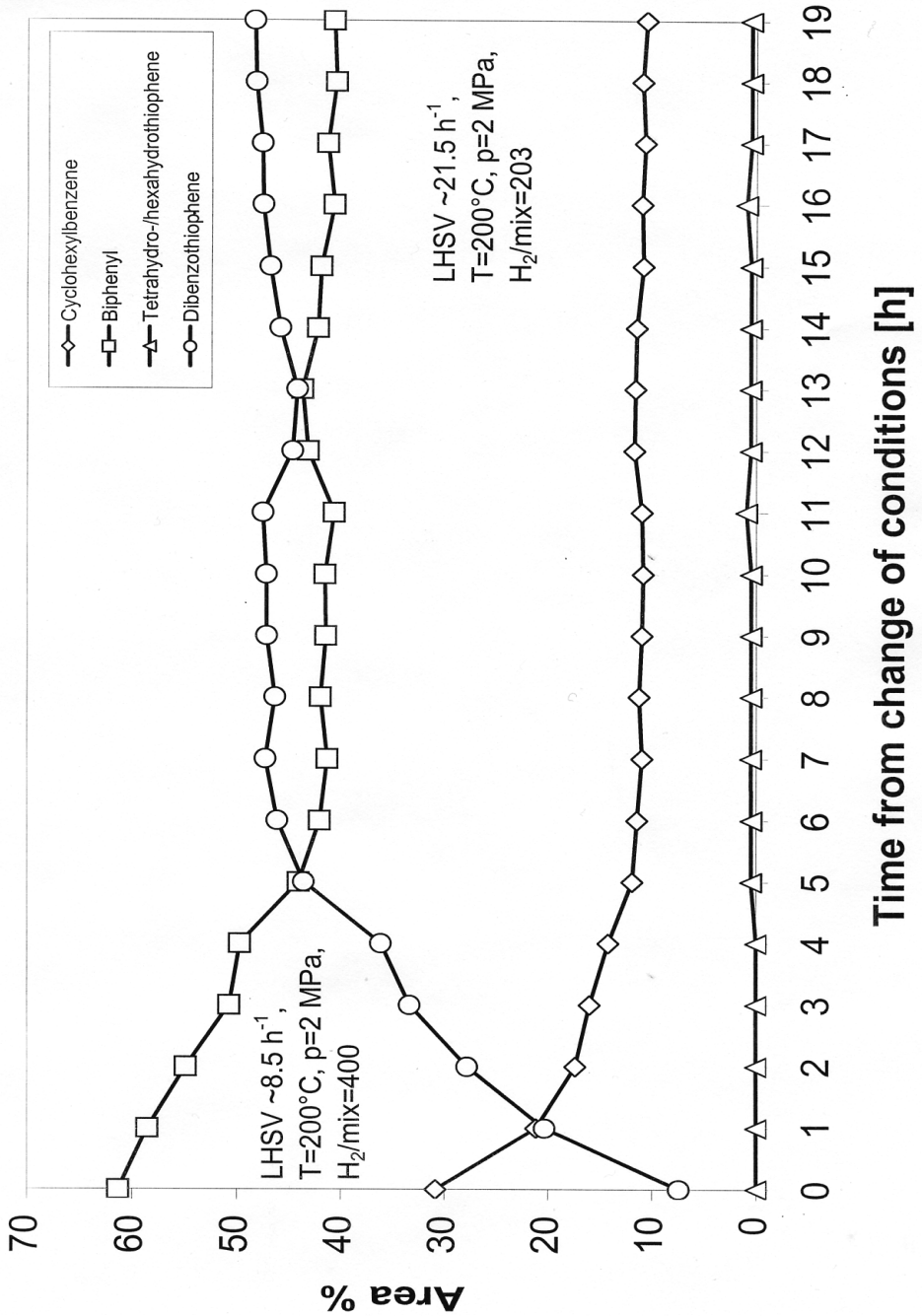
Detector : FID, 80 × 10⁻¹² Afs

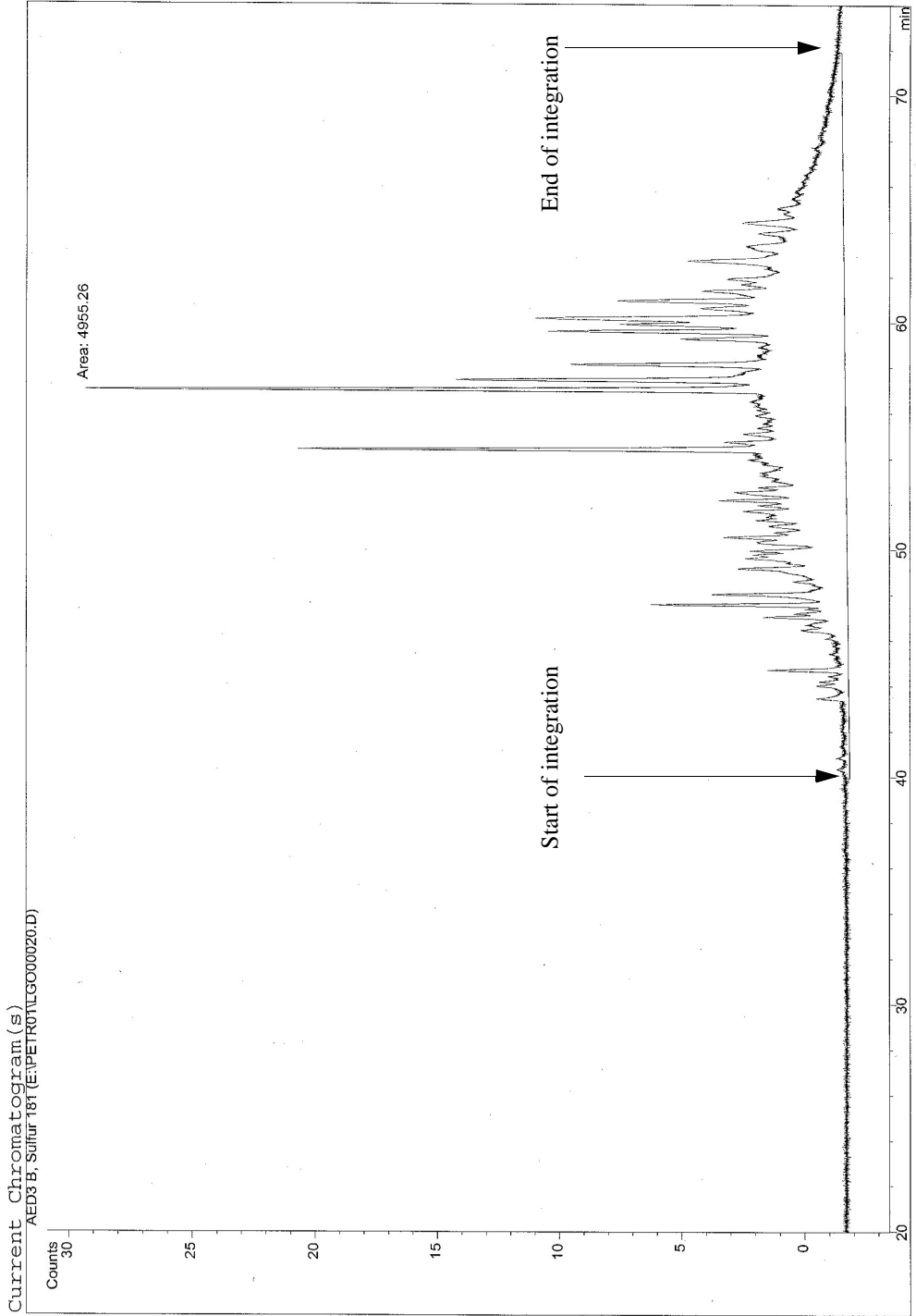
T = 250°C

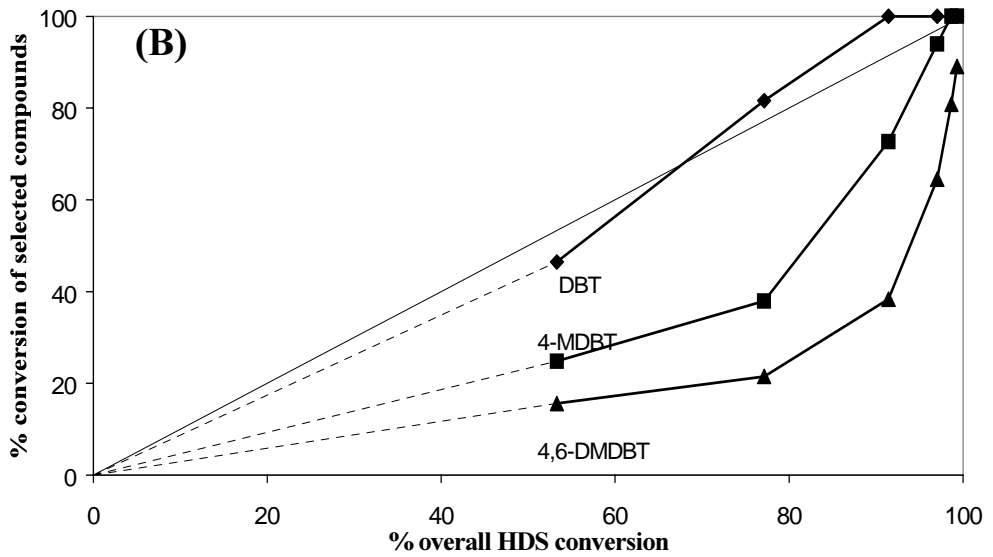
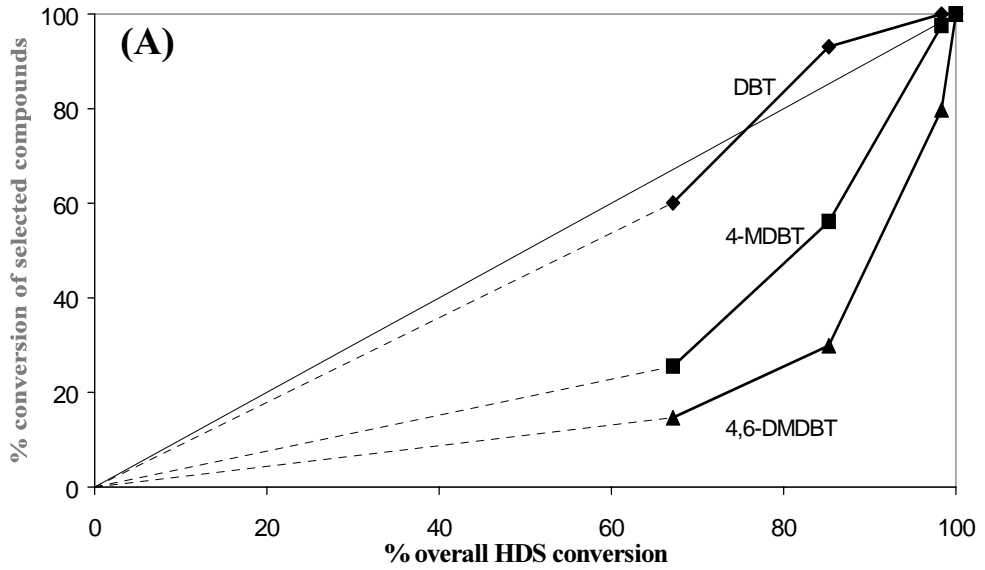
Peak identification:

1. methane
2. ethene
3. ethane, ethyne
4. propene
5. propane
6. propadiene
7. propyne
8. cyclopropane
9. isobutane
10. isobutene
11. 1-butene
12. 1, 3-butadiene
13. n-butane
14. trans-2-butene
15. cis-2-butene
16. isopentane
17. n-pentane
18. n-hexane



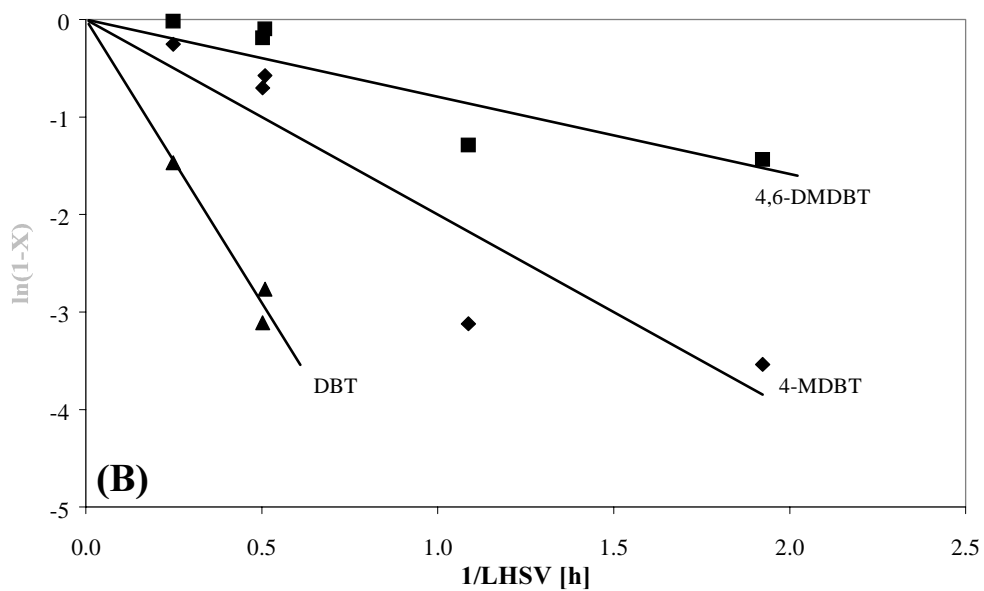
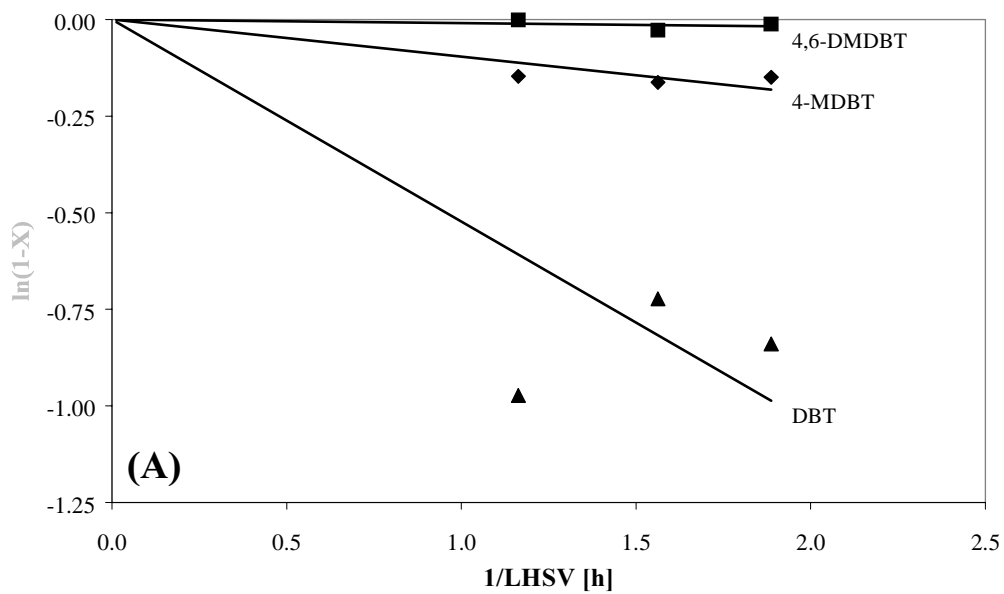






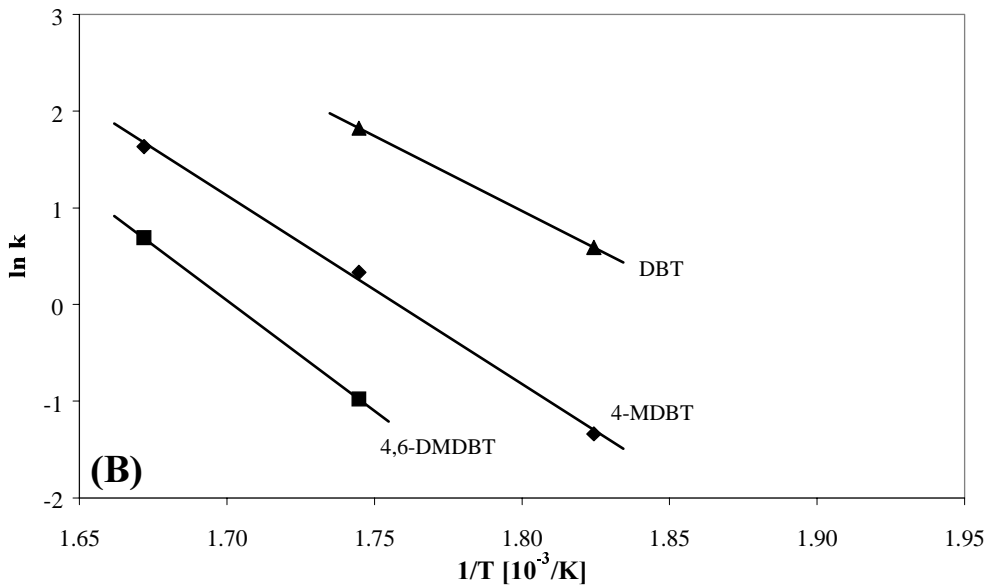
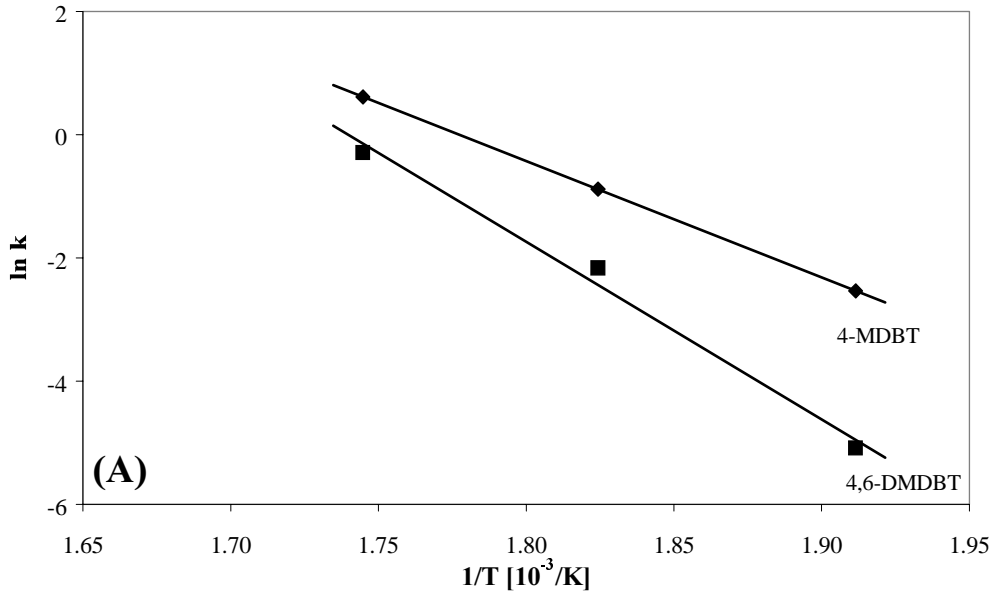
(A): LHSV = 0.5 h⁻¹.

(B): LHSV = 4.0 h⁻¹.



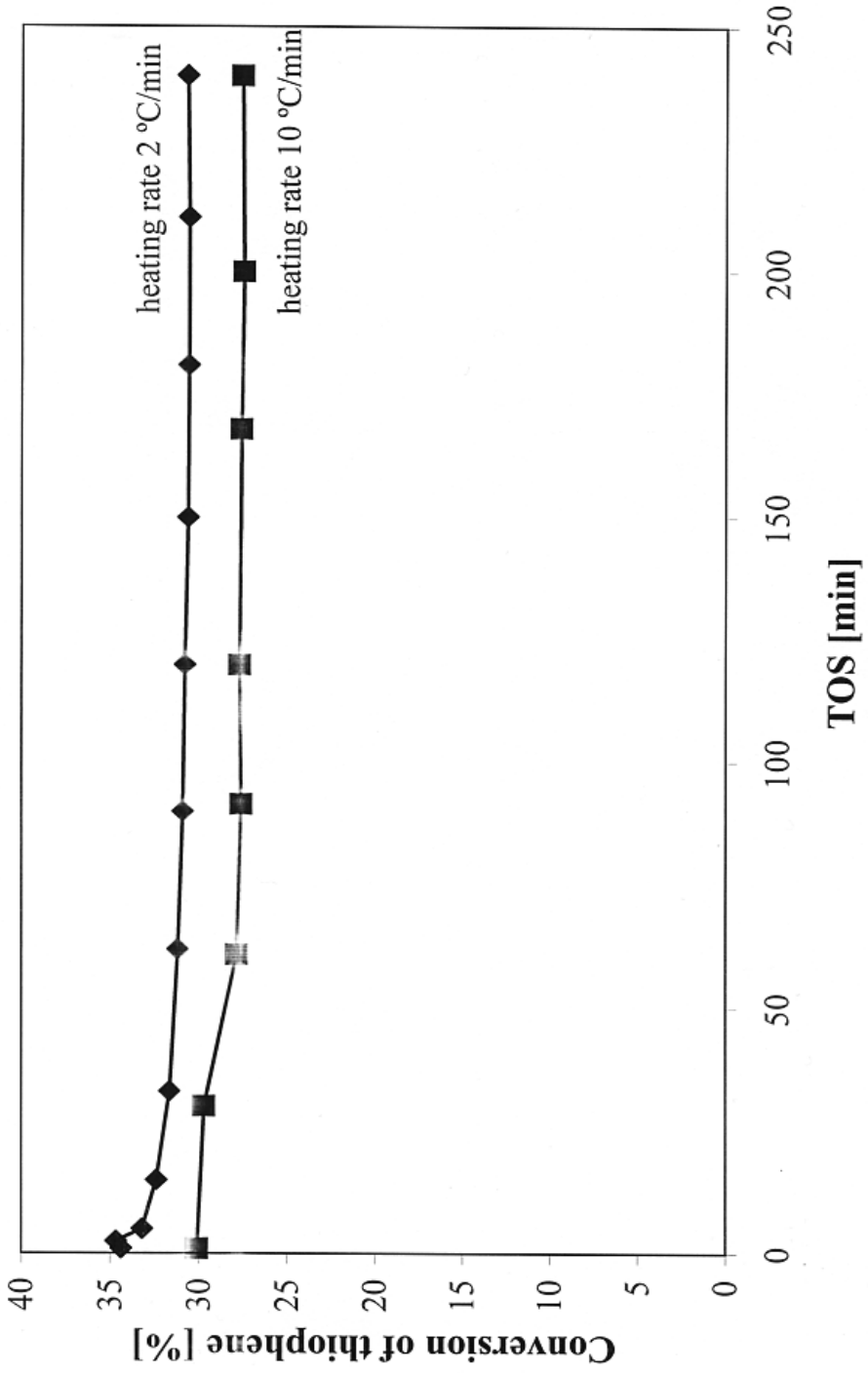
(A): Reaction temperature 250 °C.

(B): Reaction temperature 300 °C.



(A): LHSV = 0.5 h^{-1} .

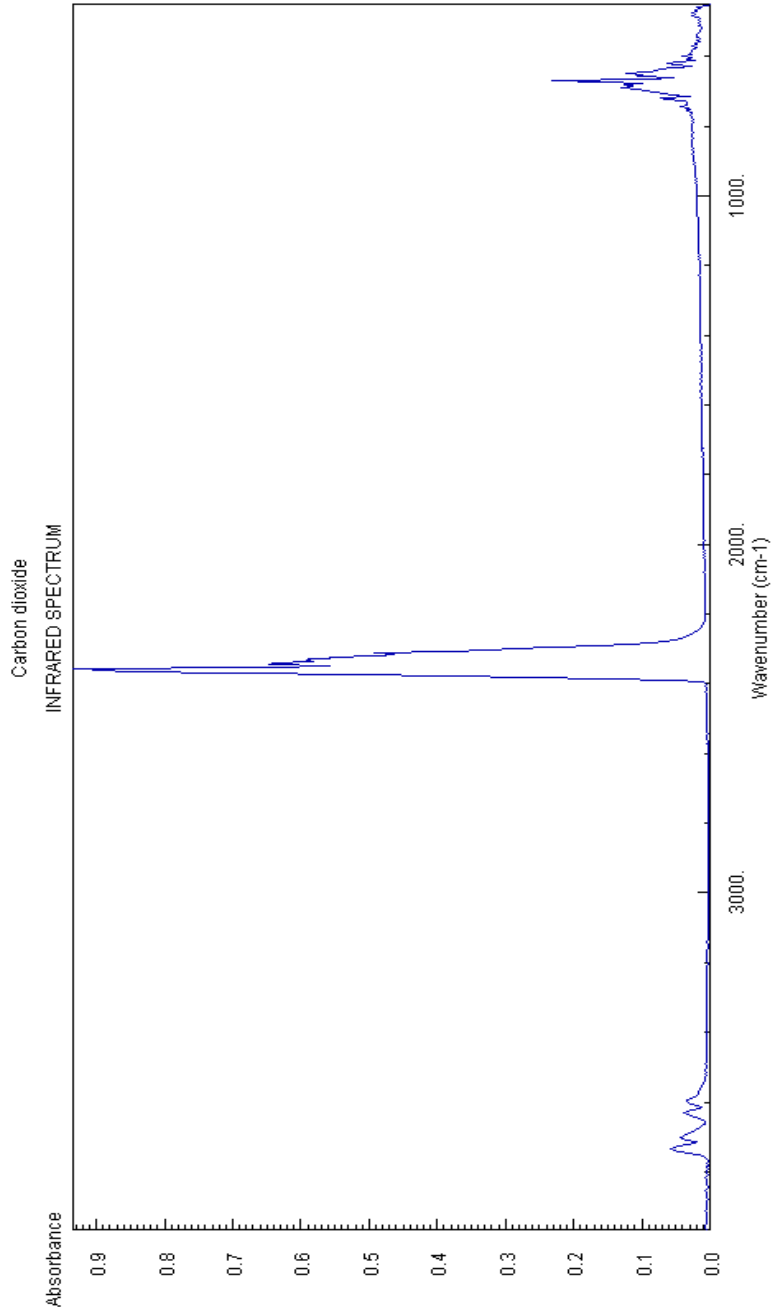
(B): LHSV = 2.0 h^{-1} .

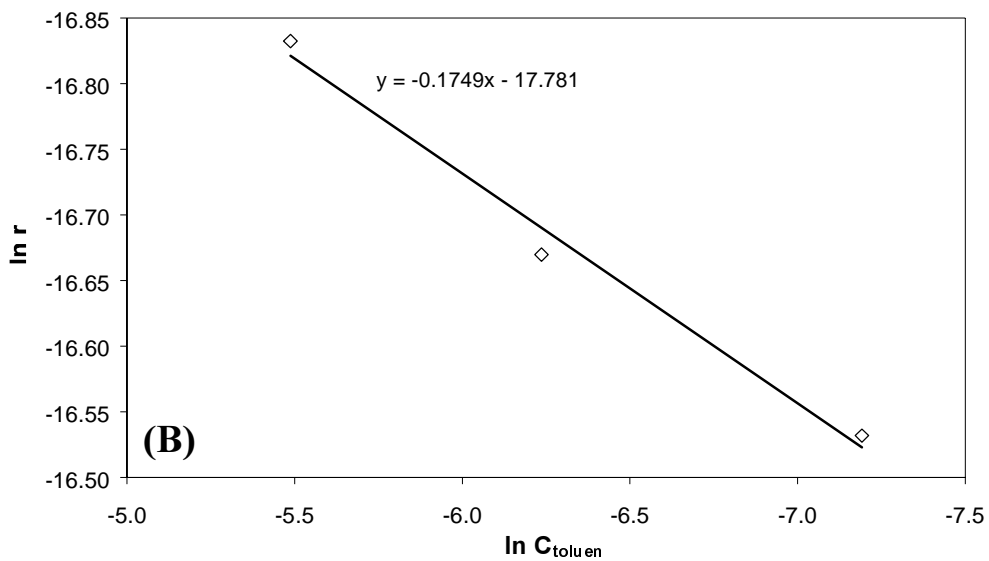
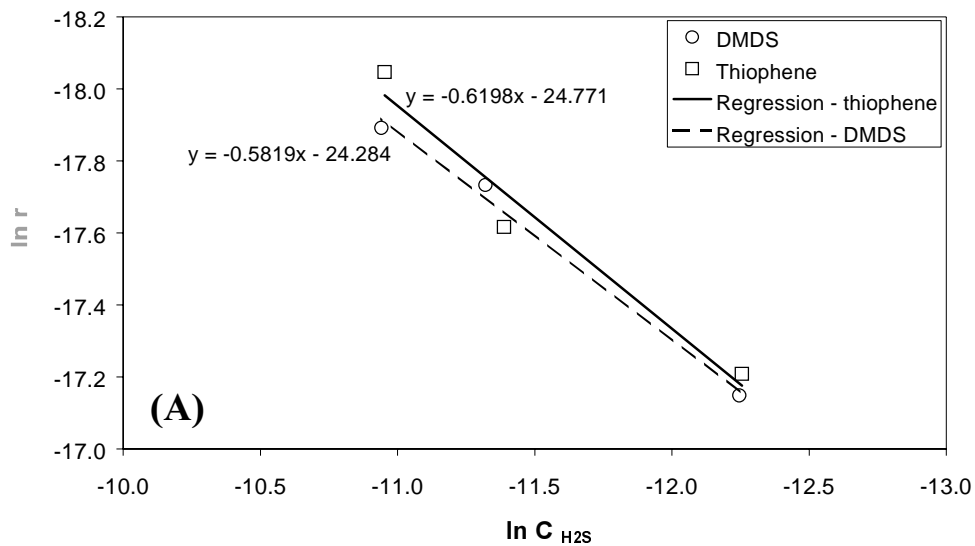


Gas Phase IR Spectrum

[Go To: Top, References, Notes / Error Report](#)

Data compiled by: NIST Mass Spec Data Center, S.E. Stein, director





(A): Reaction order with respect to H_2S during addition of DMDS and thiophene.

(B): Reaction order with respect to toluene.